

*Republic of Iraq
Ministry of Higher
Education and Scientific
Research
University of Baghdad
College of Education for
Pure Science
Ibn-AL-Haitham
Department of physics*



**computer investigations of sputtering yields for
the metals alloys (BeCu, brass, stainless -steel,
and monel-400) bombarding by different ions
(Ar, at normal and oblique
incidence.**

A Thesis

*Submitted to the Council of College of Education for Pure Science
(Ibn Al- Haitham) University of Baghdad in Partial Fulfillment of the
Requirements for the Degree of Master of Science in Physics*

By

Naeem Nahi Abd Ali

B.Sc Physics 1997

Supervised by

Lecturer Doctor: Enas Ahmed Jawad

2019 A.D

1441 A.H

بِسْمِ اللّٰهِ الرَّحْمٰنِ الرَّحِیْمِ

نَرْفَعُ دَرَجَاتٍ مِّنْ نَّشَأٍ

وَفَوْقَ كُلِّ ذِي عِلْمٍ

عَلِیْمٍ

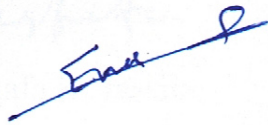
صدق الله العظيم

سورة يوسف - الآية 76

Supervisors Certification

I certify that this thesis was prepared by (NAEEM NAHI ABD ALI) under my supervision of the Physics Department, College of Education for pure Science/ Ibn Al-Haitham, University of Baghdad in partial fulfillment requirements for the Degree of Master of Science in Physics.

Signature:



Name: Dr. Enas Ahmed Jawad

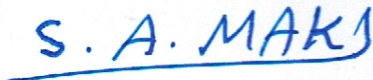
Title: Lecturer

Address: College of Education of pure Science/
Ibn Al-Haitham, University of Baghdad

Date 22/ 9 /2019

In view of the available recommendations, I forward this thesis for debate by the Examination Committee.

Signature:



Name: Dr. Samir Ata Maki


Title: Professor


Address: Chairman, Department of Physics, College of Education for pure Science/ Ibn Al-Haitham, University of Baghdad

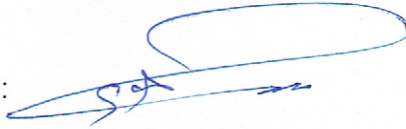
Date 23 / 9 /2019

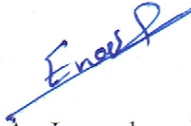
Examination Committee Certification

We certify that we have read this thesis titled "computer investigations of sputtering yields for the metals alloys (BeCu, brass, stainless –steel, and monel-400) bombarding by different ions (Ar, N₂, and O₂) at normal and oblique incidence" submitted by (NAEEM NAHI ABD ALI) and as examining committee examined the student in its content and that in our opinion, it is adequate with standard as a thesis for the Degree of Master of science in physics.


Signature: 
Name: Dr. Mustafa K. Jassim
Title: Assist. Prof.
Address: University of Baghdad
Date: 22 / 9 / 2019
(Chairman)

Signature: 
Name: Dr. Intesar H. Hashim
Title: Assist. Prof.
Address: University of Al-Mustansiriyah
Date: 22 / 9 / 2019
(Member)

Signature: 
Name: Dr. Sameera A. Ebrahiem
Title: Assist. Prof.
Address: University of Baghdad
Date: 22 / 9 / 2019
(Chairman)

Signature: 
Name: Dr. Enas A. Jawad
Title: Lecturer
Address: University of Baghdad
Date: 22 / 9 / 2019
(Member and Supervisor)

Approved by the council of the college of Education for pure sciences
Ibn-Al-Haitham / University of Baghdad.

Signature: 
Name: Dr. Hasan Ahmed Hasan
Address: / The Dean of College of Education
for Pure Science / Ibn Al-Haitham
Date: 25 / 9 / 2019

Dedication

For My loving family...

May Allah protect them

*My mother,
Brothers,
My wife,
And my daughters and sons.*

I Dedicate the Product of My Effort

Naeem

Acknowledgments

Praise and thanks to ALLAH, who gave me the health, strength, faith, and patience to get along completing this work and peace be upon the messenger of Allah, Mohammad.

I would like to express my sincere thanks and deep gratitude to my supervisor, Dr. *Enas Ahmed Jawad*, for suggesting this project, her valuable guidance and for their support and encouragement throughout the research.

I am most grateful to the Dean of the College of Education for Pure Science Ibn-AL-Haitham, and I wish to thank the head of the Physics Department and the staff of this Department.

My special thanks to my first teacher Dr. *Mustafa Kamel Jassim*, who always supports and helps me.

Naeem

Abstract

The behavior of the sputtering yield (S.Y) for metallic alloys (BeCu, Brass, Monel-400, and Stainless-Steel) which was bombarded with ions (Ar, N₂, and O₂), was studied using the TRIM (Transport of Ions in Matter) program, a program that uses the Monte Carlo algorithm to simulate the sputtering process. The selection of alloys used in this study was due to its great importance and its uses in many important applications such as precision measuring instruments and space (it is an erosion phenomenon that limits the lifetime of components used in spacecraft and satellites).

The width of the alloy used in this study is 1000Å and the number of ions is 5000 because of our results proved that any change in the number of ions leads to a slight change in the yield is not significant and the use of 5000 ion actually reduces the time of simulation.

The results showed that the theoretical study to calculate the sputtering yield of metal alloys that were bombarded by different ions (Ar, N₂, and O₂) in normal and oblique incidence depends mainly on several important parameters: ionic energy, incident angle, atomic and mass number of incident ions, mass and atomic number of target, and concentration of elements used in alloys. The results obtained for this study indicate that S.Y is directly dependent on these parameters. A slight change in the angle of the incident from the ion beam and energy leads to a significant and clear change in the sputtering yield.

Increases sputtering yield with the increasing atomic number of bombarding ions of target alloys, which are (Ar, N₂, and O₂). The Non-linear dependence of the sputtering yield on the concentrations of the elements used in the target alloys. As the results showed that a slight change in the surface binding energy (SBE) of the target (both increase and decrease) leads to a significant change in the yield of the sputtering. To illustrate the graphs between

variables, global programs such as ORIGIN8, and IGOR program were used. In addition, the results of the calculations found in the coefficients of the curves were included in the semiempirical equations of all variables.

List of Contents

Subject		Page
Abstract		I
List of contents		III
List of figures		V
List of tables		XI
List of abbreviations		XIII
Chapter One: Introduction and previous studies		
(1-1)	Introduction	1
(1-2)	Historical overview	1
(1-3)	TRIM Program	2
(1-4)	SRIM Program	3
(1-5)	The Ions	3
(1-5-1)	Argon Ion	3
(1-5-2)	Nitrogen Ion	4
(1-5-3)	Oxygen Ion	4
(1-6)	Alloys	5
(1-7)	Non – Ferrous Alloys	5
(1-8)	Alloys of Copper	6
(1-9)	Alloys of Brass	6
(1-10)	Brass Properties	6
(1-11)	Alloys of Beryllium – Copper	7
(1-12)	Stainless – Steel Alloy	8
(1-13)	Monel-400 Alloy	9
(1- 14)	Applications of Sputtering	9
(1-15)	Previous studies	10
(1-16)	The Aim of the Study	13
Chapter Tow: Sputtering Concepts and Theory		
(2-1)	Introduction	15
(2-2)	Sputtering Concepts	15
(2-3)	Mechanisms of the Sputtering Yield.	21

(2-4)	Sputtering from Compound Targets.	22
(2-5)	Results from Elastic-Collision Theory.	22
(2-6)	Basics, Concepts of Ion-Solid Interaction.	23
(2-7)	Types of Sputtering Regimes.	25
(2-8)	Sputtering Yields for Elements.	27
(2-9)	Sputtering Yields for Compounds.	29
Chapter Three: Result and Discussion		
(3-1)	Introduction	32
(3-2)	The influence of the angle of the incident ion on the sputtering yield	32
(3-2-1)	The normalized sputtering yield (NSY) vs. angle of the incident ion	43
(3-3)	The Influence Ion Energy on the Sputtering Yield	49
(3-4)	The energy for sputtering yield maxima vs. angle of the incident ion	62
(3-5)	The Effect of the Atomic Number of Ions on the sputtering yield	65
(3-6)	The effect of concentration of the elements in the alloy on the sputtering yield	68
(3-7)	Effect of the surface binding energy (SBE) on the sputtering yield	85
(3-8)	Influence of the threshold energy (E_{th}) on the sputtering yield	87
(3-9)	The Effect of the Target Atomic number on the Sputtering Yield.	90
(3-10)	The Effect of the Target Atomic Mass on the Sputtering Yield.	90
(3-11)	Conclusions	91
(3-12)	Suggestions for future work	94
References		96

LIST OF FIGURES

Figure	Title of Figure	Page
(2-1)	The interaction between the ion incident and the target.	17
(2-2)	Two dimensional diagram of a typical collision cascade	19
(2-3)	A diagram showing the possible effects of ion bombardment.	20
(2-4)	A diagram showing the process of sputtering and ion interaction with the solid surface.	24
(2-5)	Diagrams of the three sputtering regimes. (a) Single knock-on regime (b) Linear cascade regime (c) Spike regime	26
(3-1)	Incident ion angle dependence of S.Y of BeCu alloy bombard by Argon ion.	37
(3-2)	Incident ion angle dependence of S.Y of BeCu alloy bombard by Nitrogen ion.	37
(3-3)	Incident ion angle dependence of S.Y of BeCu alloy bombard by Oxygen ion.	38
(3-4)	Incident ion angle dependence of S.Y of Brass alloy bombard by Argon ion.	38
(3-5)	Incident ion angle dependence of S.Y of Brass alloy bombard by Nitrogen ion.	39
(3-6)	Incident ion angle dependence of S.Y of Brass alloy bombard by Oxygen ion.	39
(3-7)	Incident ion angle dependence of S.Y of Stainlees-Steel bombard by Argon ion.	40
(3-8)	Incident ion angle dependence of S.Y of Stainlees-Steel alloy bombard by Nitrogen ion.	40
(3-9)	Incident ion angle dependence of S.Y of Stainlees-Steel alloy bombard by Oxygen ion.	41
(3-10)	Incident ion angle dependence of S.Y of Monel-400 alloy bombard by Argon ion.	41

(3-11)	Incident ion angle dependence of S.Y of Monel-400 alloy bombard by Nitrogen ion.	42
(3-12)	Incident ion angle dependence of S.Y of Monel-400 alloy bombard by Oxygen ion.	42
(3-13)	(NSY) vs. of the angle of the ion incidence target of BeCu alloy bombarded by Argon ion.	43
(3-14)	(NSY) vs. of the angle of the ion incidence target of BeCu alloy bombarded by Nitrogen ion.	44
(3-15)	(NSY) vs. of the angle of the ion incidence target of BeCu alloy bombarded by ion Nitrogen.	44
(3-16)	The (NSY) vs. of incident ion angle, target of Brass alloy bombarded by Argon ion.	45
(3-17)	The (NSY) vs, of incident ion angle, target of Brass alloy bombarded by Nitrogen ion.	45
(3-18)	The normalized sputtering yield vs. of incident ion angle, target of Brass alloy bombarded by Oxygen ion.	46
(3-19)	The normalized sputtering yield vs. of incident ion angle, Stainless-Steel alloy bombarded by Argon ion.	46
(3-20)	The normalized sputtering yield vs. of incident ion angle, Stainless-Steel alloy bombarded by Nitrogen ion.	47
(3-21)	(NSY) vs. of the angle, of Stainless-Steel alloy bombarded by Oxygen ion.	47
(3-22)	(NSY) vs. of the angle, of Monel-400 alloy bombarded by Argon ion.	48
(3-23)	(NSY) vs. of the angle, of Monel alloy-400 bombarded by Nitrogen ion.	48
(3-24)	(NSY) vs. of the angle, of Monel alloy-400 bombarded by Oxygen ion.	49
(3-25)	Energy dependence of S.Y of the incident for the bombarded by Ar^+ on BeCu alloy.	56
(3-26)	Energy dependence of S.Y of incident Nitrogen ions on BeCu alloy.	57
(3-27)	Energy dependence of S.Y of incident Oxygen ions on BeCu	57

	alloy.	
(3-28)	Energy dependence of S.Y of incident Argon ions on Brass alloy.	58
(3-29)	Energy dependence of S.Y of incident Nitrogen ions on Brass alloy.	58
(3-30)	Energy dependence of S.Y of the incident for the bombarded by Oxygen ion on Brass alloy.	59
(3-31)	Energy dependence of S.Y of incident Argon ions on Stainless-Steel alloy.	59
(3-32)	Energy dependence of S.Y of incident Nitrogen ions on Stainless-Steel alloy.	60
(3-33)	Energy dependence of S.Y of incident Oxygen ions on Stainless-Steel alloy.	60
(3-34)	Energy dependence of S.Y of incident Argon ions on Monel-400 alloy.	61
(3-35)	Energy dependence of S.Y of incident Nitrogen ions on the Monel-400 alloy.	61
(3-36)	Energy dependence of S.Y of incident Oxygen ions on the Monel-400 alloy.	62
(3-37)	Ion energy for S.Y maxima vs. angle. (BeCu alloy)	63
(3-38)	Ion energy for E (S. Y_m) vs. angle. (Brass alloy)	63
(3-39)	Ion energy for E (S. Y_m) vs. angle. (Stainless-Steel alloy)	64
(3-40)	Ion energy for E (S. Y_m) vs. angle. (Monel-400 alloy)	64
(3-41)	S.Y vs. atomic number of ions (Ar, N_2 , O_2) that bombardment the BeCu alloy (Be 50%, Cu 50%).	66
(3-42)	S.Y vs. atomic number of ions (Ar, N_2 , O_2) that bombardment the Brass alloy (Zn 33%, Cu 34%, Pb 33%).	66
(3-43)	S.Y vs. atomic number of ions (Ar, N_2 , O_2) that bombardment the Stainless - Steel alloy (Cr 33%, Fe 34%, Ni 33%).	67
(3-44)	S.Y vs. atomic number of ions (Ar, N_2 , O_2) that bombardment the Monel - 400 alloy (Mn 25%, Fe 25%, Ni	67

	25%, Cu 25%).	
(3-45)	The S.Y as a function of the incident Angle (different concentration in BeCu alloy), Bombarded by Ar^+ .	68
(3-46)	The S.Y as a function of the incident Angle (different concentration in BeCu alloy), Bombarded by Nitrogen ion.	69
(3-47)	The S.Y as a function of the incident Angle (different concentration in BeCu alloy), Bombarded by Oxygen ion.	69
(3-48)	The S.Y as a function of ion energy (for different concentrations in the BeCu alloy). Bombarded by Ar^+ .	70
(3-49)	The S.Y as a function of ion energy (for different concentrations in the BeCu alloy). Bombarded by Nitrogen ion.	70
(3-50)	The S.Y as a function of ion energy (for different concentrations in the BeCu alloy). Bombarded by Oxygen ion.	71
(3-51)	The SY as a function of the incident Angle (different concentration in Brass alloy), Bombarded by Ar^+ .	71
(3-52)	The SY as a function of the incident Angle (different concentration in Brass alloy), Bombarded by Nitrogen ion.	72
(3-53)	The SY as a function of the incident Angle (different concentration in Brass alloy), Bombarded by Oxygen ion.	72
(3-54)	The SY as a function of ion energy (different concentrations in the Brass alloy). Bombarded by Ar^+ .	73
(3-55)	The SY as a function of ion energy (different concentrations in the Brass alloy). Bombarded by Nitrogen ion.	73
(3-56)	The SY as a function of ion energy (different concentrations in the Brass alloy). Bombarded by Oxygen ion.	74
(3-57)	The SY as a function of the incident Angle (different concentration in the Stainless-Steel alloy), Bombarded by Ar^+ .	74
(3-58)	The SY as a function of the incident Angle (different concentration in the Stainless-Steel alloy), Bombarded by Nitrogen ion.	75
(3-59)	The S.Y as a function of the incident Angle (different concentration in the Stainless-Steel alloy), Bombarded by Oxygen ion.	75

(3-60)	The S.Y as a function of ion energy (different concentrations in the Stainless-Steel alloy). Bombarded by Argon ion.	76
(3-61)	The S.Y as a function of ion energy (different concentrations in the Stainless-Steel alloy). Bombarded by Nitrogen ion.	76
(3-62)	The S.Y as a function of ion energy (different concentrations in the Stainless-Steel alloy). Bombarded by Oxygen ion.	77
(3-63)	The S.Y as a function of the incident Angle (different concentration in the Monel-400 alloy), Bombarded by Argon ion.	77
(3-64)	The S.Y as a function of the incident Angle (different concentration in the Monel-400 alloy), Bombarded by Nitrogen ion.	78
(3-65)	The S.Y as a function of the incident Angle (different concentration in the Monel-400 alloy), Bombarded by Oxygen.	78
(3-66)	The S.Y as a function of ion energy (different concentrations in the Monel-400 alloy). Bombarded by Argon ion.	79
(3-67)	The S.Y as a function of ion energy (different concentrations in the Monel-400 alloy). Bombarded by Nitrogen ion.	79
(3-68)	The S.Y as a function of ion energy (different concentrations in the Monel-400 alloy). Bombarded by Oxygen ion.	80
(3-69)	Energy dependence of sputtering yields of Cu, Be, and BeCu under Ar ⁺ bombardment.	81
(3-70)	Energy dependence of sputtering yields of Cu, Zn, Pb, and Brass Alloy under Ar ⁺ bombardment.	81
(3-71)	Energy dependence of sputtering yields of Cr, Fe, Ni, and Stainless - Steel Alloy under Ar ⁺ bombardment.	82
(3-72)	Energy dependence of sputtering yields of Cu, Fe, Ni, Mn, and Monel - 400 Alloy under Ar ⁺ bombardment.	82
(3-73)	Sputtering yields dependence of Angle incident of Cu, Be, and BeCu Alloy under Ar ⁺ bombardment.	83
(3-74)	Sputtering yields dependence of Angle incident of Cu, Zn, Pb, and Brass Alloy under Ar ⁺ bombardment.	83
(3-75)	Sputtering yields dependence of Angle incident of Cr, Ni, Fe,	84

	and Stainless-Steel Alloy under Ar ⁺ bombardment.	
(3-76)	Sputtering yields dependence of Angle incident of Cu, Ni, Fe, Mn, and Monel-400 Alloy under Ar ⁺ bombardment.	84
(3-77)	Sputtering yield vs. surface binding energy of target material (Be, Cr, Mn, Fe, Ni, Cu, Zn, Pb) bombarded by Ar ⁺ .	86
(3-78)	Sputtering yield vs. (SBE) of the target material (Be, Cr, Mn, Fe, Ni, Cu, Zn, Pb) bombarded by Nitrogen.	86
(3-79)	Sputtering yield vs. (SBE) of the target material (Be, Cr, Mn, Fe, Ni, Cu, Zn, Pb) bombarded by Oxygen ions	87
(3-80)	Sputtering yield vs. sputtering threshold energy for alloy elements BeCu (Be, Cr, Mn, Fe, Ni, Cu, Zn, Pb) target materials bombarded by (Ar, N ₂ , and O ₂) ions.	88
(3-81)	Sputtering yield vs. sputtering threshold energy for alloy elements Brass (Be, Cr, Mn, Fe, Ni, Cu, Zn, Pb) target materials bombarded by (Ar, N ₂ , and O ₂) ions.	88
(3-82)	Sputtering yield vs. sputtering threshold energy for alloy elements Stainless-Steel (Be, Cr, Mn, Fe, Ni, Cu, Zn, Pb) target materials bombarded by (Ar, N ₂ , and O ₂)	89
(3-83)	Sputtering yield vs. sputtering threshold energy for alloy elements Monel-400 (Be, Cr, Mn, Fe, Ni, Cu, Zn, Pb) target materials bombarded by (Ar, N ₂ , and O ₂)	89
(3-84)	Sputtering yield vs. atomic number target for (Be, Cr, Mn, Fe, Ni, Cu, Zn, and Pb) bombarded by (Ar, N ₂ , and O ₂) ions	90
(3-85)	Sputtering yield vs. atomic Mass target for (Be, Cr, Mn, Fe, Ni, Cu, Zn, and Pb) bombarded by (Ar, N ₂ , and O ₂)	91

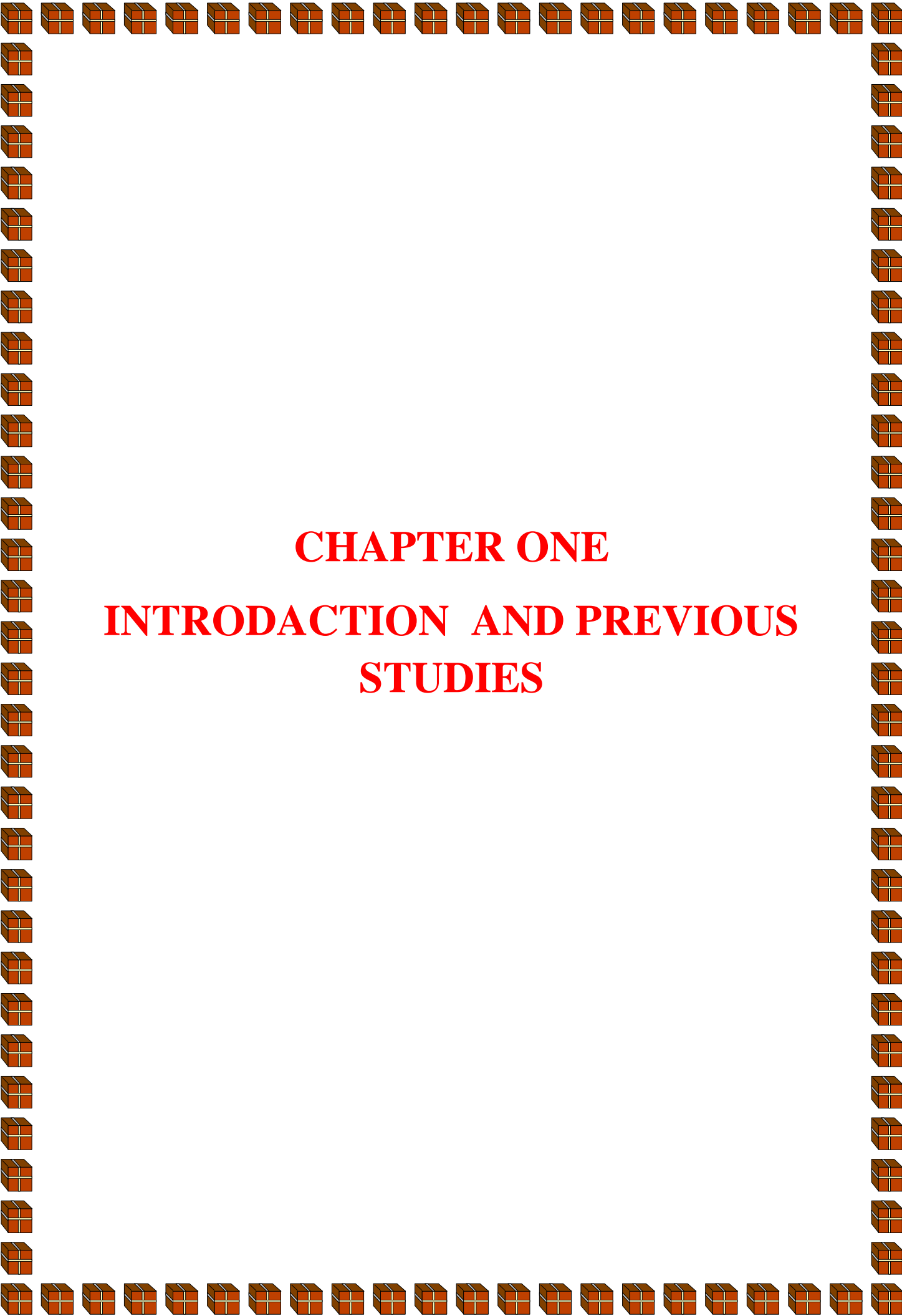
List of tables

Table	Title	Page
2-1	Comparison table between sputtering systems.	26
3-1	Parameters of equation (3-1) plotted in Figure (3-1) from Argon ions When you bombard BeCu alloy.	33
3-2	Parameters of equation (3-1) plotted in Figure (3-2) from Nitrogen ions When you bombard BeCu alloy.	33
3-3	Parameters of equation (3-1) plotted in Figure (3-3) from Oxygen ions When you bombard BeCu alloy.	34
3-4	Parameters of equation (3-1) plotted in Figure (3-4) from Argon ions When you bombard Brass alloy.	34
3-5	Parameters of equation (3-1) plotted in Figure (3-5) from Nitrogen ions When you bombard Brass alloy.	34
3-6	Parameters of equation (3-1) plotted in Figure (3-6) from Oxygen ions When you bombard Brass alloy.	34
3-7	Parameters of the equation (3-1) Argon ions bombarding of Stainless - steel alloy target, shown in figure (3-7).	35
3-8	Parameters of the equation (3-1) Nitrogen ions bombarding of Stainless - steel alloy target, shown in figure (3-8).	35
3-9	Parameters of the equation (3-1) Oxygen ions bombarding of Stainless - steel alloy target, shown in figure (3-9).	35
3-10	Parameters of the equation (3-1) Argon ions bombarding of (Mone1-400) alloy target, shown in figure (3-10).	36
3-11	Parameters of the equation (3-1) Nitrogen ions bombarding of Monel - 400 alloy target, shown in figure (3-11).	36
3-12	Parameters of the equation (3-1) plotted from Oxygen ions bombarding of Mone1-400 alloy target, shown in figure (3-12)	36
3-13	Parameters of the equation (3-2) plotted from Argon ions bombarding of BeCu alloy target, shown in figure (3-25).	50
3-14	Parameters of the equation (3-2) plotted from Nitrogen ions bombarding of BeCu alloy target, shown in figure (3-26).	51
3-15	Parameters of the equation (3-2) plotted from Oxygen ions	51

	bombarding of BeCu alloy target, shown in figure (3-27).	
3-16	Parameters of the equation (3-2) plotted from Argon ions bombarding of brass alloy target, shown in figure (3-28).	52
3-17	Parameters of the equation (3-2) plotted from Nitrogen ions bombarding of brass alloy target, shown in figure (3-29).	52
3-18	Parameters of the equation (3-2) plotted from Oxygen ions bombarding of brass alloy target, shown in figure (3-30).	53
3-19	Parameters of the equation (3-2) plotted from Argon ions bombarding of Stainless-Steel alloy target, shown in figure (3-31).	53
3-20	Parameters of the equation (3-2) plotted from Nitrogen ions bombarding of Stainless-Steel alloy target, shown in figure (3-32).	54
3-21	Parameters of the equation (3-2) plotted from Oxygen ions bombarding of Stainless-Steel alloy target, shown in figure (3-33).	54
3-22	Parameters of the equation (3-2) plotted from Argon ions bombarding of Monel-400 alloy target, shown in figure (3-34).	55
3-23	Parameters of the equation (3-2) plotted from Nitrogen ions bombarding of Monel-400 alloy target, shown in figure (3-35).	55
3-24	Parameters of the equation (3-2) plotted from Oxygen ions bombarding of Monel-400 alloy target, shown in figure (3-36).	56
3-25	Parameters for equation (3 -3) fitting for sputtering yield as a function of atomic number of incident ion (Z), bombarding of (Ar, N ₂ and O ₂) ion, target, in (BeCu, Brass, Stainless-Steel, Monel-400) alloy are shown in figures (3-41) to (3 – 44).	65
3-26	shows the elements involved in these alloys (targets).	85
3-27	Max. Sputter yields vs. Energy for Argon ion.	93
3-28	Max. Sputter yields vs. Energy for Nitrogen ion.	93
3-29	Max. Sputter yields vs. Energy for Oxygen ion.	93
3-30	Max. Sputter yields vs. Incident Angle for Argon ion.	94
3-31	Max. Sputter yields vs. Incident Angle for Nitrogen ion.	94
3-32	Max. Sputter yields vs. Incident Angle for Oxygen ion.	94

List of abbreviations

Symbol	Description
TRIM	Transport of Ions in Matter.
SRIM	Stopping and Range of Ions in Matter.
BeCu	Beryllium – Copper
S.Y	Sputtering Yield.
PKAs	Primary knock-on Atoms or Primary Recoils.
SBE	Surface Binding Energy.
NSY	Normalized Sputtering Yield.
MCs	Monte Carlo Eimulates.
ppmv	Part of the Million.
U_d	Lattice Displacement Energy.
U_b	Surface Binding Energy.
E_{th}	The Sputtering Threshold Energy.
M_1, M_2	Atomic Mass of Ion and Target Respectively.
Z_1, Z_2	Atomic Number of Ion and Target Respectively.
$d\sigma$	Cross Section.
Ze	Nuclear Charge.
T_m	Maximum Energy Transfer.
T	The Energy Transferred to the Target Atom.
$S_n(E)$	Nuclear Stopping Cross Section per Atom.
e	Electronic Charge.
ϵ_0	Permittivity of a Vacuum.
a_0	Bohr Radius.
ρ	The Target Density.
N	Avogadro's Number.
r	The Average Interatomic Spacing.
E	Energy of the Incident Particle.
γ	Energy Transfer Factor.
$Se(\epsilon)$	The Electronic Stopping Power.
ϵ	The Reduced Energy.
KE	Kinetic Energy



CHAPTER ONE
INTRODACTION AND PREVIOUS
STUDIES

(1-1) Introduction

This chapter contains the sputter definition. It also provides a brief history of sputtering, and its applications have been reviewed. The SRIM / TRIM program used in this study was explained. Then reviewed the alloys used in the thesis, its components, characteristics, and the uses. Finally, a brief overview of some of the previous studies and current studies.

(1-2) Historical overview

The sputtering can be stated as the physical removal of atoms from the surface by the bombardment of energetic particles. The term 'sputtering' was possibly derived from Thompson, who used the word 'spluttering' to describe the wear of a cathode in a vacuum tube [1]. In 1852 a description of the use of wire as a source of sputtering to be deposited on the surface was published [2].

In 1926, A. Von Hippel proposed a thermal evaporative sputter theory, where it was thought that when a reacts high energy ion with the target, a localized area of extremely high temperatures will lead to the evaporation of the target material (creating the source of sputtered particles) [3].

In the middle of the 20th century, Sigmund, Thompson, and Lindhard separately refine the theories of momentum transfer more. Sigmund's model presented the standard sputtering model that is accepted to this today. Many research papers and wide-ranging applications of technologies and concepts participator in sputtering yield studies have been published on the subject. One of the first studies that have been developed is the phenomenon of sputtering because the uses extend to fields far away from that in which sputtering phenomena were first studies and developed (e.g. found an application of sputtering to blood cells, to remove surface layers of red blood cells [4].

Many of the Monte Carlo computer simulations have been produced in recent years to emulate the sputtering process, most notably SRIM / TRIM,

developed by Ziegler and Biersack in the early 1980s. Yamamura, Matsunami, Eckstein, and Bodhansky developed a comprehensive experimental formula with any ion/target combination [3].

(1-3) TRIM Program

The TRIM Program name comes from the first letters of the phrase (The **TR**ansport of **I**ons in **M**atter) 2013 is the portion of the SRIM 2013 (Stopping and Range of Ions in Matter) software package designed by Ziegler and Biersack. SRIM 2013 set of software that calculates the stopping range of ions in this matter [5]. TRIM software simulates ion bombardment with specified target and ion properties. The user sets the target and ion elements, the number of incoming ions, incidence energy, and incidence angle. TRIM was developed to transfer ions in the matter with the primary objective of providing a computer-efficient program that still maintains a high degree of accuracy for simulating different surfaces [6].

Written in the early 1980 by Biersack and Eckstein, TRIM was the first computer simulation in the TRIM family to follow the paths and collisions of the recoil atoms as well as the projectiles. The acronym stands for ‘Transport of ions in matter’ as it was developed to deal primarily with sputtering and other surface effects [7].

The theoretical and semi-empirical calculations provide valuable analytical terms that describe the useful physical mechanisms related to sputtering and the corresponding dependencies of several variables. However, these calculations also show that the solutions are more than often complicated and simplified assumptions have to be made. So, many software packages have been developed which simulate the evolution of the collision cascade inside the target.

(1-4) SRIM program

The version used in this exercise, SRIM 2013, is the latest in a long line of ion implantation Monte-Carlo simulations beginning with TRIM85 in 1985. This family of programs is also based off TRIM, the original simulation that laid the grounds for TRIM, but was developed in a slightly different manner. The code is credited to Ziegler, et.al with contributions from many others [7].

(1 – 5) The Ions

An ion is an atom or molecule that has a net electrical charge. Since the charge of the electron (considered negative by convention) is equal and opposite to that of the proton (considered positive by convention), the net charge of an ion is non-zero due to its total number of electrons being unequal to its total number of protons. A cation is a positively charged ion, with fewer electrons than protons, while an anion is negatively charged, with more electrons than protons. Because of their opposite electric charges, cations and anions attract each other and readily form ionic compounds [8].

(1 – 5 – 1) Argon Ion

Argon is a chemical element with the symbol Ar and atomic number 18. It is in group 18 of the periodic table and is a noble gas. Electron configuration [Ne] $3s^2 3p^6$. Argon is the third-most abundant gas in the Earth's atmosphere, at 0.934% (9340 ppmv). It is more than twice as abundant as water vapor (which averages about 4000 ppmv), but, varies greatly 23 times as abundant as carbon dioxide (400 ppmv), and more than 500 times as abundant as neon (18 ppmv). Argon is the most abundant noble gas in Earth's crust, comprising 0.00015% of the crust.

Argon ions are then formed, and their amount is continually increased by collisions of free electrons with neutral Argon atoms up to an equilibrium situation where a steady-state plasma is formed [9].

(1 – 5 – 2) Nitrogen Ion

Nitrogen is the chemical element with the symbol N and atomic number 7. A nitrogen atom has seven electrons. In the ground state, they are arranged in the electron configuration $1s^2 2s^2 2p^3$. Nitrogen is classified as non-metallic, and in normal conditions of pressure and temperature, N_2 is a diatomic gas, colorless, tasteless and odorless. Nitrogen has two stable isotopes: ^{14}N and ^{15}N . The first is much more common, making up 99.634% of natural nitrogen, and the second (which is slightly heavier) makes up the remaining 0.366%.

(1 – 5 – 3) Oxygen Ion

Oxygen is the $[He] 2s^2 2p^4$ chemical element with the symbol O and atomic number 8, meaning its nucleus has 8 protons. The number of neutrons varies according to the isotope: the stable isotopes have 8, 9, or 10 neutrons. Oxygen is a member of the chalcogen group on the periodic table, a highly reactive nonmetal, and an oxidizing agent that readily forms oxides with most elements as well as with other compounds. By the mass, oxygen is the third-most abundant element in the universe, after hydrogen and helium. At standard temperature and pressure, two atoms of the element bind to form dioxygen, a colorless and odorless diatomic gas with the formula O_2 . Diatomic oxygen gas constitutes 20.8% of the Earth's atmosphere. As compounds, including oxides, the element makes up almost half of the Earth's crust [10].

(1-6) Alloys

An alloy is a combination of a metal with at least one other metal or nonmetal. The combination must be part of a solid solution, a compound, or a mixture with another metal or nonmetal in order for it to be considered an alloy. The most common way to combine metals into an alloy is by melting them, mixing them together, and then allowing them to solidify and cool back to room temperature.

The mineral material is widespread of two types - ferrous and non-ferrous materials. This classification mainly depends on the number of materials used worldwide. They are classified into [11]:

1. Ferro alloys: Those in which iron is the main element, include steel and cast iron.
2. Non – ferrous alloys: These alloys do not contain iron as a major component, e.g., alloys (zinc, nickel, aluminium, and lead).

(1- 7) Non – Ferrous alloys

Non-ferrous alloys that do not contain iron (ferrite) in appreciable amounts. Generally, costlier than ferrous metals, non-ferrous metals are used because of desirable properties such as low weight (e.g. Aluminium), higher conductivity (e.g. Copper), non-magnetic property or resistance to corrosion (e.g. Zinc) [12].

These alloys contain (Al, Pb, Cu, Zn) as the principal alloying constituent. The properties are [11]:

- They have good corrosion resistance and low density.
- They have high electrical and thermal conductivity.
- They are easily castable and can be cold worked.

- They have a low coefficient of friction and can be fabricated easily.
- Most of the alloys have wide applications in the engineering fields.
- They possess attractive colors, softness, and lower melting points as compared to ferrous alloys.

(1 – 8) Alloys of Copper

These alloys contain copper as the principal constituent (brasses and bronzes). The copper metal is highly resistant to corrosion. It is ductile, malleable, having moderate to high hardness and strength. It is used for:

- It is used for making marine fittings, condenser tubes, valves.
- It is used for making springs and chains.

(1-9) Alloys of Brass

Brass is an alloy made primarily of copper and zinc. The proportions of the copper and zinc are varied to yield many different kinds of brass. Basic brass is 62% copper and 35% zinc. However, the amount of copper may range from 55% to 95% by weight, with the amount of zinc varying from 5% to 40%. Lead is commonly added to the brass at a concentration of around 3%. The lead addition improves the machinability of brass. However, significant lead leaching often occurs, even in brass that contains a relatively low overall concentration of lead. Uses of brass include musical instruments, firearm cartridge casing, radiators, architectural trim, pipes and tubing, screws, and decorative items [11].

(1 – 10) Brass Properties

- Brass often has a bright gold appearance, however, it can also be reddish-gold or silvery-white. A higher percentage of copper yields a rosy tone, while more zinc makes the alloy appear silver.

- Brass has higher malleability than either bronze or zinc.
- Brass has desirable acoustic properties appropriate for use in musical instruments.
- The metal exhibits low friction.
- Brass is a soft metal that may be used in cases when a low chance of sparking is necessary.
- The alloy has a relatively low melting point.
- It's a good conductor of heat.
- Brass resists corrosion.
- Brass is easy to cast.
- Brass is not ferromagnetic. Among other things, this makes it easier to separate from other metals for recycling.

(1-11) Alloys of Beryllium - Copper

Beryllium - Copper high strength and Copper 98.1% based alloys with the addition of beryllium (0.4 to 2%) with about (0.3 to 2.7%) of other alloying elements such as (Ni, Co, and Fe or Pb) The Beryllium Copper alloys are the most versatile of all copper alloys. They combine a wide range of properties that make alloys ideal materials to meet the exacting requirements of many products demanding high specifications. The Beryllium copper alloys offer a wide combination of mechanical and electrical properties, combining with excellent performance which is unique for copper alloys. The mechanical strength achieved after simple heat treatment, at low temperature, ranks highest in all the copper-based alloys, and combined with a high electrical conductivity outperforms any bronze alloys. Exhibit a wide range of desired properties such as high fatigue strength, and abrasion resistance. It is also non-magnetic and non-sparking. It has properties [11].

- It has good resistance to corrosion.
- It has good conductivity.
- It is used in making electrical switch.

(1-12) Stainless – Steel alloy

Stainless steel in all environments is highly corrosion resistant. The basic alloy element is chromium, with a concentration of at least 11% chromium element. Chromium produces a thin layer of oxide on the surface of the steel known as the 'passive layer'. This prevents any further corrosion of the surface. Increasing the amount of Chromium gives an increased resistance to corrosion. There are numerous grades of stainless steel with varying chromium and molybdenum contents to suit the environment the alloy must endure. Resistance to corrosion and staining, low maintenance, and familiar luster make stainless steel an ideal material for many applications where both the strength of steel and corrosion resistance are required. Resistance to corrosion can also be enhanced by adding element Ni and element Mo [11].

Stainless steel is rolled into sheets, plates, bars, wire, and tubing to be used in cookware, cutlery, surgical instruments, major appliances; construction material in large buildings, industrial equipment (for example, in paper mills, chemical plants, water treatment); and storage tanks and tankers for chemicals and food products (for example, chemical tankers and road tankers). Corrosion resistance, the ease with which it can be steam cleaned and sterilized, and unnecessary need for surface coatings have also influenced the use of stainless steel in commercial kitchens and food processing plants [13].

(1-13) Monel-400 alloy

Monel alloy-400 is a collection of the most common nickel-copper alloys. It consists primarily of nickel (from 52 - 67%) copper, with low amounts of the element (Fe, Mn, C, and Si). It has great corrosion resistance. Because both Ni and Cu are dissoluble in all respects, it is a one-phase alloy. Compared to steel, it is very hard to manufacture a Monel machine because it works with great force. The Monel- 400 is usually much more expensive than stainless- steel.

At sub-zero temperatures, it retains excellent mechanical properties. Increased strength and stiffness with a slight loss of pliancy and shock resistance. The Monel-400 is also resistant to corrosion and corrosion in most fresh and industrial waters. Therefore, they are widely used in marine engineering, chemical and hydrocarbon treatment equipment, pumps, valves, shafts, and heat exchangers. Safety wires are used in aircraft maintenance to ensure that fasteners cannot be undone, usually in high-temperature areas; stainless wires are used in other areas for economic purposes [14].

(1- 14) Applications of Sputtering

Currently, sputtering processes are involved in many important fields, include [15,16,17,18].

- High energy physics, manufacturing, and space science/applications.
- Creation of surface property changing, thin-film coatings where sputtered particles are used to coat other materials.
- Thin-film coatings are used heavily in the semiconductor, optical glass, and architectural glass industries.
- Many consumer products today are coated with sputtered atoms (e.g. decorative jewelry coatings, eyewear lenses).

- Sputtering is also used in surface preparation to remove contaminants and polishing.
- The deposition of thin films on a substrate is one of the most useful applications of sputtering.
- Sputtering is also used to clean and modify the micro-surfaces.
- In microscopy/spectroscopy applications, a specimen's surface can be sputtered and the resulting sputtered particle masses can be identified.
- In fusion research, the walls of reactors are constantly sputtered by very high energy neutral atoms and neutrons have also been identified as an important process high energy.
- Solar particle-induced sputtering on astronomical bodies that lack significant atmospheres (e.g. the moon).

Sputtering is both a nuisance to scientific apparatus and an important industrial too. Besides destroying the ion thruster hardware, sputtering damages in electron microscopes and membranes and targets in particle accelerators [12].

(1-15) Previous studies

In 1960: Nils Laegreid and G. K. Wehner were measured the sputtering yield of the targets of the polycrystalline metal and semiconductors under normal bombardment Ar^+ and Ne^+ ion in range the energy from 50 to 600 eV [19].

In 1976: P. K. Hafft. In particular, the physical model was offered to describe some sputtering sides of alloy targets. Expressions were developed for the partial yield of dual systems in the expression of initial sputtering

average, surface binding energy, and the stoichiometry concentrations [20].

In 1977: Z. L. Liao and et.al. Artificial changes in binary alloys and compounds have been observed as an outcome of noble gases sputtering in the energy range (20-80) keV [21].

In 1979: Peter Sigmund was studied the recoil planting and the composition of the ion beam surface change in the targets of the alloys and compounds. Recoil implantation of alloys leads to distinctly different changes in the structure after the low and high Ar⁺ bombardment [22].

In 1980: T. okutani, and et.al had investigated the changes that occur in the surface compositions of (Copper and Nickel) alloy under 3 keV Ar⁺ bombardment [23]4.

In 1981: G. Betz and el.at. investigate the surface composition in binary alloys, when bombarded with ion. It generally enriches one component surface where the energy of the bombarding ions Neon, Argon or Xenon is changed from (0.5 - 5) keV [24].

In 1981: L. Rivaud and et.al have the effect of low energies (200-3000 eV) was investigated using an argon ion to bombardment a target of Oversaturation copper in alloys. The results were always in the Sputtering this is done by using scanning transmission electron microscopy and Auger electron spectroscopy [25].

In 1981: M. P. Seah. An analysis of the published groups of the Sputtering yield of the pure element is provided using (500 to 1000) eV Argon ions to predict data for elements that do not contain measurements. [26].

In 1982: Yamamura, and et.al give Matsunami's experimental formula in theoretical investigations of sputtering yield. and propose a new

experimental formula. Use for several ions (D, H, He, Ne, Ar) and targets (Be, Cu, Ni, Fe, Au) [27].

In 1985: Ri - Sheng LI, and et.al, were studied the alloys (gold and copper) ion bombed by argon with ion energy (1 keV). The energy dependence was studied for surface composition changes [28].

In 1995: K.W. Pierson a. I., and et.al. The study of obtaining the sputtering yield of Alloys (Silver/Copper) by bombardment from the low-energy argon ion [29].

In 1998: M. Kustener and W. Eckstein, et al. have studied the angular dependence of the S.Y of rough beryllium element surfaces [30].

In 2003: W. Eckstein and R. Preuss. Energy formulas and angular dependence are proposed for sputtering yield. Although they are experimental, they provide the Best description of the S.Y datum, especially close to the minimum energy for several ions (T, He, N, Ne, Ar) and targets (Be, C, Ni) [31].

In 2004: M. P. Seah, and et.al, a semi-experimental formula was developed based on the of Matsunami, Tawara, Yamamura, and Other from an analysis of the Sputtering yield data from 28 single-component solid materials in energy (250-10000) eV [32].

In 2005: T.A. Cassidy and R.E. Johnson. The expulsion of atoms and molecules into a variety of target surfaces was studied due to the flow of biomolecules and radiation kinds [33].

In 2005: M. P. Seah., and et.al, a historical analysis of the 28 mono-elemental argon ion in the energy range from (250 to 10000) eV has been

analyzed to develop an improved semi-experimental formula based on the Matsunami and et.al formulations [34].

In 2007: V. I. Bachurin, etal, consider the interaction of ions of Ar⁺ and nitrogen to the surface of SiO₂ to measure the Sputtering yield [35].

In 2015: Huda M. Tawfeek, et.al, sputtering yield conduct of target bombarded by Ar⁺ beam was studied through the reduction of TRIM simulation data [36].

In 2018: H. Gu, et. al, Monte Carlo calculations of the atmospheric sputtering yields on Titan [37].

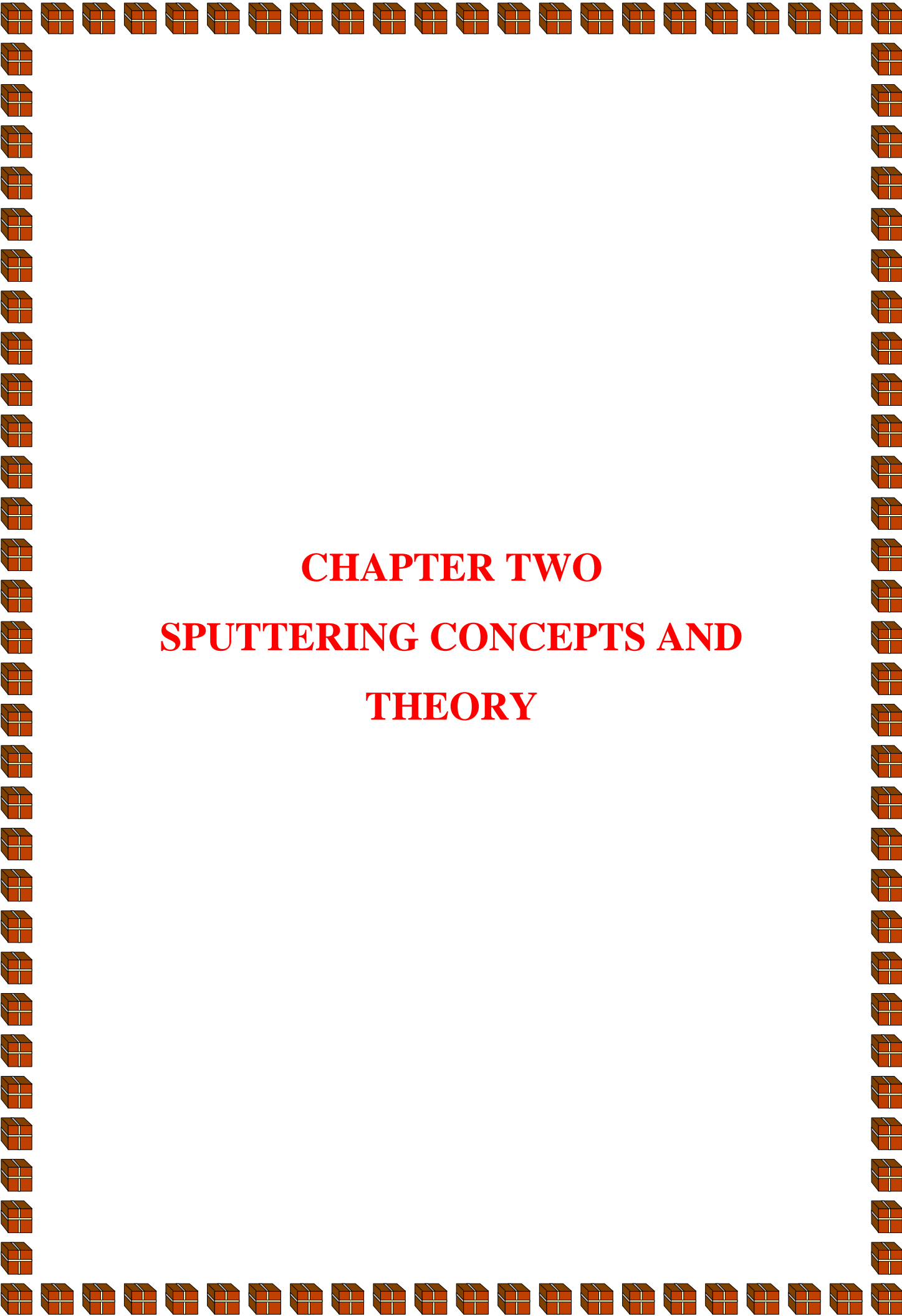
(1- 16) The aim of the study

In this study, the interaction of three ions was verified (Ar, N₂, and O₂) with four alloys (BeCu, Brass, Stainless – Steel, Monel – 400) using the TRIM program.

An understanding of the sputtering behavior of alloys targets is of primary importance for several reasons.

- i) Varying composition of the target provides an extra dimension to fundamental sputtering studies that may yield a clue to the understanding of the material dependence of the S.Y.
- ii) Applications of sputtering in the production and analysis of thin films almost invariably deal with multiple component targets.

Through our study of the amount of sputtering yield in alloys (BeCu, Brass, Stainless – Steel, Monel - 400) targeted by ions (Ar, N₂, and O₂) most of which are in the atmosphere, which can be exposed to metallic materials. The alloys where the sputtering yield is low are determined. After completing the current study, an alloy can be suggested where there is as little sputtering as possible in order to reduce the economic damage caused by sputtering, including scientific and industrial devices.



CHAPTER TWO
SPUTTERING CONCEPTS AND
THEORY

1. (2-1) Introduction

In this chapter, we will deal with the physics of sputtering and the basic concepts of ion interaction with the solid surface and the terms that describe the sputtering and provides a basic discussion of the theory of sputtering systems. The models presented will analyze total yields at normal incidence, total yields at oblique incidences.

(2-2) Sputtering Concepts

If an energetic ion collides with a target surface and has at least a certain amount of kinetic energy, atoms will be ejected from the target surface. This removed process of surface atoms by energetic ions is called the sputtering yield. Quantified sputtering yield S.Y the mean rate, number of atoms removed per incident particle S.Y as stated in Eq. (2-1) [39,40].

$$S.Y = \frac{\text{atoms removed}}{\text{incident particle}} \dots \dots \dots (2 - 1)$$

As the definition of sputtering yield, it is assumed that the number of atoms, removed the surface is proportional to the number of particles in the incident beam while holding all other factors constant. The S.Y depends heavily on the kinetic energy (KE) of the bombarding ion. Sputtering yield increases with increasing ion energy, ion incidence angle, ion mass, and target material properties. This process occurs for all materials for incident particle energies that exceed certain threshold energy. The sputtering threshold, E_{th} , is known as the minimum kinetic energy of the under ion bombardment for sputtering to occur [41].

Much of the early effort in sputtering theory dealt with the expected sputtering energy threshold. In general, the definition of threshold energy for

sputtering is a sensitive task, usually of little value. In fact, since sputtering yield is a statistical variable, fluctuations must be calculated once the yield is small sputtering begins at the energy limit, which depends on the efficiency of moving the momentum to the target. This depends on the mass match. It also depends on the Surface Binding Energy (SBE) of the atoms in the target.

The ejection of the atom from solid surfaces to active ion bombardment is called sputtering. Sputtering elements have been widely investigated in the past years [42]. However, it has been found that the sample that occurs sputtering as alloys and compounds often changes the composition of the surface [43,44]. So, the understanding of the process of sputtering of alloys is very necessary for quantitative analysis. The typical sputtering event begins when active particles collide with the target solid surface. Several possible processes may occur [45].

If the bombarding ion transfers kinetic energy (KE) more than the lattice displacement energy, U_d , of the target atoms, surface damage takes place. (U_d) can be defined as is the energy a target atom needs to move more than one atomic distance from its original position. If the atoms of the lattice move to new lattice sites, surface migration and surface damage occur [46]. When a target atom recoils to a new position it loses a certain amount of energy called the lattice binding energy [39].

Physically, referred to the sputtering process, as the process of collision taken into account transmission of kinetic energy and momentum of bombarding ions to target atoms, if (KE) enough to overcome the surface binding energy (SBE) sputtering occurs from the surface atoms Target.

When the ion beam collides with the target, they lose energy by two mechanisms: the nuclear elastic collision, and the electronic non-elastic collisions.

Depending on the energy, these ions can, recoil directly or they can be reflected from the surface after a series of cascaded collisions. or they could be in a rest state in the last of the eventual, where implantation in the target at a certain depth within the target. As the collision is an inelastic collision, therefore will lose ions a large amount of energy become at the end electrically neutral, as can that eject secondary electrons. As a result, the collision Occur Inelastic scattering lead produce phonons [44].

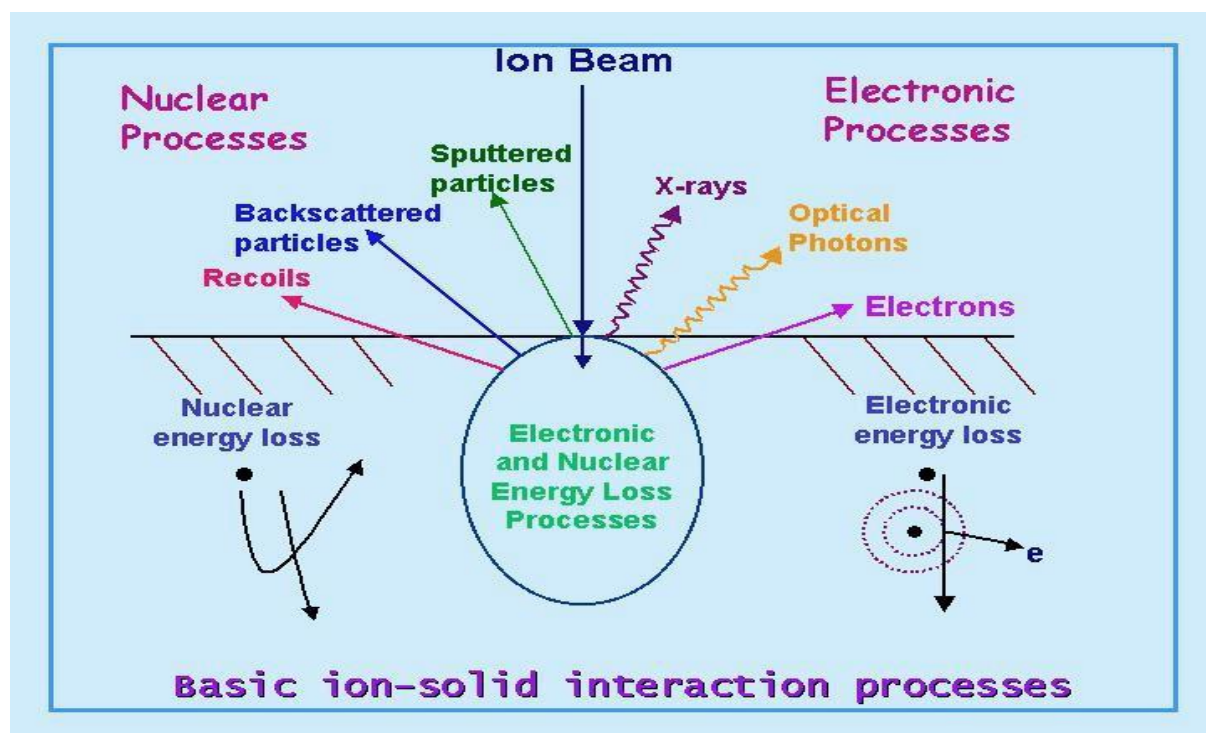


Fig. (2-1) The interaction between the incident ion and the target [47].

The atoms that collide directly with the incident particle are known as primary recoils (or primary knock-on atoms, PKAs). These primary recoil atoms, in turn, are generally displaced from their lattice positions (overcoming the lattice displacement energy, U_d this is the energy that a bounce atom needs

to beat the forces the lattice and move more than one atomic distance from its original position. If the bounce atom does not move more than one atomic distance, it is supposed that it will return to its original position and give up its bounce energy. Typical values the lattice binding energy are about (15 eV) for semiconductors and (25 eV) for the conductors. For fragile materials such as polymers, lower worth (2 – 5) eV [48].

Sputtering is usually of the total (S.Y) (units: atoms/ion), hence the sputter yield as illustrated in Fig. (2.2) is $S.Y = 3$ atoms/incident particle. The sputter yield is a statistical measure in that an individual incident particle may create more or less sputtered atoms than the value S.Y, but a large group of N incident particles will sputter $Y \times N$ atoms. Molecules, Ions, neutral atoms, neutrons, electrons, or energetic photons can induce sputtering. We will focus on sputtering by ion beam on alloy targets (i.e., targets comprised of more than one element) [47,48].

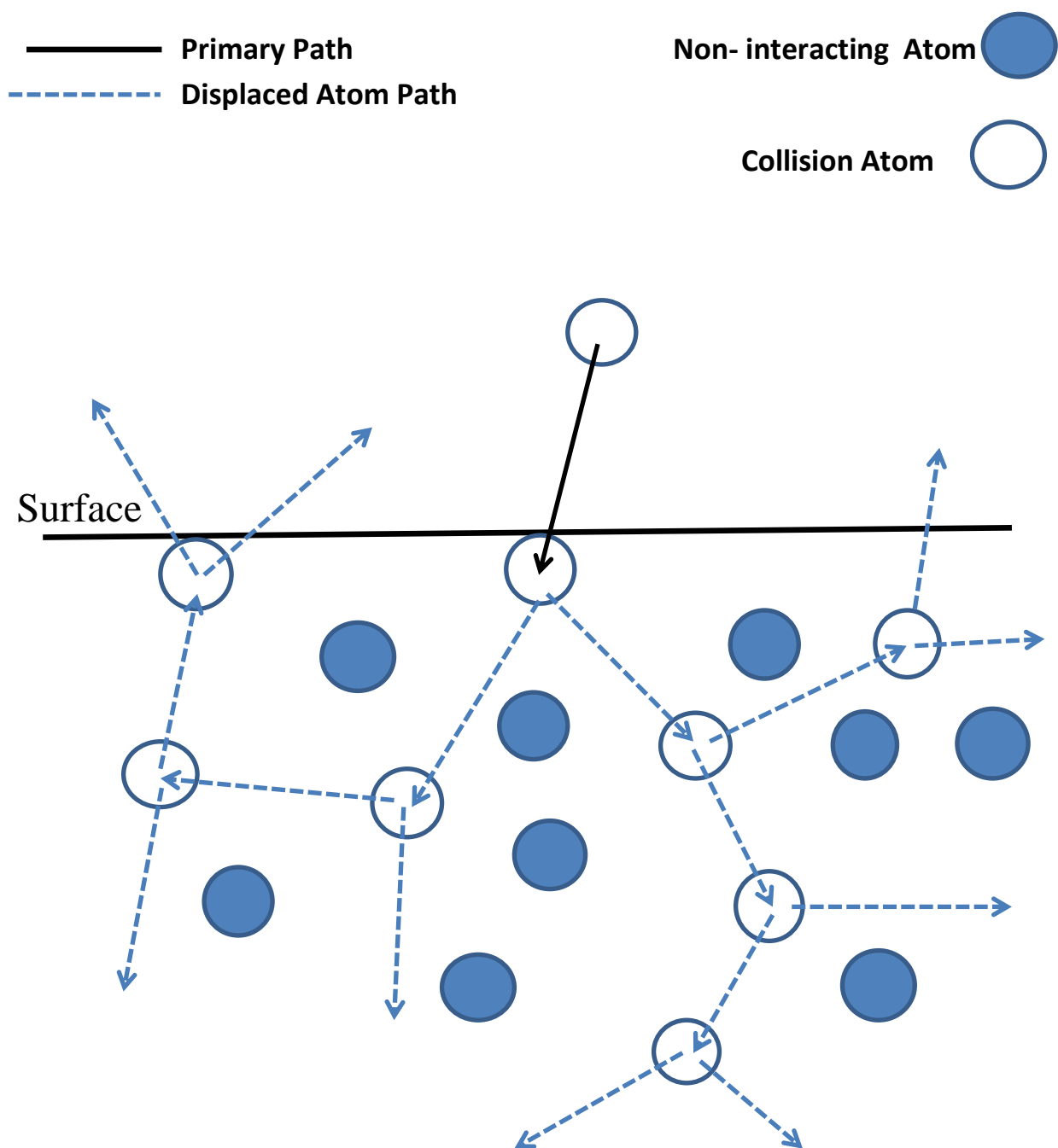


Fig. (2-2): Two dimensional diagram of a typical collision cascade [49].

In figure (2-2) there are three particles escaping from one particle surface of an accident give $S.Y = 3$ atoms/ion as shown in the two-dimensional diagram of a typical collision series [49].

Several different types of events may occur as a result of the ion beam effect on a target surface. Some of these events include electron or photon emission, electron transfer (both ion-surface and surface-ion), scattering, adsorption, and sputtering (i.e. Ejection of atoms from the surface). In Fig. (2-3) diagram of various ion-surface interactions (non-exhaustive). (1) Incoming ion; (2) Scattering; (3) Neutralization and scattering; (4) Sputtering or recoiling; (5) Electron emission; (6) Photon emission; (7) Adsorption; (8) Displacement [50].

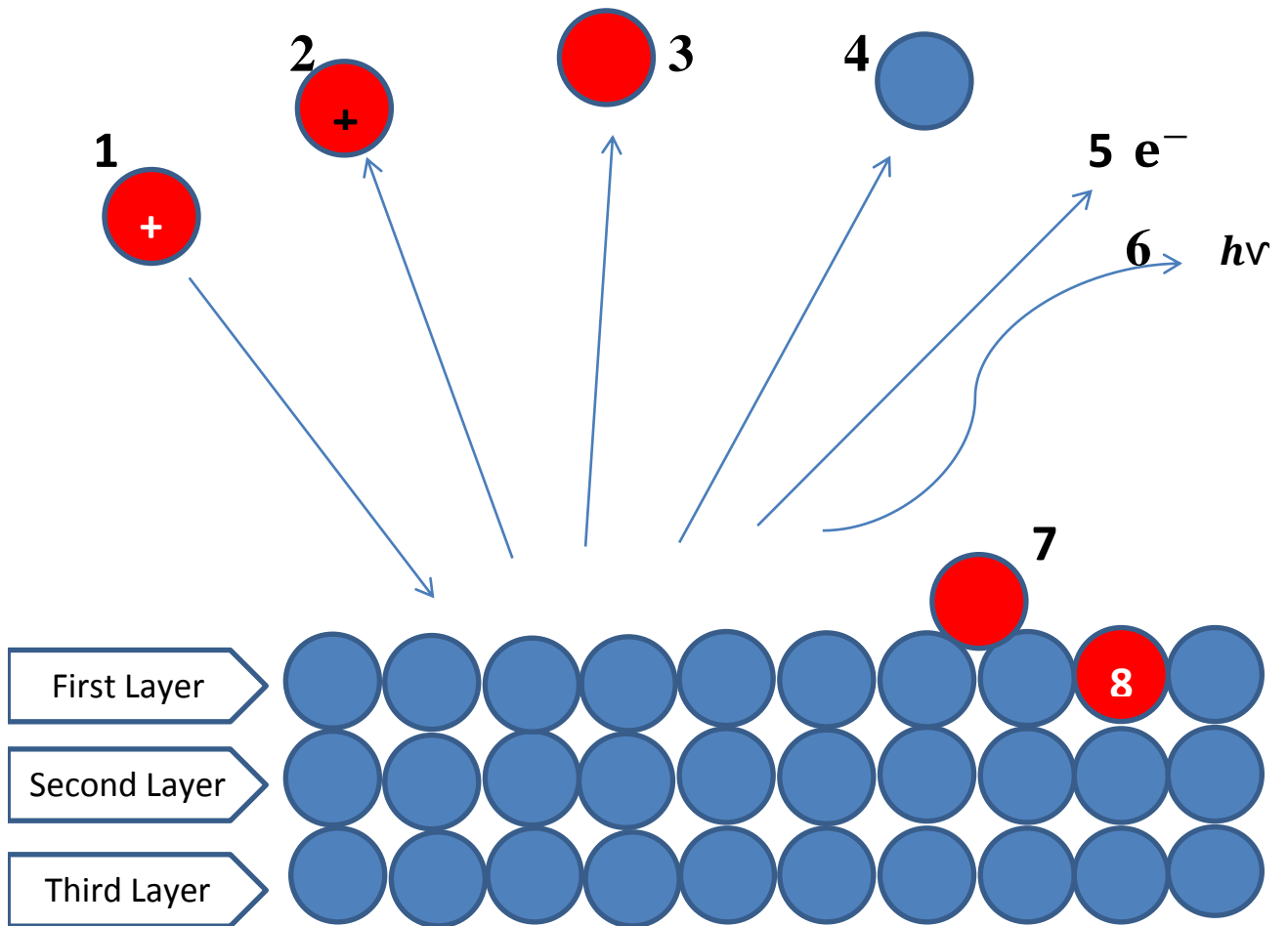


Fig. (2-3): A diagram showing the possible effects of ion bombardment.

(2-3) Mechanisms of the Sputtering Yield

The definition of threshold energy for sputtering is a delicate task, and usually of little value. The (KE) of the bombarding particle must, therefore, be greater than the sputtering threshold, E_{th} , [40].

S.Y depends on the properties of both the incident ion and the target as follows [40, 51]:

• Incident Particle Properties:

- Energy.
- Mass.
- Incidence angle.

• Target Properties:

- Atomic Mass.
- Surface binding energy.
- Surface topography.
- Crystal orientation.

If the incident ion energy is lower than the (E_{th}) the sputtering yields will not happen, but above (E_{th}) sputtering generally increasing with the increase of incidence ion mass, increase with increasing incident ion energy [52]. Yields will start to decline due to the incident ion's energy being deposited too far away from the surface layer where most sputtered particles originate [53]. The definition sputtering yield is assumed that the number of atoms removed proportionally with the number of incident particles while all the other factors remain constant, and where the target is a solid material, and that the package ions bombards energy E_0 and incident angle (θ°), it leads to a series of elastic collisions when neglecting electronic excitation of the target [54]. The atom of

target atoms will move recoil, after gaining energy of the collision process and can cause recoil movement of other atoms.

(2-4) Sputtering from compound targets

When a multi-component solid material is bombarded with energetic particles, the structural change near the surface is a real phenomenon is called sputtering and thermal processes. The driver's forces of surface atom separation are the energy of stress. The proportional importance of each process depends on the system of alloys, elements, the energy of the bombarding ions, and the temperature of irradiation [55].

(2-5) Results from Elastic-Collision Theory

When the incident ion energy is more than the threshold, the Sputtering process can be analyzed as a sequence of independent binary collisions resembling a three-dimensional billiards game with atoms [39].

Under conservation laws for energy and momentum, the energy transmitted (an elastic collision) is between two atoms. An atom 1 with initial energy E can at most transfer energy [54].

$$T_m = \gamma E \dots \dots \dots (2 - 2)$$

where

$$\gamma = \frac{4 M_1 M_2}{(M_1 + M_2)^2} \dots \dots \dots (2-3)$$

To an atom 2 with zero initial energy, and this requires a central (head-on) collision.

where:

M_1 and M_2 are the mass of the incident particle and target particle, respectively.

T : is the energy that is transferred to the target atom.

E : is the initial energy of the incident particle.

T_m : the maximum energy transfer, happen during a head-on collision.

The probability distribution of the energy transfer T is determined by the cross section $d\sigma (E, T)$ [55].

$$d\sigma (E, T) = \pi \frac{M_1}{M_2} Z_1^2 Z_2^2 e^4 \frac{dT}{ET^2} \quad ; \quad 0 \leq T \leq T_m \dots\dots\dots(2 - 4)$$

Where Z_1e and Z_2e are nuclear charges. This ($d\sigma$) strongly prefers collisions with small (T) ($T \ll T_m$) and, moreover, the reduction in absolute magnitude with increasing the initial energy of the incident particle [55].

(2 - 6) Basics, Concepts of Ion-Solid Interaction:

The basic concepts of ion-solid interactions, on which the theory of sputtering is built. Quantitative analysis of sputtering requires both an understanding of the energy transfer mechanisms in atomic collisions and penetration phenomena [56]. to understand the sputtering yield process, we must understand the interaction between the energetic particle and the alloy, due to the elastic collision between the energetic particle and the target atoms, the ion's momentum is transferred to the target atoms and as a result, the sputtering occurs. If the surface atom gained enough (KE) to overcome the (SBE) of the target material can be removed as a sputtered particle. Which determines the interaction between the ion incident and the target is the primary (KE) of the ion. Thus, if the ions are not dispersed from the target surface, the ions will stop at the end, at a certain depth within the target, an ion is implanted Fig. (2-5) [57].

Particles in sputtering

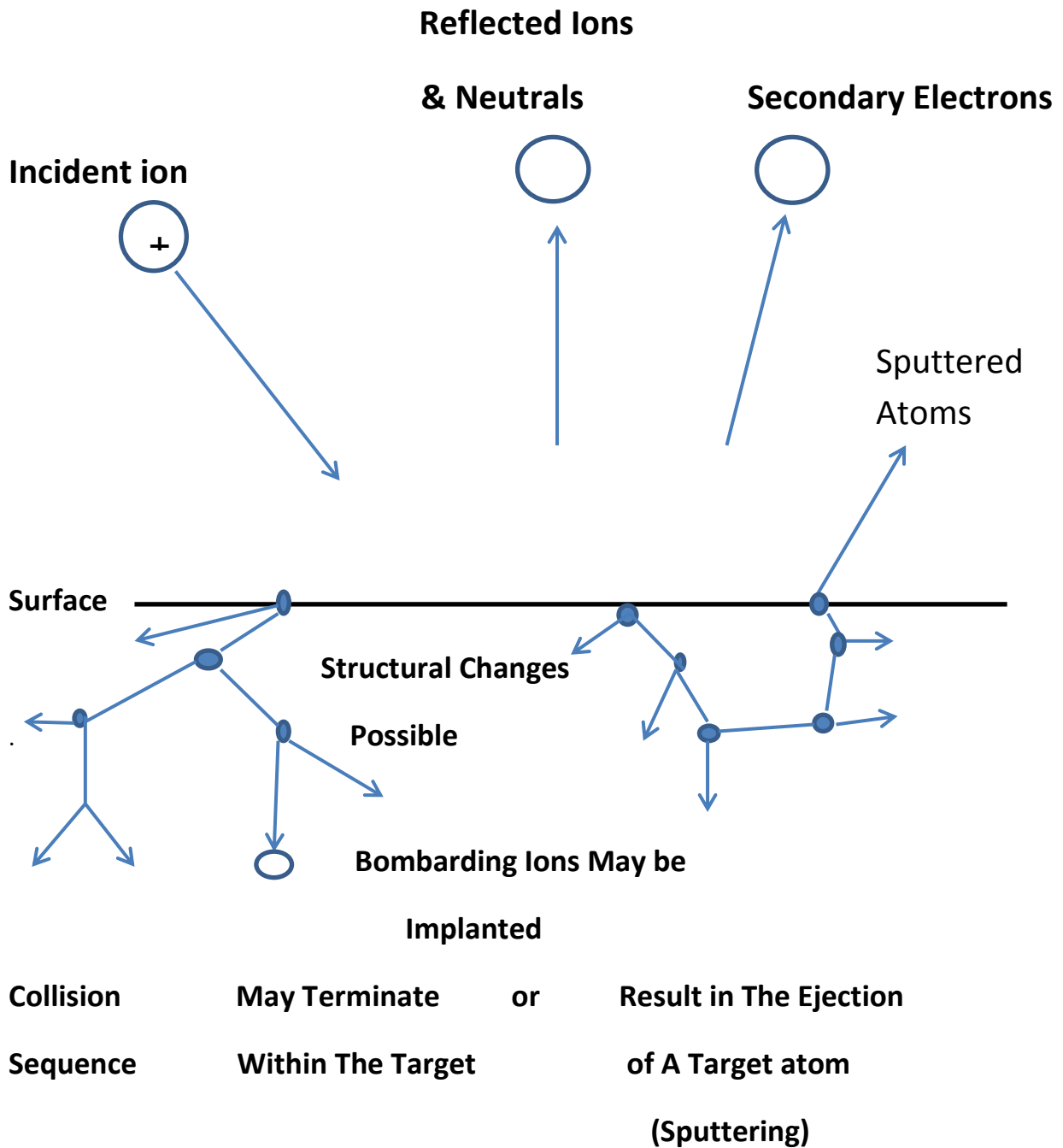


Fig. (2-4): A diagram the process of sputtering and ion interaction with the solid surface.

(2-7) Types of Sputtering Regimes

Sigmund has identified three sputtering regimes that can be classified as energy - dependent [58]. Table (2-1), Fig. (2-5).

- (a) The single knock-on regime: In this regime the ion transfers enough energy (approx. In the energy range less than 1 keV) of the target atoms to create PKAs (primary knock – on atoms), some of which are sputtered, but the process is not enough to generate recoil cascades. Figure (2-5a).
- (b) The linear cascade regime: Is characterized by the generation of a full collision cascade, in which the interaction of two moving target atoms is negligible. The linear cascade framework lends itself to being described by transport theory Figure (2-5b).
- (c) The spike regime: produces collision cascades, except that the interaction between moving atoms and other target atoms is no longer negligible. The sputtering process is caused by collision cascades generated by ions backscattered from the interior of the solid. Figure (2-5c).

The theoretical description of sputtering in the single knock- on and spike regime is less developed than in the linear collision cascade regime.

In ion propulsive devices undergoing sputtering at low energy and relatively low flux, most sputtering occurs in the single knock-on regime, with a smaller amount happening in the linear cascade regime. Unfortunately, the single knock-on regime has the least extensive theoretical underpinnings and is also the hardest of the regimes to measure yields experimentally [59].

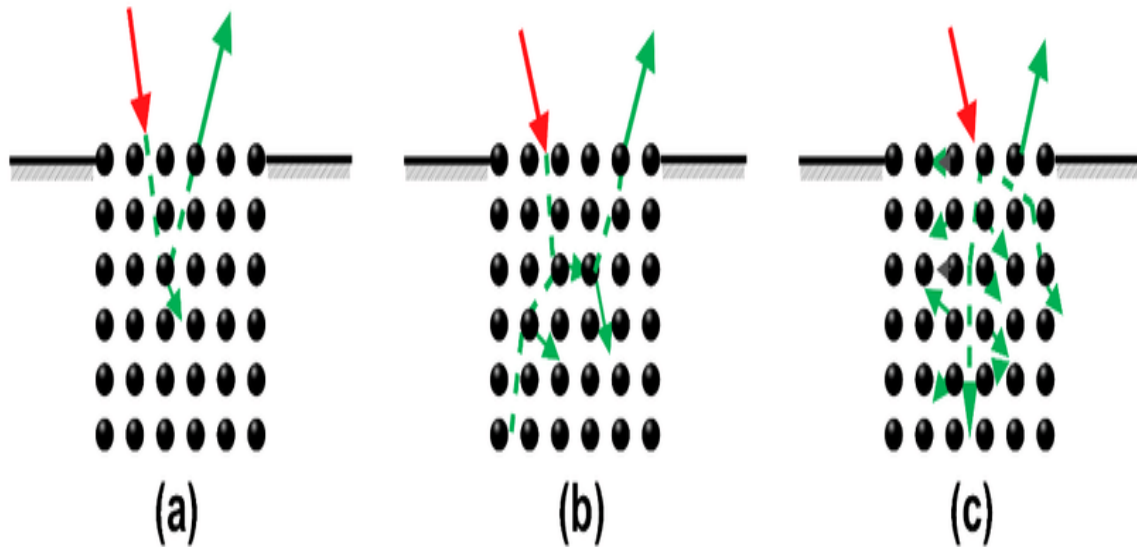


Figure (2-5): diagrams of the three sputtering regimes [60].

Table 2-1: Comparison table between types of sputtering systems [58].

Regime	Approx. Energy Range	Characteristic
Single knock – on	Less than 1 keV	Only primary recoils are created (PKAs). Without recoil cascades.
Linear cascade	From 1 to 300 keV	The recoil atoms receive enough energy from the collisions with the incident particles to generate a recoil cascade. In this case, the density of recoil atoms is low.
Spike	More than 100 keV, when ions reach high levels of flux, they can occur at lower energies.	Produces collision cascades, except that the interaction between moving atoms and other target atoms is no longer negligible.

(2 - 8) Sputtering yields for elements:

The sputtering yield gives by Sigmund's theory [61,62] as:

$$S.Y = \frac{C Q}{U_b} \frac{\alpha S_n(E)}{1 + AS_e(\epsilon)} \left\{ 1 - \left[\frac{E_{th}}{E} \right]^{\frac{1}{2}} \right\}^{2.8} \dots \dots \dots (2 - 6)$$

where $S_n(E)$ is the nuclear stopping cross section per atom.

The coefficient C is constant.

E : is the initial energy of the incident particle.

E_{th} : threshold energy.

Here, the $S_n(E)$ is known by [63].

$$S_n(E) = 4\pi Z_1 Z_2 \frac{e^2}{4\pi\epsilon_0} a_{12} \frac{M_1}{M_1 + M_2} s_n(\epsilon) \dots \dots \dots (2 - 7)$$

where:

Z_1 and M_1 are the atomic number and mass of the primary ion and Z_2 and M_2 are similarly for the target atoms

e : electron charge.

ϵ_0 : permittivity of a vacuum.

a_{12} :The parameter is given by:

$$a_{12} = \left[\frac{9\pi^2}{128} \right]^{\frac{1}{3}} \frac{a_0}{\left(Z_1^{2/3} + Z_2^{2/3} \right)^{\frac{1}{2}}} \dots \dots \dots (2 - 8)$$

where a_0 is the Bohr radius of 0.529 \AA and, depending on Matsunami et al. [64] and Lindhard, Scharff and Schiott's theory [65],

$$s_n(\epsilon) = \frac{3.441\epsilon^{1/2} \ln(\epsilon + 2.718)}{1 + 6.355\epsilon^{1/2} + \epsilon(6.882\epsilon^{1/2} - 1.708)} \dots \dots \dots (2 - 9)$$

When offsetting transaction values in Eq. (2-7) gives:

$$S_n(E) = \frac{84.78 Z_1 Z_2}{\left(Z_1^{2/3} + Z_2^{2/3}\right)^{1/2}} \frac{M_1}{M_1 + M_2} S_n(\varepsilon) \dots\dots\dots (2 - 10)$$

The reduced energy (ε) is given by:

$$\varepsilon = \frac{0.03255}{Z_1 Z_2 \left(Z_1^{2/3} + Z_2^{2/3}\right)^{1/2}} \frac{M_2}{M_1 + M_2} E \dots\dots\dots (2 - 11)$$

In Eq. (2-6), $s_e(\varepsilon)$ is the inelastic, electronic stopping power where

$$s_e(\varepsilon) = k \varepsilon^{1/2} \dots\dots\dots (2 - 12)$$

and [64]

$$k = G^{1/2} \frac{(M_1 + M_2)^{3/2}}{M_1^{3/2} M_2^{1/2}} \frac{Z_1^{2/3} Z_2^{1/2}}{\left(Z_1^{2/3} + Z_2^{2/3}\right)^{3/4}} \dots\dots\dots (2 - 13)$$

where: G is constant.

In the formulation of Matsunami et al [62].

$$A = D U_b \dots\dots\dots(2-14)$$

where:

D: constant.

$$\alpha = 0.08 + 0.164 \left(\frac{M_2}{M_1}\right)^{0.4} + 0.0145 \left(\frac{M_2}{M_1}\right)^{1.29} \dots\dots\dots (2 - 15)$$

with

$$\frac{E_{th}}{U_b} = 1.9 + 3.8 \left(\frac{M_1}{M_2}\right) + 0.134 \left(\frac{M_2}{M_1}\right)^{1.24} \dots\dots\dots(2-16)$$

Q: for each element. [62]:

$$Qr^3 = g^3 \left\{ \exp\left[-\frac{(M_2-b)^2}{2c^2}\right] \right\} + h^3 \left\{ 1 - \exp\left[-\frac{(M_2-d)^2}{f^2}\right] \right\} \dots\dots\dots(2-17)$$

where: b, c, d, f, g, h are constant

r : Average distances between spaces, is known by:

$$r^3 = \frac{M_2}{1000 \rho N} \dots\dots\dots(2-18)$$

r^3 : The most important parameter of Q and, is part of Sigmund's theory [62].

where:

ρ : is the target density in kg/m³

N : is Avogadro's number.

(2-9) Sputtering yields for compounds

According to the Bragg's rule, for compounds, stopping power would be a linear combination of the initial stopping forces measured [66]. This has finite accuracy, especially when M_1 is medium between two widely different compound masses M_{2A} and M_{2B} notes that Sigmund [63]. And computing with the target is proposed to be "elemental" at an atomic number average,

$$Z_2 = X_A Z_{2A} + X_B Z_{2B}$$

Where X_A is the atomic fraction of A in the compound of A, and B, etc.

When calculating the sputtering yield of the compounds, in the current work values the basic parameters in Eq. (2-6) are interpolated from the values of separated elements to find an efficient value. The (Qr^3 , α , $S_n(E)$, E_{th} , and k) of Eq. (2-17), (2-15), (2-10), (2-16), and (2-13) but the mean interatomic spacing, r , is evaluated from the apparent density of the alloy except if otherwise stated. U_b is discussed below. By interpolation, for instance, $Q_{2A}r_{2A}^3$ and $Q_{2B}r_{2B}^3$ for M_{2A} and M_{2B} are calculated from equation (2-17) and then Qr^3 is taken as $X_A(Q_{2A}r_{2A}^3) + X_B(Q_{2B}r_{2B}^3)$

Instead of directly from the Eq. (2-17) for the average value of M_2 .

For U_A^S and U_B^S , of pair bond theory with zero heat mixture assumptions in the compound and that random order:

$$U_A^S = X_A^S U_A + 0.5X_B^S (U_A + U_B) \dots\dots\dots(2-19)$$

$$U_B^S = X_B^S U_B + 0.5X_A^S (U_A + U_B) \dots\dots\dots(2-20)$$

these Eqs. are for a changeable surface layer that perhaps more than a monolayer layer.

Here, U_A and U_B are the energies to remove A and B atoms from pure A and B. U_A^S and U_B^S are the energies to remove A and B atoms from the compound surface.

In Eq. (2-19) and (2-20). The sputtering process will be made the assumption of randomness more right.

Anders and Urbassek's [66] got a result

$$\frac{X_A^S}{X_B^S} = \frac{X_A}{X_B} \frac{U_A^S}{U_B^S} \dots\dots\dots(2-21)$$

Combining equations (2-19), (2-20) and (2-21), together with $X_A^S + X_B^S = 1$ and $X_A + X_B = 1$, leading to expression for X_A^S :

$$X_A^S = \frac{[p^2 + (1 - p^2)X_A]^{0.5 - p}}{1 - p} \dots\dots\dots(2-22)$$

where

$p = U_B/U_A$. From equations (2-19) and (2-20), U_A^S and U_B^S may then be obtained.

The emission rate of in the surface layer and its binding surface energy, the surface atoms will be largely subject to fracture. Any model needs a calculate X_A^S , X_B^S , U_A^S , and U_B^S . The ratio of the yield including a simple

preferential sputtering (Y_{ps}) to that from interpolation (Y_{int}) without considering preferential sputtering is now calculated. This ratio is given by [67]:

$$\frac{Y_{PS}}{Y_{int}} = \frac{X_A^S/U_A^S + X_B^S/U_B^S}{1/U_{int}} \dots\dots\dots(2-23)$$

where

$$U_{int} = X_A U_A + X_B U_B \dots\dots\dots(2-24)$$



CHAPTER THREE
RESULTS AND CONCLUSIONS

(3-1) Introduction

In this chapter, we introduce our results about the Sputtering Yield (S.Y) behavior, for (Beryllium - Copper, Brass, Stainless Steel, Monel - 400) alloys and different incident ion types (Ar, N₂, and O₂) as a function of the incident ion energy and incident angle are usually acquired from MCs of several processes for the energy influence. Our count is completely based on data that calculated by TRIM.

The width of the alloy is 1000Å, and the number of the ions used for these calculations is 5000. The data of sputtering yield are fitted using IGOR Program and Origin8 program.

(3-2) The influence of the angle of the incident ion on the sputtering yield

For this study, we have fitted the curves of the sputtering yield versus incident angle to get a semi-empirical equation in figures (3-1) - (3-12) showing the sputtering yield versus of incident angle. The fitted data are given by a fourth-degree polynomial as in the equation below

$$S.Y = k_0 + k_1 \theta + k_2 \theta^2 + k_3 \theta^3 + k_4 \theta^4 \dots\dots\dots (3-1)$$

where k_0, k_1, k_2, k_3, k_4 are parameters depending for incident angle and the tables (2-1) to (2-12) gives the values of these parameters according to the different energy ions.

Figures (3-1) - (3-12) show the relationship between sputtering yield and incidence angle from incidence ions (Ar, N₂, and O₂) to a target of alloy (Beryllium - Copper, Brass, Stainless Steel, Monel-400) respectively, at an energy of incident ions is (0.5, 1, 1.5, 3, 4.5, 5) keV respectively. The sputtering yield depends on the angle of incident, measured from the surface normal. In all the cases investigated, the sputtering yield has a slight increase

from the incident angle of (0°) to (60°), because of a cascade progressing more nearby to the surface, and then a significant increase typically between (60°) to (80°) of incident angle. The reason for the increase of the S.Y is that the deposited energy is transferred to the nearest surface of the target, after crossing the maximum, it decreases rapidly at an angle greater than (80°), where it begins the sieving effect of contiguous atoms of target surface that prevents the bombarding ions from entering the target alloy. Eventually, it decreases significantly because all incident ions are reflected without giving the incident ion energy to the target alloys. The present results also reveal a relatively stronger angular effect for Brass alloy than BeCu and Monel – 400. And less angular effect at Stainless-Steel.

Table (3-1): parameters of equation (3-1) plotted in Figure (3-1) as Argon ions bombarding BeCu alloy.

Ion energy (keV)	k_0	k_1	k_2	k_3	k_4
0.5	2.3335	-0.012032	0.00074486	1.7798e-8	-8.7124e-8
1	3.4923	0.0021866	-4.5757e-5	3.071e-5	-3.5476e-7
1.5	4.1266	0.01818	-0.00087047	6.1389e-5	-6.173e-7
3	5.2315	0.10746	-0.0072374	0.00022114	-1.7181e-6
4.5	5.9768	0.10488	-0.0069732	0.00022933	-1.8289e-6
5	6.1028	0.089248	-0.0063428	0.00023099	-1.9017e-6

Table (3-2): parameters of equation (3-1) plotted in Figure (3-2) as Nitrogen ions bombarding BeCu alloy.

Ion energy (keV)	k_0	k_1	k_2	k_3	k_4
0.5	1.5715	- 0.0027741	2.7563e-5	9.6164e-6	-1.1579e-7
1	2.1371	0.015228	-0.0011085	4.0122e-5	-3.3941e-7
1.5	2.3683	0.02164	-0.0019441	6.79e-5	-5.5227e-7
3	1.5715	-0.0027741	2.7563e-5	9.6164e-6	-1.1579e-7
4.5	2.5836	0.077754	-0.0059361	0.0001657	-1.2026e-6
5	2.5485	0.10464	-0.0078125	0.0002040	-1.4337e-6

Table (3-3): parameters of equation (3-1) plotted in Figure (3-3) as Oxygen ions bombarding BeCu alloy.

Ion energy (keV)	k_0	k_1	k_2	k_3	k_4
0.5	1.7826	0.0052025	-0.0003123	1.4835e-5	-1.4448e-7
1	2.3521	0.012719	-0.00088195	3.905e-5	-3.5369e-7
1.5	2.7326	0.032612	-0.0023539	7.4548e-5	-5.9297e-7
3	3.071	0.069019	-0.0049614	0.00014097	-1.0483e-6
4.5	2.9816	0.099347	-0.0071022	0.00019406	-1.4035e-6
5	3.1478	0.07276	-0.0060757	0.00018181	-1.3562e-6

Table (3-4): parameters of equation (3-1) plotted in Figure (3-4) as Argon ions bombarding Brass alloy.

Ion energy (keV)	k_0	k_1	k_2	k_3	k_4
0.5	3.5352	-0.01472	0.0011132	-4.5703e-6	-8.6966e-8
1	5.2313	0.016299	-0.0002452	3.926e-5	-4.5688e-7
1.5	6.481	0.070294	-0.0036036	0.00011761	-9.9497e-7
3	8.2317	-0.011524	0.00057495	0.00010326	-1.2297e-6
4.5	8.8017	0.10469	-0.0072572	0.00028162	-2.3864e-6
5	8.9179	0.20022	-0.01324	0.00040222	-3.1271e-6

Table (3-5): parameters of equation (3-1) plotted in Figure (3-5) as Nitrogen ions bombarding Brass alloy.

Ion energy (keV)	k_0	k_1	k_2	k_3	k_4
0.5	2.3747	0.00038354	-5.0084e-5	1.2708e-5	-1.5091e-7
1	3.1186	0.024487	-0.0015128	5.3814e-5	-4.6149e-7
1.5	3.4393	0.034931	-0.0023975	8.2878e-5	-6.8874e-7
3	3.8947	0.07211	-0.0056698	0.00016865	-1.2751e-6
4.5	3.9033	0.0085945	-0.0014341	9.3649e-5	-8.6942e-7
5	3.9295	0.12153	-0.0091295	0.00024707	-1.7737e-6

Table (3-6): parameters of equation (3-1) plotted in Figure (3-6) as Oxygen ions bombarding Brass alloy.

Ion energy (keV)	k_0	k_1	k_2	k_3	k_4
0.5	2.652	0.001086	-9.6015e-5	1.4882e-5	-1.7289e-7
1	3.5936	0.0045131	-8.9407e-5	2.8812e-5	-3.348e-7
1.5	4.0963	0.038387	-0.0028889	9.6043e-5	-7.8228e-7
3	3.071	0.069019	-0.0049614	0.00014097	-1.0483e-6
4.5	4.6516	0.060729	-0.0055561	0.00017916	-1.3966e-6
5	4.6827	0.13238	-0.010218	0.0002821	-2.0445e-6

Table (3-7): parameters of the equation (3-1) as Argon ions bombards of Stainless - steel alloy target which are shown in figure (3-7).

Ion energy (keV)	k_0	k_1	k_2	k_3	k_4
0.5	1.6091	-0.0039491	0.00034482	5.1381e-6	-9.9033e-8
1	2.3396	0.0172	-0.00065675	3.554e-5	-3.4409e-7
1.5	2.9817	0.011751	-0.00085206	5.5151e-5	-5.319e-7
3	3.8832	0.038822	-0.0028156	0.00011898	-1.0281e-6
4.5	4.2612	0.039386	-0.0032811	0.00014885	-1.2962e-6
5	4.4606	0.073216	-0.0062459	0.0002155	-1.7147e-6

Table (3-8): parameters of the equation (3-1) as Nitrogen ions bombarding of Stainless - steel alloy target which are shown in figure (3-8).

Ion energy (keV)	k_0	k_1	k_2	k_3	k_4
0.5	1.2253	-0.00055734	-2.5195e - 5	8.5141e-6	-9.7319e-8
1	1.6347	0.011443	-0.00090804	3.461e-5	3.461e-5
1.5	1.7795	0.033788	-0.0022834	6.5668e-5	-4.9826e-7
3	1.9508	0.053097	-0.0039589	0.00011041	-8.0427e-7
4.5	2.0129	0.065921	-0.0051539	0.00014272	-1.0279e-6
5	2.0254	0.086839	-0.0065847	0.0001702	-1.1841e-6

Table (3-9): parameters of the equation (3-1) as Oxygen ions bombarding of Stainless - steel alloy target which are shown in figure (3-9).

Ion energy (keV)	k_0	k_1	k_2	k_3	k_4
0.5	1.3532	0.0027881	-0.00015766	1.1058e-5	-1.1472e-7
1	1.8432	-0.00016253	-0.00012495	2.1387e-5	-2.2917e-7
1.5	2.0639	0.022674	-0.001723	5.9157e-5	-4.8041e-7
3	2.378	0.042837	-0.0036442	0.00011085	-8.3785e-7
4.5	2.3105	0.046723	-0.0040536	0.00012971	-9.9176e-7
5	2.3087	0.088165	-0.0067041	0.00017972	-1.2767e-6

Table (3-10): parameters of the equation (3-1) Argon ions bombarding of Mone1-400 alloy target which are shown in figure (3-10).

Ion energy (keV)	k_0	k_1	k_2	k_3	k_4
0.5	2.0276	0.0027092	0.0027092	8.1419e-6	-1.2057e-7
1	3.249	-0.018224	0.0015098	-3.8705e-6	-1.3461e-7
1.5	3.8665	0.021565	-0.00094865	5.6367e-5	-5.5446e-7
3	5.0658	0.062197	-0.0037621	0.00014263	-1.2166e-6
4.5	5.789	0.09793	-0.0066741	0.00022354	-1.7976e-6
5	6.0719	0.074262	-0.0059044	0.0002214	-1.8339e-6

Table (3-11) parameters of the equation (3-1) as Nitrogen ions bombarding of Monel - 400 alloy target which are shown in figure (3-11).

Ion energy (keV)	k_0	k_1	k_2	k_3	k_4
0.5	1.5358	-0.0041566	0.00018253	4.9256e-6	-8.1185e-8
1	1.9918	0.018873	-0.0011923	4.1136e-5	-3.4527e-7
1.5	2.3099	0.021833	-0.0017287	5.995e-5	-4.9111e-7
3	2.5885	0.042635	-0.0037748	0.00011712	-8.9241e-7
4.5	2.63	0.066568	-0.0054002	0.00015673	-1.1569e-6
5	2.6569	0.10121	-0.0077015	0.00020052	-1.4056e-6

Table (3-12): parameters of the equation (3-1) as Oxygen ions bombarding of Mone1-400 alloy target which are shown in figure (3-12)

Ion energy (keV)	k_0	k_1	k_2	k_3	k_4
0.5	1.7032	0.003355	-0.00016467	1.0768e-5	-1.1464e-7
1	2.3235	0.0057769	-0.00050433	3.0081e-5	-2.9122e-7
1.5	2.5944	0.024592	-0.0016045	5.8901e-5	-4.9952e-7
3	3.1261	0.042818	-0.0035858	0.00011513	-8.9759e-7
4.5	2.9002	0.080339	-0.0059128	0.00017134	-1.2726e-6
5	3.1546	0.079839	-0.0064794	0.0001864	-1.3722e-6

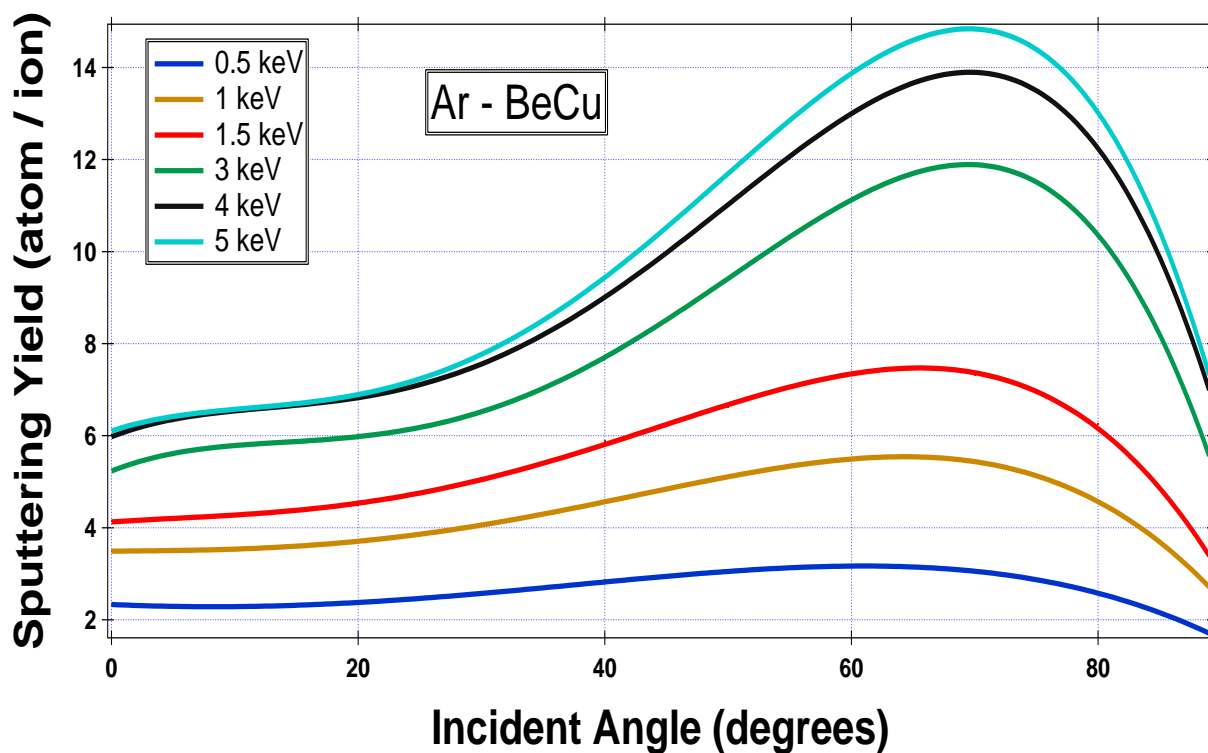


Figure (3-1): incident ion angle dependence of S.Y of BeCu alloy bombard by Argon ion.

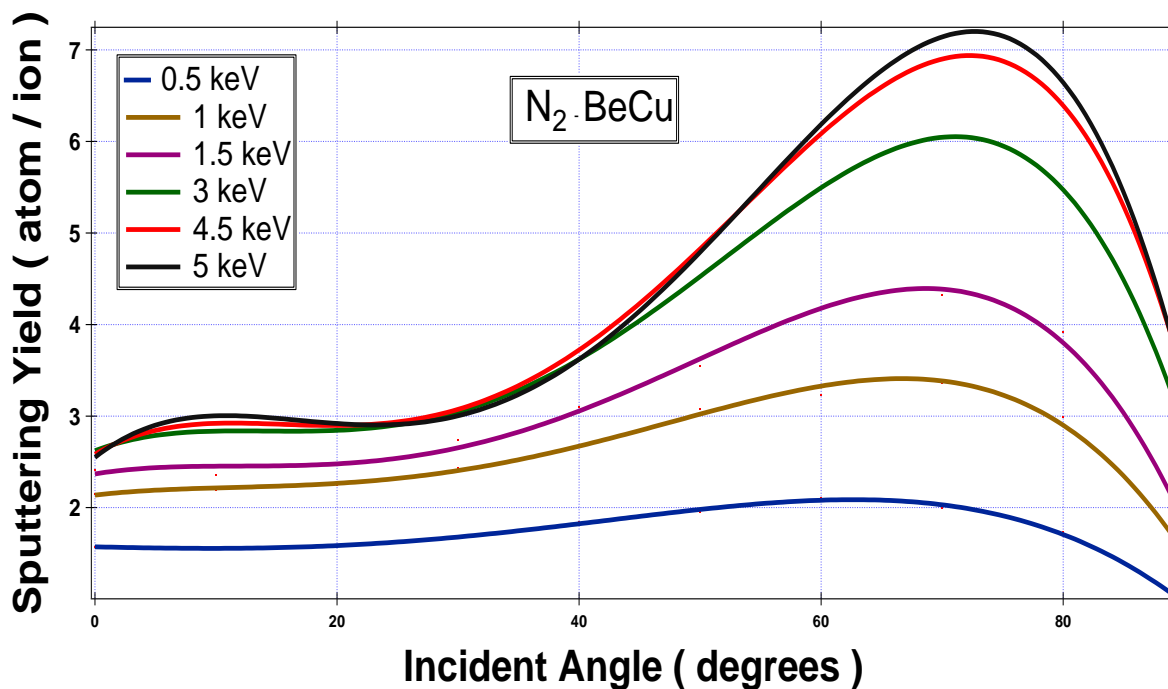


Fig. (3-2): incident ion angle dependence of S.Y of BeCu alloy bombard by Nitrogen ion.

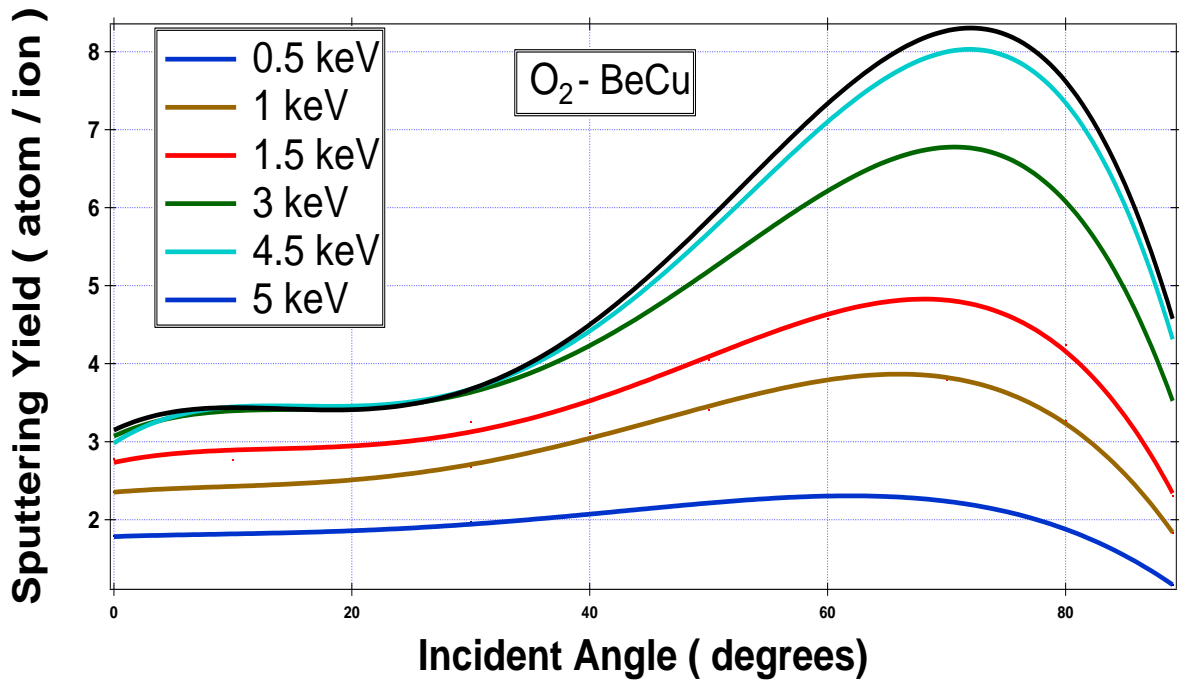


Figure (3-3): incident ion angle dependence of S.Y of BeCu alloy bombard by Oxygen ion.

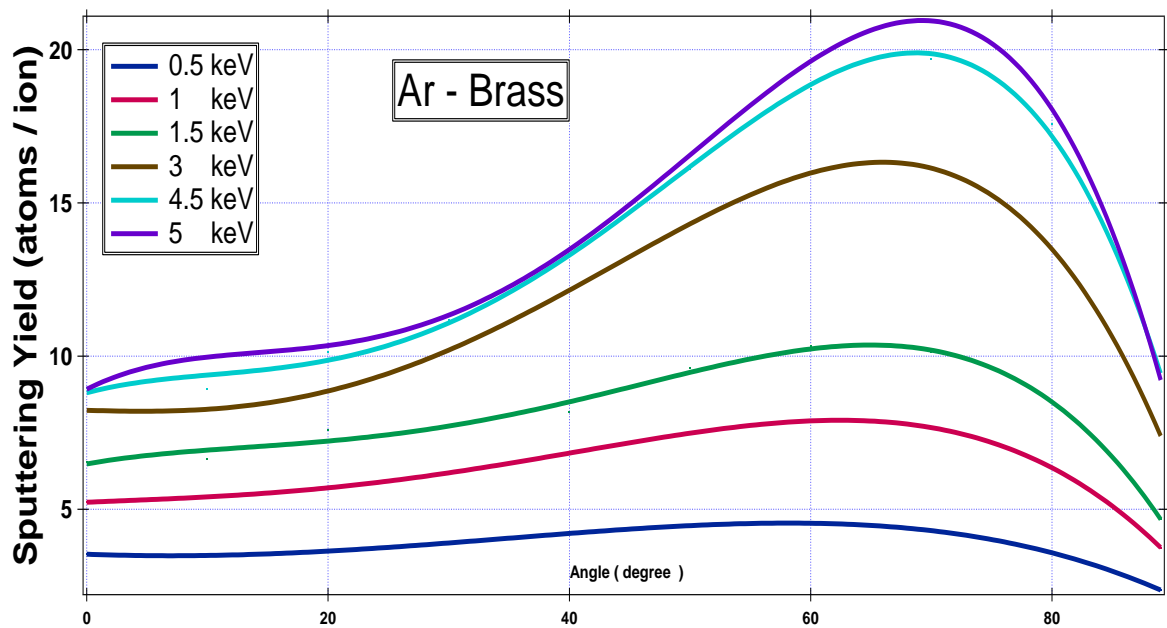


Figure (3-4): ion angle dependence of S.Y of Brass alloy bombard by Argon ion.

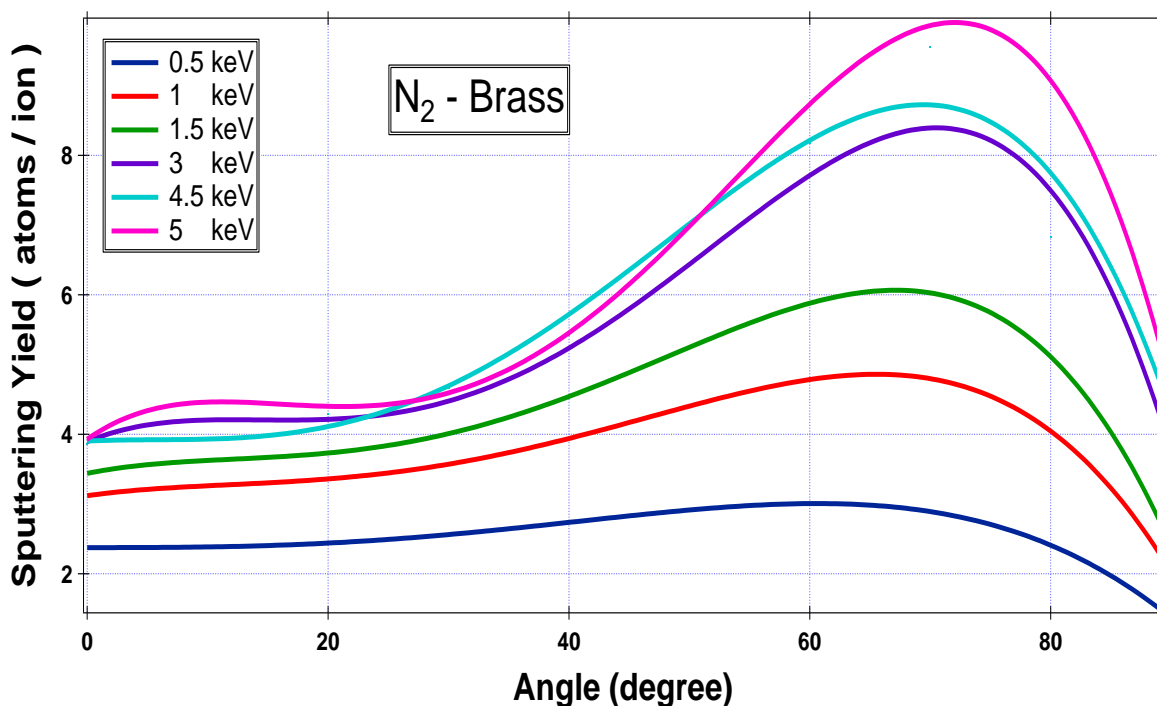


Figure (3-5): incident ion angle dependence of S.Y of Brass alloy bombard by Nitrogen ion.

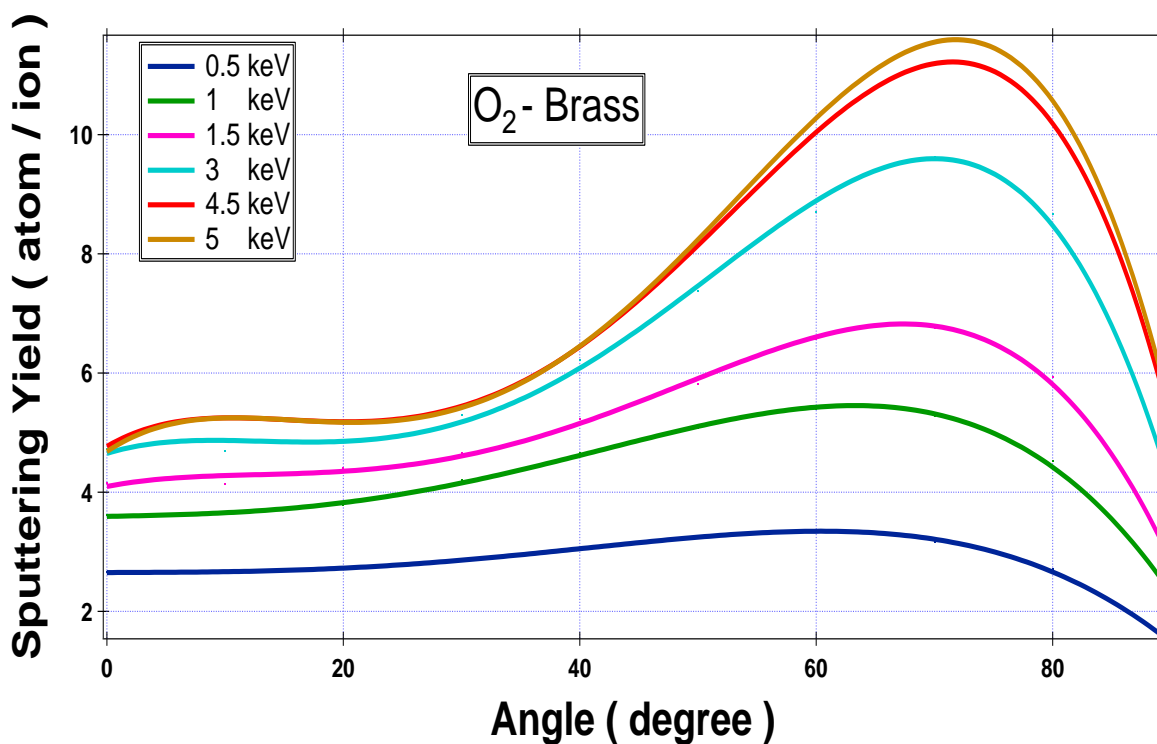


Fig. (3-6): incident ion angle dependence of S.Y of Brass alloy bombard by Oxygen ion.

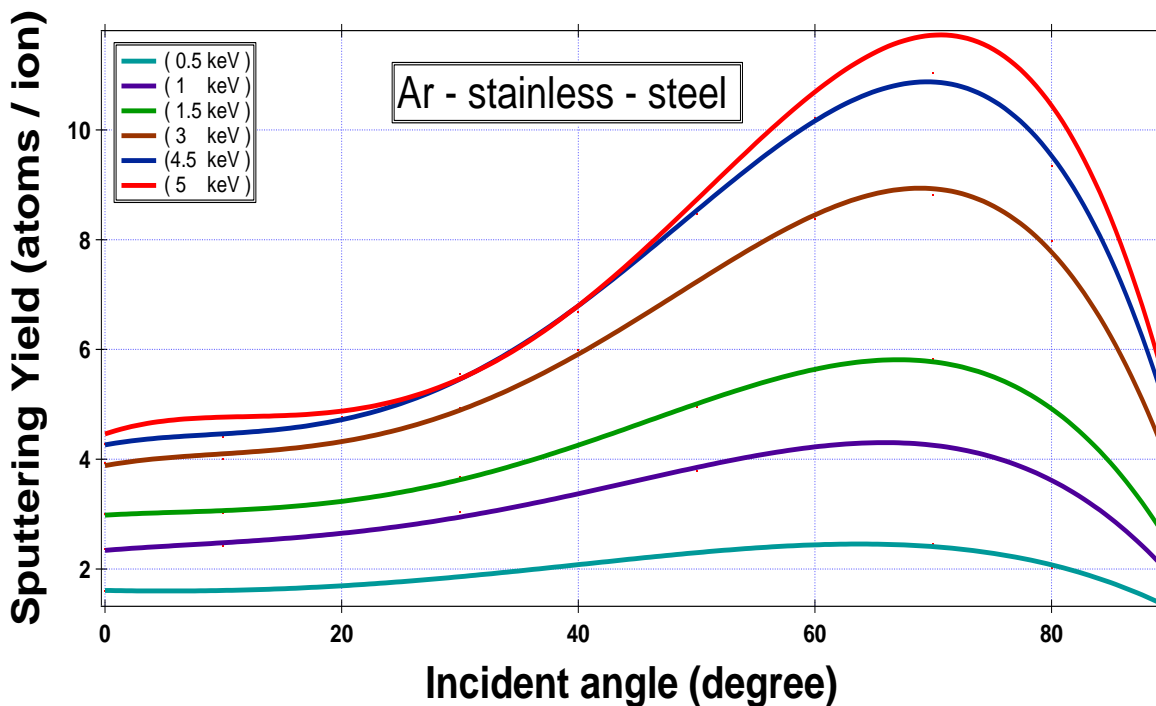


Fig. (3-7): incident ion angle dependence of S.Y of Stainless-Steel alloy bombard by Argon ion.

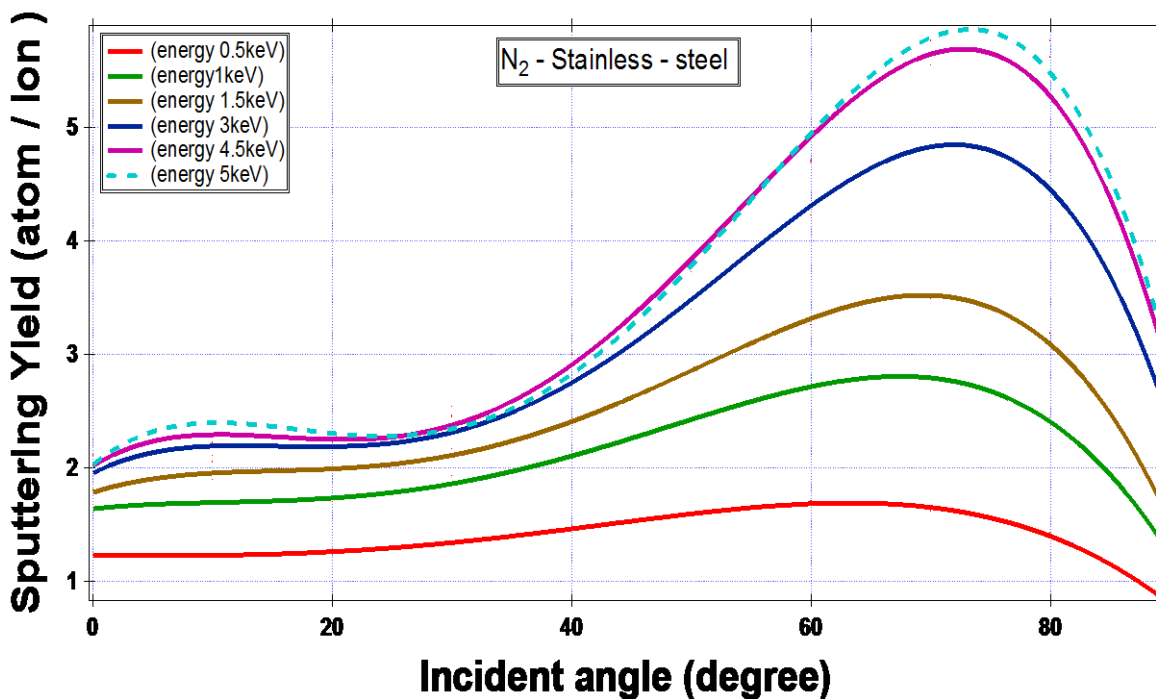


Figure (3-8): incident ion angle dependence of S.Y of Stainless-steel alloy bombard by Nitrogen ion.

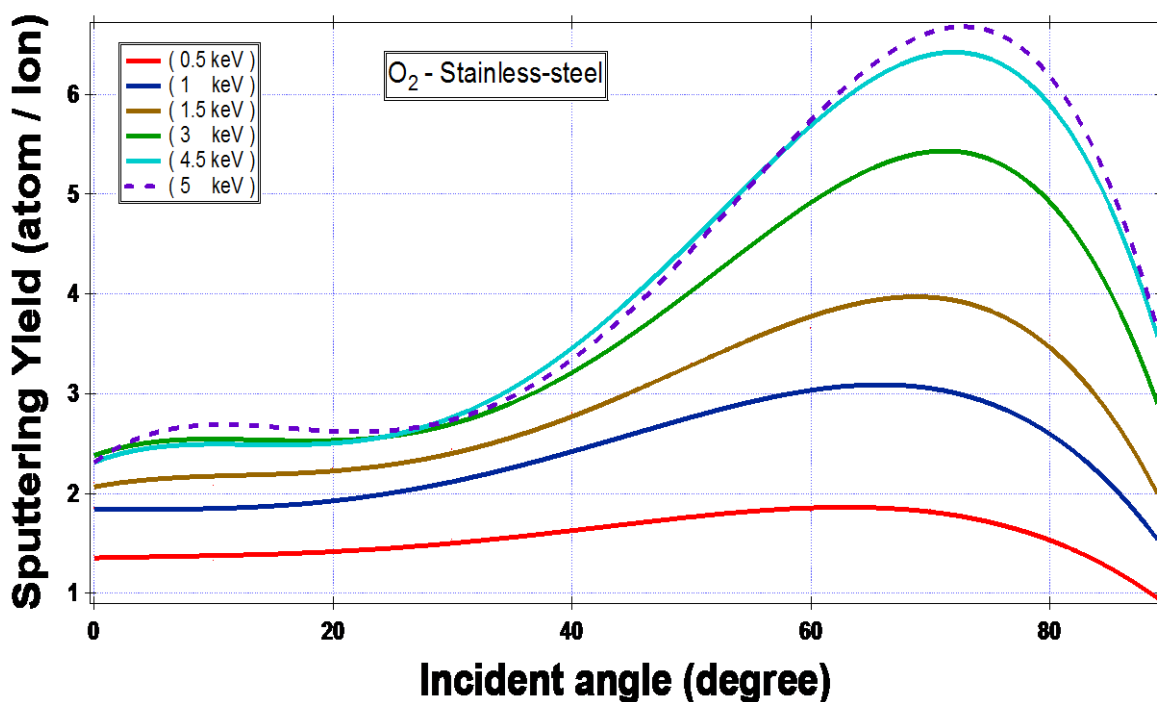


Figure (3-9): incident ion angle dependence of S.Y of Stainless-Steel alloy bombard by Oxygen ion.

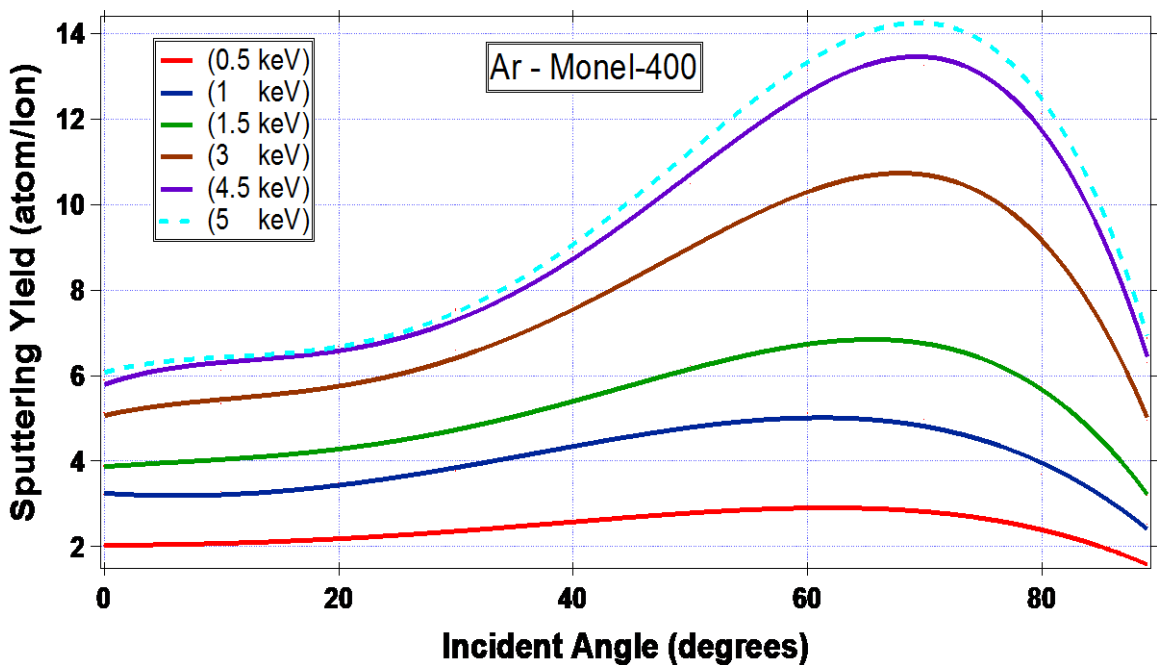


Figure (3-10): incident ion angle dependence of S.Y of Monel-400 alloy bombard by Argon ion.

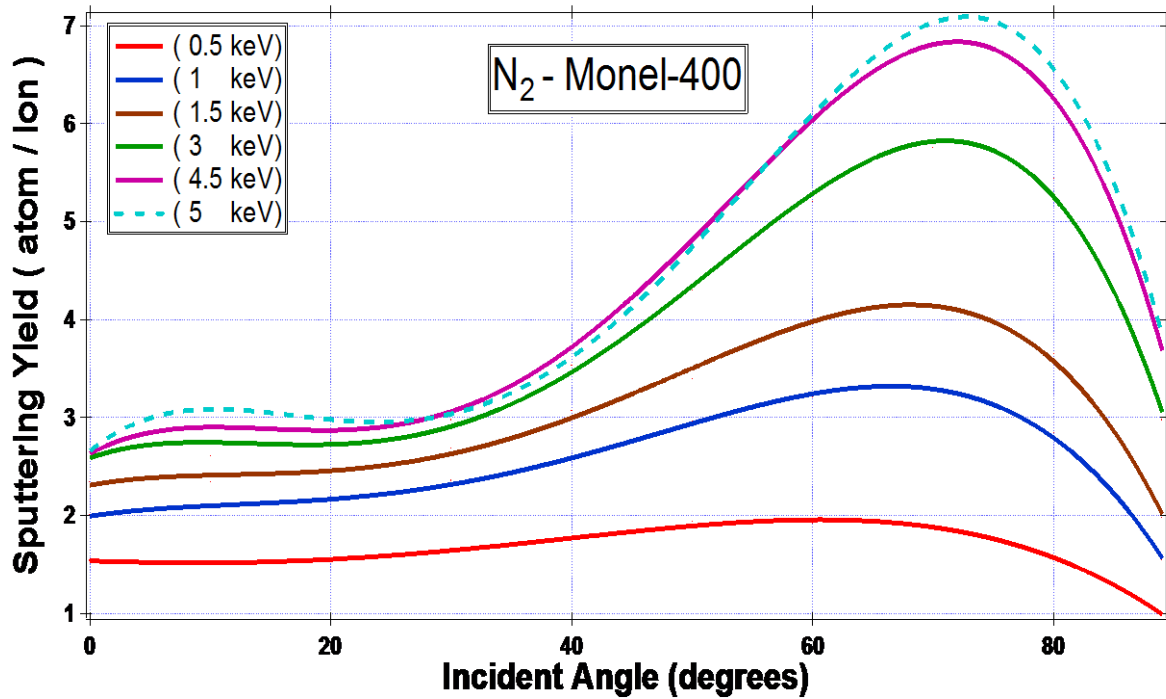


Figure (3-11): incident ion angle dependence of S.Y of Stainless-steel alloy bombard by Nitrogen ion.

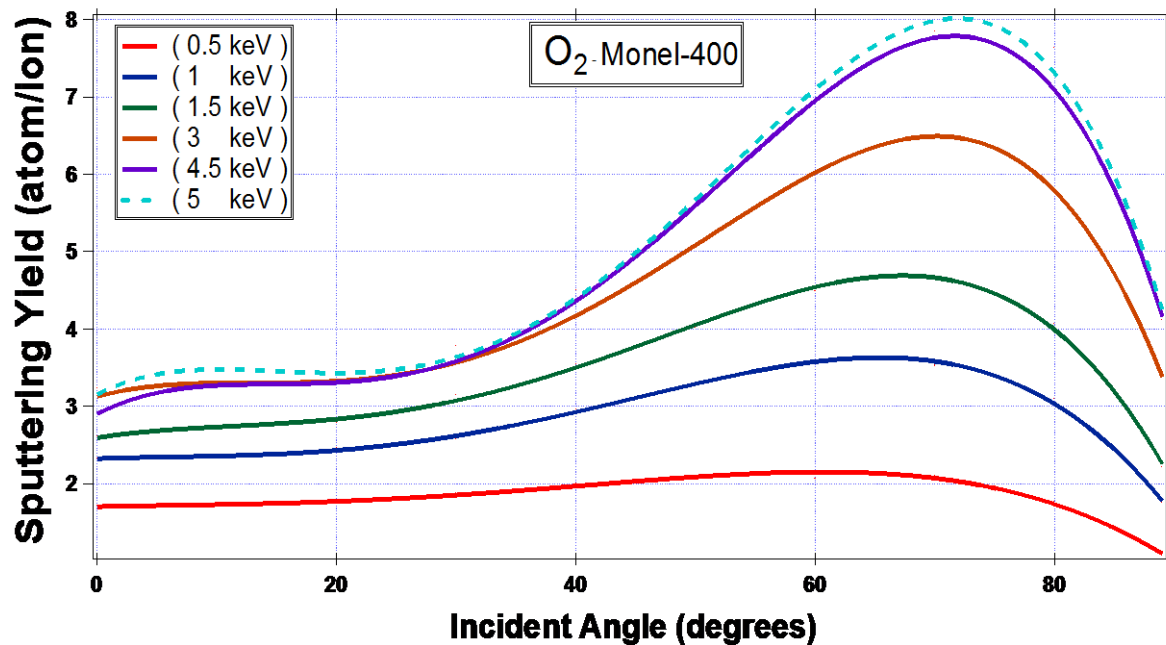


Figure (3-12): incident ion angle dependence of S.Y of Mone1-400 bombard by Oxygen ion.

(3-2-1) The normalized sputtering yield (NSY) vs. angle of the incident ion

It is often usually for the researchers on the topic of sputtering to use normalized sputter yield rather than direct sputter yield as soon as they treat with ion angle of incidence dependence.

The normalized sputter yield is the value ratio of sputter yield at a certain angle with respect to that at normal incidence ($\frac{Y_{\theta}}{Y_0}$). It is noted that a slight increase of the angle of incidence yields to a gradual increase in the normalized sputter yield reaching to the highest point of the angle 70° and then it drops rapidly towards low values as it approaches 89° .

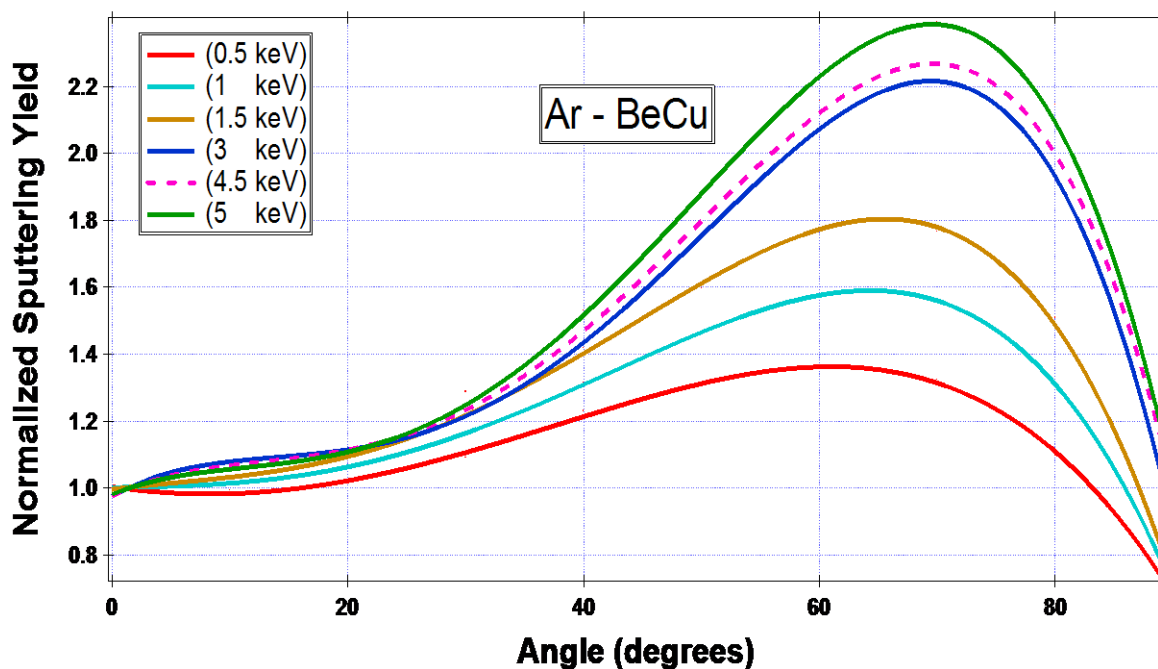


Figure (3-13): (NSY) vs. of the angle of ion incidence at BeCu alloy bombarded by Argon ion.

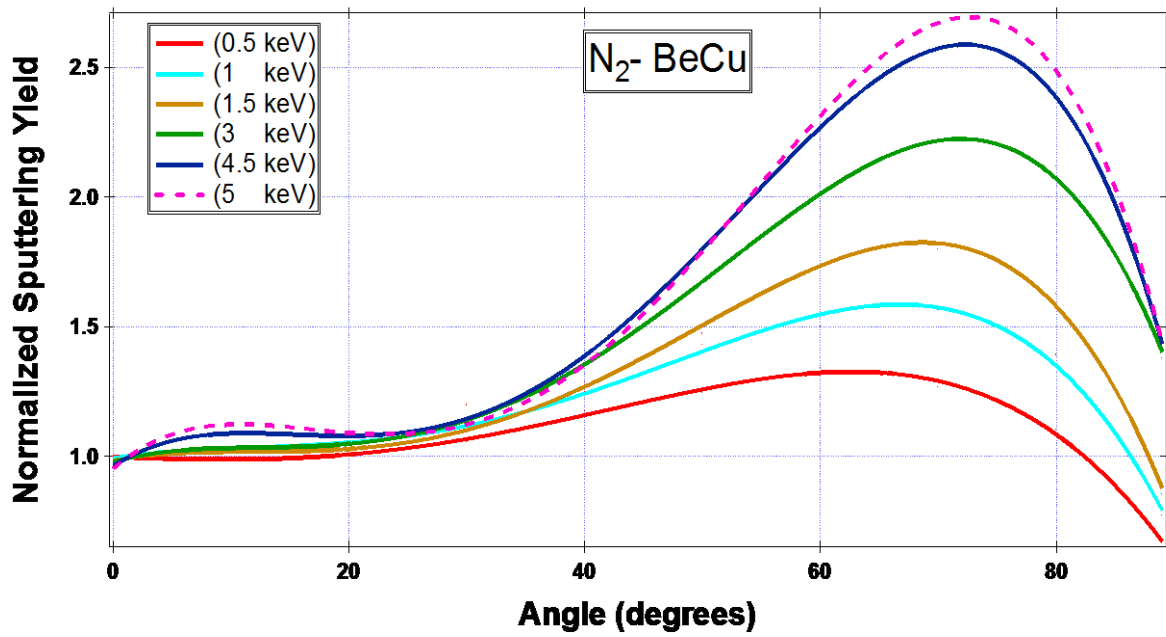


Figure (3-14): The (NSY) vs. of incident ion angle, the target of BeCu alloy bombarded by Nitrogen ion.

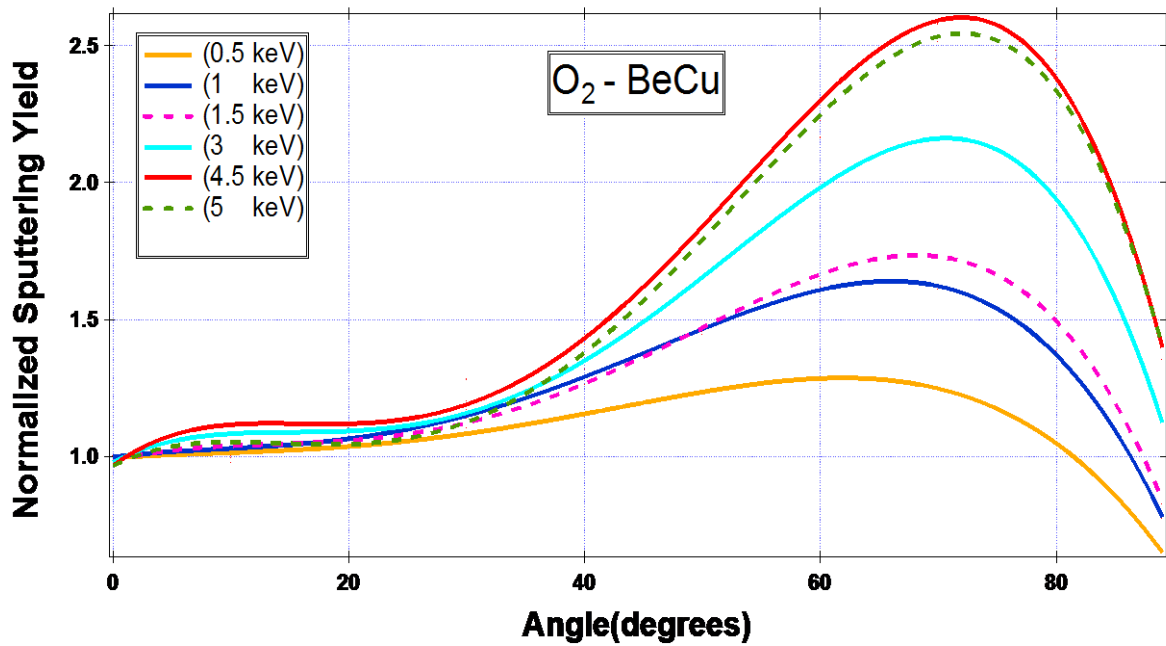


Figure (3-15): The (NSY) vs. of incident ion angle, the target of BeCu alloy bombarded by Oxygen ion.

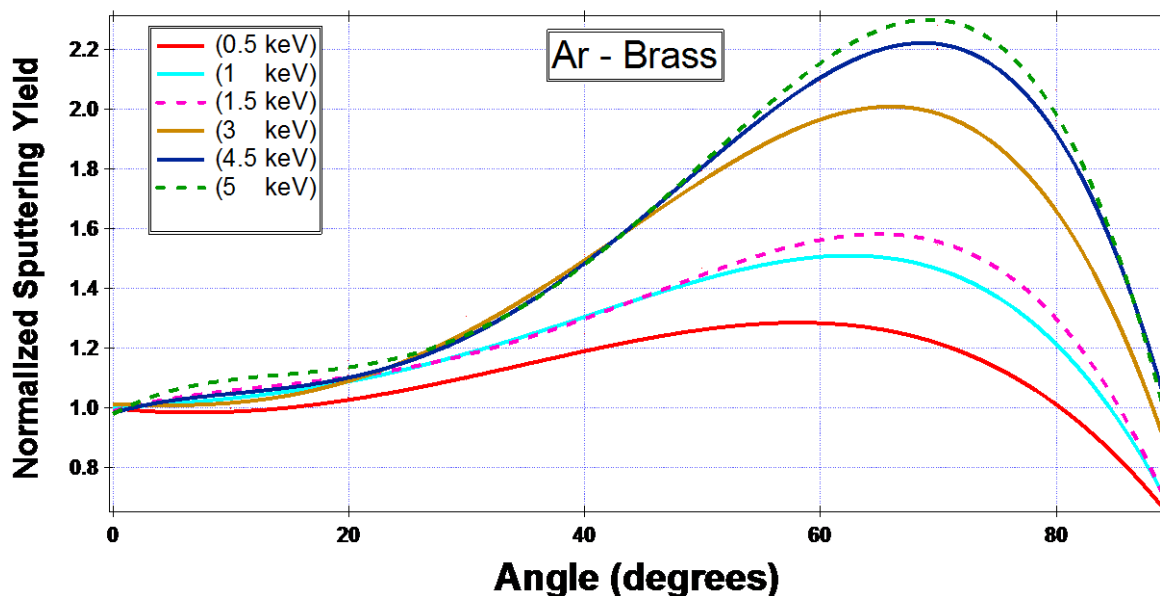


Figure (3-16): The (NSY) vs. of incident ion angle, the target of Brass alloy bombarded by Argon ion.

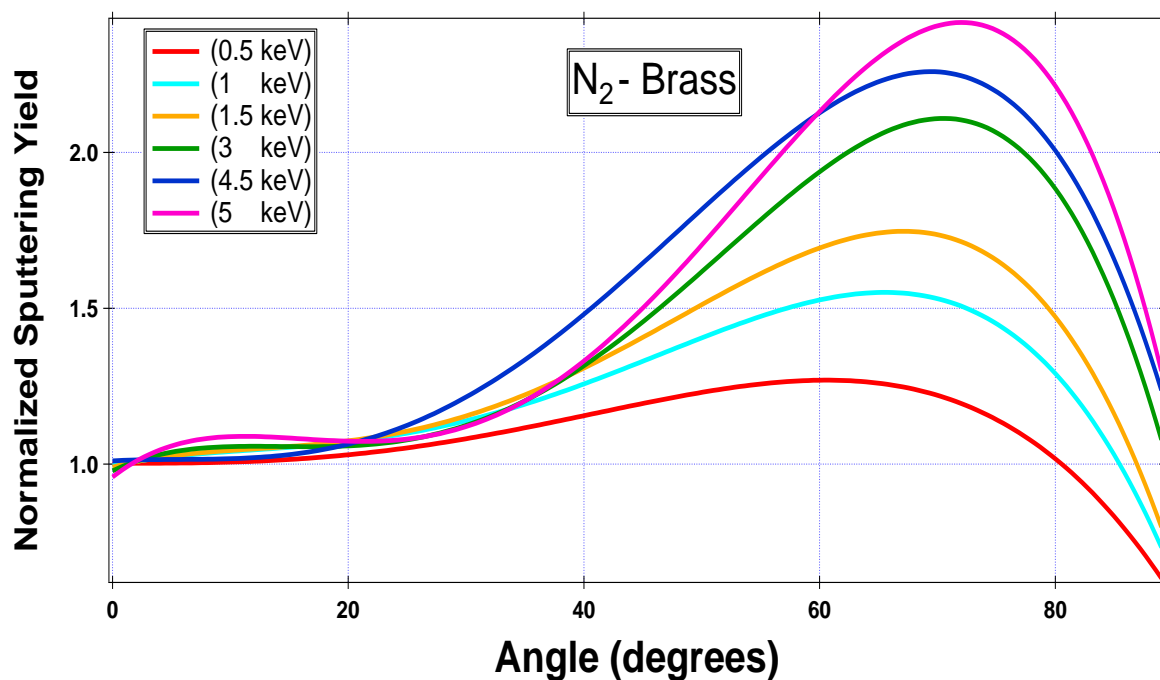


Figure (3-17): The (NSY) vs, of incident ion angle, the target of Brass alloy bombarded by Nitrogen ion.

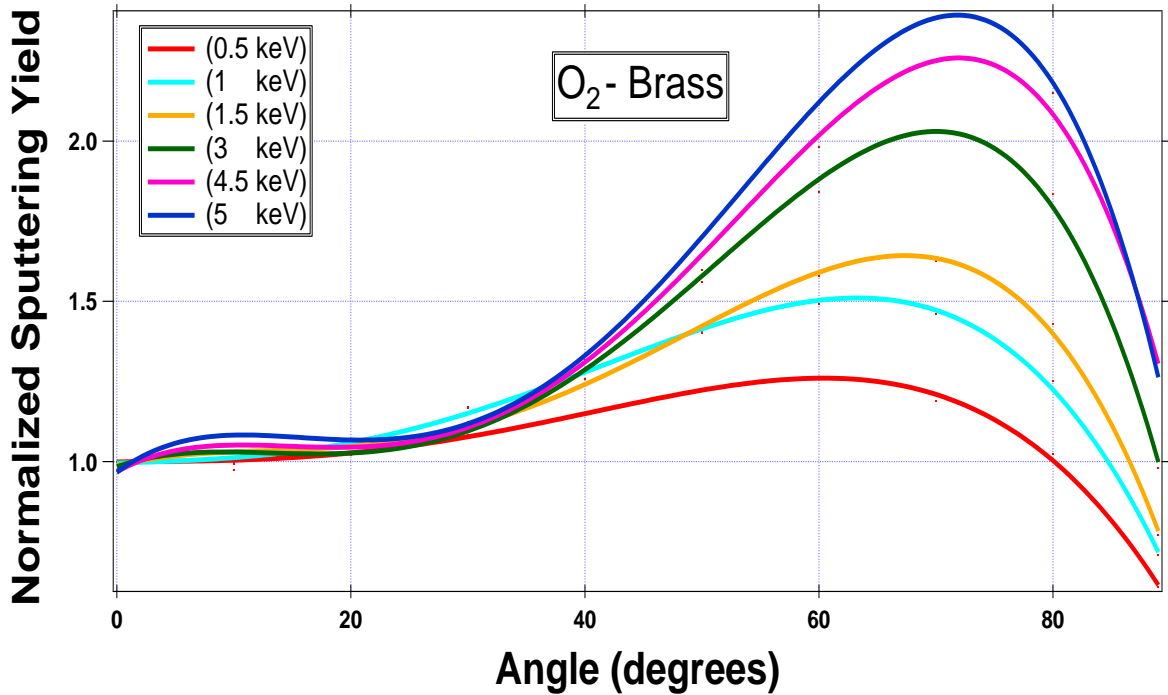


Figure (3-18): The normalized sputtering yield vs. of incident ion angle, the target of Brass alloy bombarded by Oxygen ion.

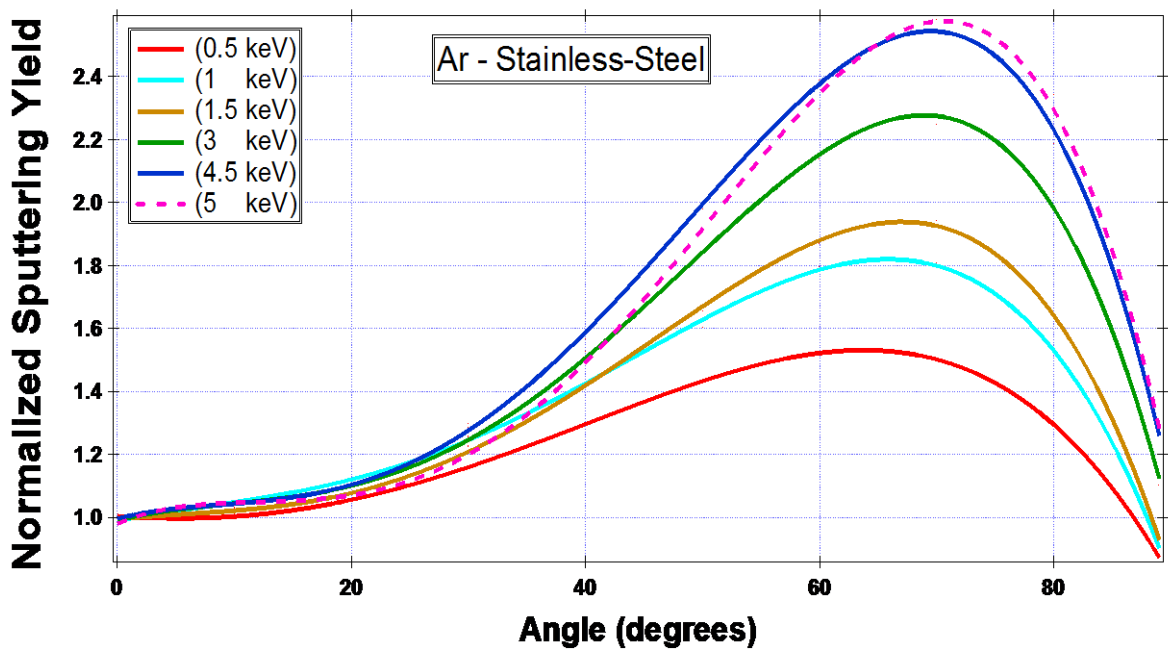


Figure (3-19): The normalized sputtering yield vs. of incident ion angle, the target of Stainless-Steel alloy bombarded by Argon ion.

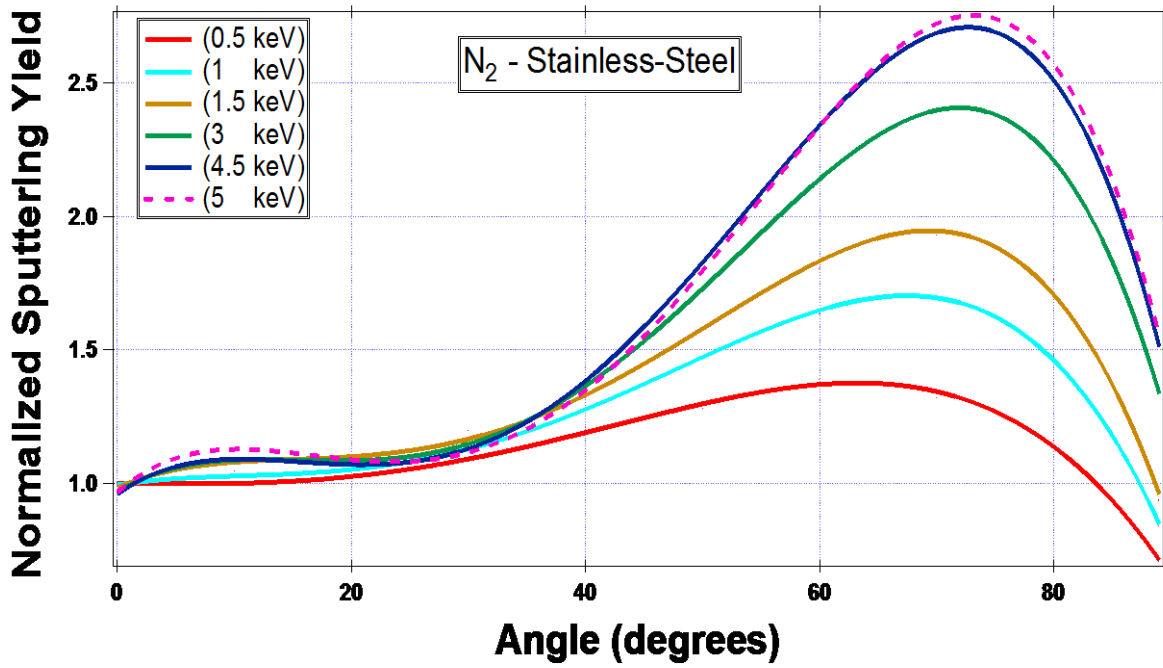


Figure (3-20): The normalized sputtering yield vs. of incident ion angle, the target of Stainless-Steel alloy bombarded by Nitrogen ion.

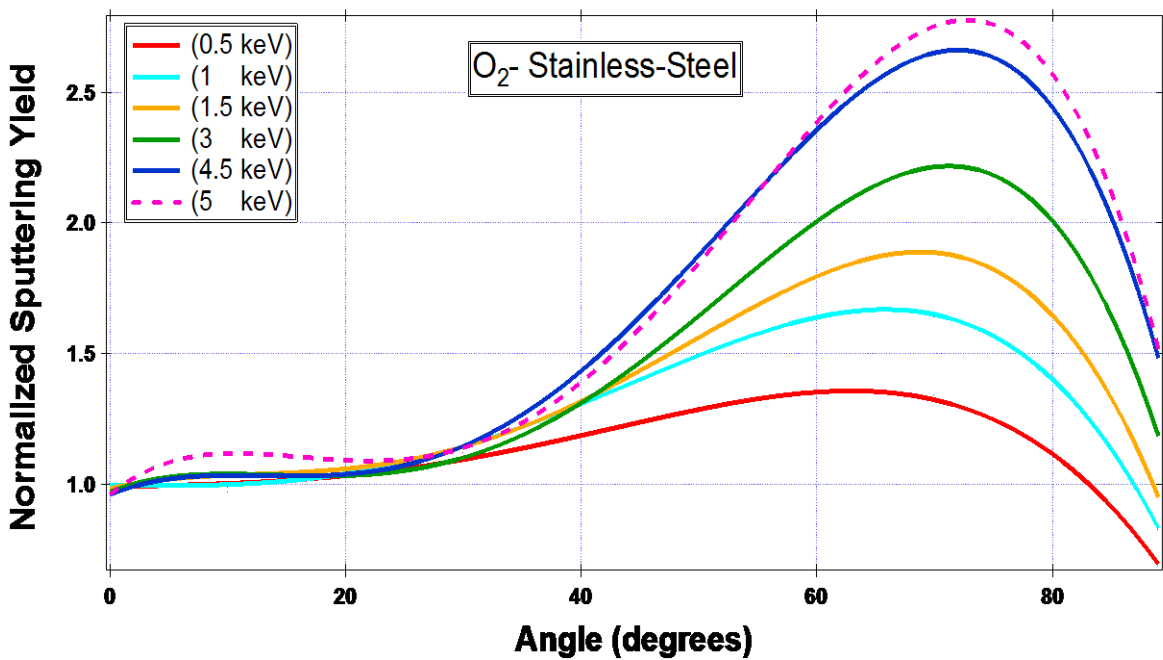


Fig. (3-21): (NSY) vs. of the angle, the target of Stainless-Steel alloy bombarded by Oxygen ion.

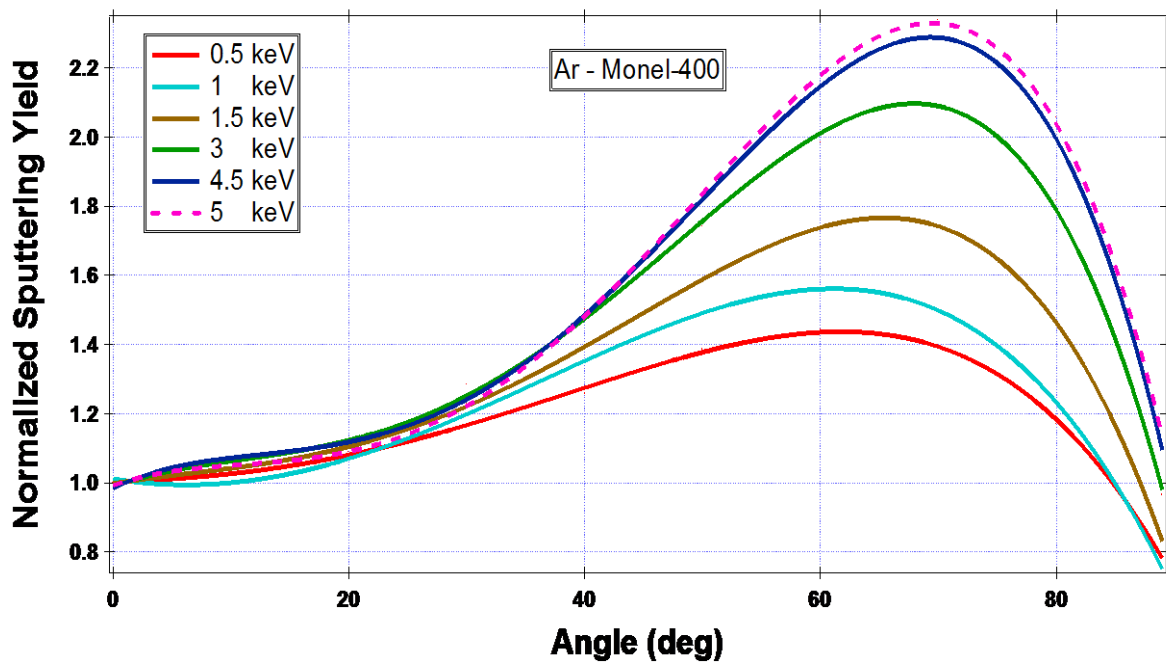


Figure (3-22) :(NSY) vs. of the angle, target of Monel-400 alloy bombarded by Argon ion.

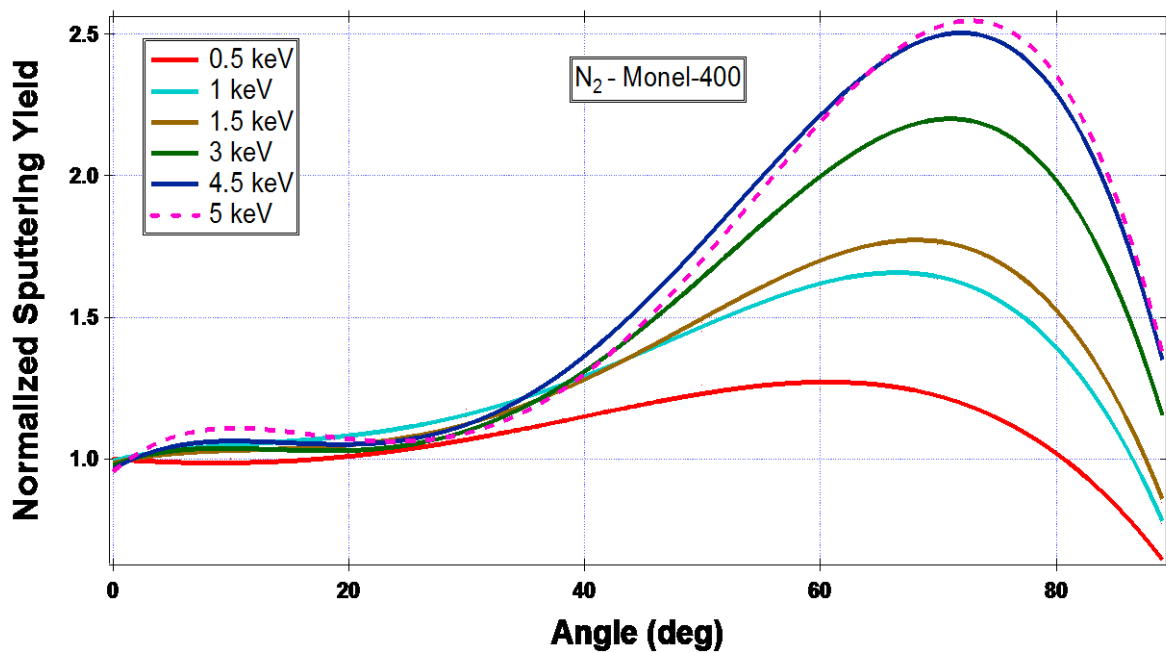


Figure (3-23): (NSY) vs. of the angle, the target of Monel alloy-400 bombarded by Nitrogen ion.

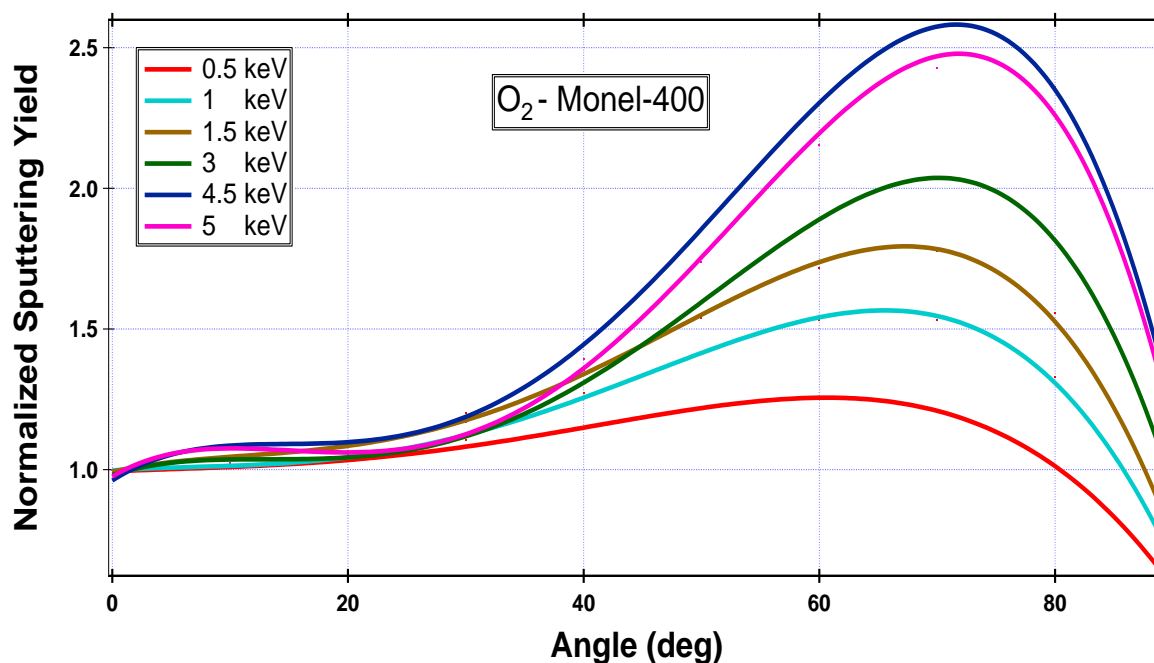


Figure (3-24): (NSY) vs. of the angle, the target of Monel alloy-400 bombarded by Oxygen ion.

(3-3) The influence of ion energy on the sputtering yield

Figures (3-25) to (3-36) show the sputtering yield vs. ion energy for (Beryllium - Copper, Brass, Stainless Steel, Monel - 400) alloys at a direct incident of (Ar, N₂, and O₂) ions, respectively. The width of each target is 1000Å, and the ion number used for these calculations is 5000. This huge of the ion number will interact per second with the target atoms at a direct bombardment and will stop at a certain range of the target. The maximum energy transferred by ions to the target occurs approximately at a half distance of the ion range in the target. Therefore, the collision cascades regions extend from the surface to the distance of maximum energy deposited into the target. Sputtering yield increases with incident ion energy and then begins to decline, the reason for this is attributable to the incident ions of high - energy because it does not happen to sputter, but implemented ions from the target sputtering will not occur, At incident ion energies below the threshold energy (E_{th}), The

S.Y display a threshold minimum which the energy transmitted to atoms of the target are too small for them to beat energy that surface atoms binding (U_b).

We have fitted the curves of the sputtering yield vs. ion energy to get a semi-empirical equation (3-2) for figures (3 - 25) - (3 - 36). The fitted data are given by:

$$S.Y = Y_0 + A \exp \left\{ -\frac{\left(\ln \frac{E}{X_0} \right)^2}{w} \right\} \dots \dots \dots (3-2)$$

Where (Y_0 , A , X_0 , and w) are parameters depending for the ion energy. And the tables (3-13) to (3-24) give the values of these parameters according to the different incident angle (0° , 10° , 20° ,, 89°).

Table (3-13): parameters of equation (3-2) as Argon ions bombarding of BeCu alloy target which are shown in figure (3-25)

θ°	Y_0	A	X_0	w
0	-0.18276	7.587	18.906	3.4382
10	0.0072488	7.3976	17.115	3.252
20	-0.25194	8.2771	16.924	3.301
30	-0.079732	9.4609	17.488	3.1381
40	-0.0080058	11.877	22.864	3.2175
50	0.090208	12.416	28.231	3.3023
60	-0.030139	20.665	38.391	3.1763
70	0.18501	29.045	73.599	3.2733
80	219.18	-218.35	0.16263	13.884
89	283.74	-282.89	0.20306	20.996

Table (3-14): parameters of equation (3-2) plotted as Nitrogen ions bombarding of BeCu alloy target which are shown in figure (3-26)

θ°	Y_0	A	X_0	w
0	-0.99086	3.657	4.9286	3.9429
10	-0.66565	3.3896	4.8148	3.6112
20	-0.74672	3.6304	5.0723	3.6328
30	-0.5432	3.8285	5.6204	3.3837
40	-0.47618	4.3804	6.2799	3.2167
50	-0.32146	5.1833	7.8611	3.0719
60	-0.020898	6.4012	9.8589	2.8061
70	-0.055278	8.4402	16.006	2.9232
80	-0.055431	11.072	43.975	3.2978
89	0.032936	7.7299	127.33	3.8561

Table (3-15): parameters of equation (3-2) as Oxygen ions bombarding of BeCu alloy target which are shown in figure (3-27).

θ°	Y_0	A	X_0	W
0	-0.44994	3.668	5.5467	3.4222
10	-0.33059	3.599	5.4544	3.2966
20	-0.49705	3.9744	5.9467	3.4155
30	-0.3591	4.283	6.3201	3.2302
40	-0.3474	5.0835	7.5709	3.1531
50	-0.17138	6.1232	8.5296	2.9136
60	-0.13297	7.822	12.026	2.9357
70	0.094484	9.9086	17.735	2.8659
80	0.11098	13.318	50.524	3.2306
89	-0.18659	10.79	357.55	4.5462

Table (3-16): parameters of equation (3-2) as Argon ions bombarding of the brass alloy target which are shown in figure (3-28).

θ°	Y_0	A	X_0	w
0	-0.30676	11.115	17.873	3.4887
10	-0.35201	11.323	17.082	3.4512
20	-0.26168	12.037	16.316	3.3423
30	0.082976	13.591	16.687	3.1197
40	-0.13744	16.742	19.477	3.1752
50	-0.28032	21.72	25.801	3.221
60	0.26304	28.72	35.73	3.0756
70	55.067	-54.551	0.17897	4.8169
80	300.62	-299.96	0.15515	13.867
89	261.38	-260.69	0.18821	17.108

Table (3-17): parameters of equation (3-2) as Nitrogen ions bombarding of brass alloy target which are shown in figure (3-29).

θ°	Y_0	A	X_0	w
0	-0.99086	3.657	4.9286	3.9429
10	-0.66565	3.3896	4.8148	3.6112
20	-0.74672	3.6304	5.0723	3.6328
30	-0.5432	3.8285	5.6204	3.3837
40	-0.47618	4.3804	6.2799	3.2167
50	-0.32146	5.1833	7.8611	3.0719
60	-0.020898	6.4012	9.8589	2.8061
70	-0.055278	8.4402	16.006	2.9232
80	-0.055431	11.072	43.975	3.2978
89	0.032936	7.7299	127.33	3.8561

Table (3-18): parameters of equation (3-2) plotted as Oxygen ions bombarding of the brass alloy target which are shown in figure (3-30).

θ°	Y_0	A	X_0	w
0	-0.56407	5.3982	5.5053	3.3287
10	-1.0572	5.8856	5.728	3.671
20	-0.77865	5.9356	5.6151	3.3883
30	-0.38691	6.2222	6.1875	3.0991
40	-0.42623	7.3321	7.0522	3.0782
50	-0.37016	8.7939	8.63	3.0092
60	-0.2606	11.073	12.003	2.9882
70	0.023532	14.129	18.951	2.9297
80	0.19069	18.495	52.854	3.2442
89	21.487	-21.198	0.12843	6.6059

Table (3-19): parameters of equation (3-2) plotted as Argon ions bombarding of Stainless-Steel alloy target which are shown in figure (3-31).

θ°	Y_0	A	X_0	w
0	-0.036868	5.1069	17.966	3.3599
10	0.026917	5.1523	15.784	3.1591
20	-0.021337	5.6569	15.644	3.1545
30	-0.057884	6.7427	17.054	3.1507
40	-0.092858	8.5511	19.528	3.1235
50	-0.12814	11.3	24.377	3.1311
60	0.073965	15.465	33.252	3.0452
70	0.43962	21.327	54.2	2.9986
80	49.118	-48.987	0.20333	6.2584
89	212.26	-211.86	0.15908	21.237

Table (3-20): parameters of equation (3-2) as Nitrogen ions bombarding of Stainless-Steel alloy target which are shown in figure (3-32).

θ°	Y_0	A	X_0	w
0	-0.07693	2.1271	4.5768	3.1809
10	-0.28008	2.3331	4.5646	3.4461
20	0.20457	2.0304	5.7779	2.5231
30	-0.10685	2.5954	5.1832	3.0984
40	-0.052045	3.0909	5.9758	2.9001
50	-0.053048	3.9268	6.9771	2.8345
60	-0.081304	5.0515	9.2142	2.8452
70	-0.046931	6.6806	14.561	2.8638
80	0.18199	8.5822	36.05	3.0212
89	0.026564	6.4574	136.73	3.8656

Table (3-21): parameters of equation (3-2) as Oxygen ions bombarding of Stainless-Steel alloy target which are shown in figure (3-33).

θ°	Y_0	A	X_0	w
0	-0.26464	2.6745	5.1968	3.4245
10	-0.1917	2.6305	5.4738	3.3116
20	-0.30099	2.9173	5.5566	3.3574
30	-0.35582	3.2949	6.0781	3.3768
40	-0.10521	3.7657	6.7802	2.9531
50	-0.16451	4.794	8.2487	2.9442
60	-0.09083	6.0813	10.746	2.8688
70	0.12	7.9005	16.672	2.7767
80	0.067956	10.429	41.829	3.1322
89	-0.16667	8.5751	293.71	4.453

Table (3-22): parameters of equation (3-2) as Argon ions bombarding of Monel-400 alloy target which are shown in figure (3-34).

θ°	Y_0	A	X_0	w
0	-0.15478	7.0903	19.008	19.008
10	-0.16299	7.2063	16.843	3.3053
20	-0.28075	7.8409	17.284	3.3523
30	-0.062805	9.0575	18.178	18.178
40	-0.10023	11.35	20.824	3.1116
50	0.045352	14.763	24.865	3.0026
60	0.01188	19.995	38.202	3.1129
70	0.41744	27.533	61.149	3.0346
80	0.46551	37.866	171.91	3.3357
89	162.74	-162.34	0.16573	16.557

Table (3-23): parameters of equation (3-2) as Nitrogen ions bombarding of Monel-400 alloy target which are shown in figure (3-35).

θ°	Y_0	A	X_0	w
0	-0.011263	2.7567	4.9527	2.9163
10	-0.05016	2.7853	4.9741	3.0274
20	-0.061835	2.9582	5.1446	3.0122
30	-0.33567	3.5475	5.6976	3.1919
40	-0.32396	4.1282	6.4099	3.1295
50	-0.43009	5.1253	7.6285	3.1696
60	-0.17391	6.3881	10.662	2.9226
70	0.095512	8.2056	15.321	2.7312
80	0.17062	10.656	36.498	2.9778
89	-0.12819	8.4065	210.23	4.2192

Table (3-24): parameters of equation (3-2) as Oxygen ions bombarding of Monel-400 alloy target which are shown in figure (3-36).

θ°	Y_0	A	X_0	w
0	-0.28672	3.4537	5.8252	3.3691
10	-0.27869	3.4778	5.7436	3.2911
20	-0.1187	3.5494	5.9593	3.11
30	-0.25992	4.1071	6.9044	3.2281
40	-0.22911	4.8918	7.5209	3.0611
50	-0.11097	6.0499	8.8541	2.8631
60	-0.082271	7.6335	11.762	2.8473
70	0.11121	9.932	18.658	2.8098
80	0.31279	12.981	45.327	2.981
89	14.805	-14.553	0.11467	6.6439

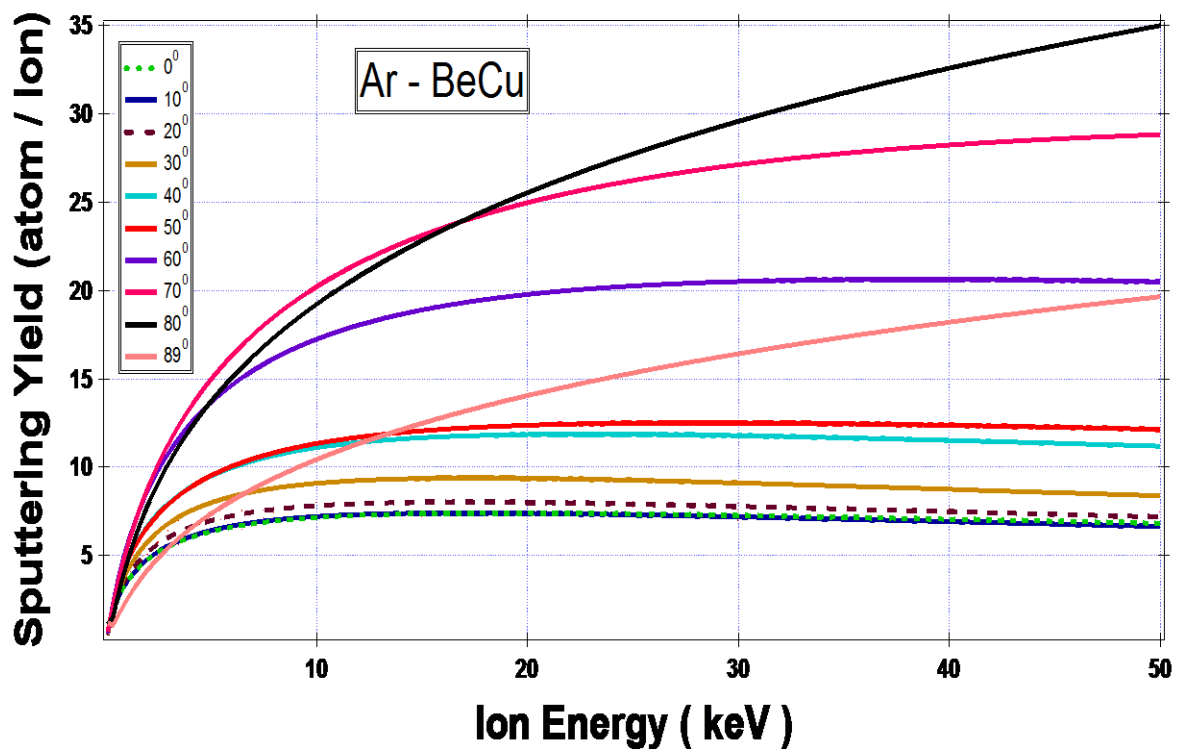


Figure (3-25): Energy dependence of S.Y of the incident for the bombarded by Ar^+ on BeCu alloy.

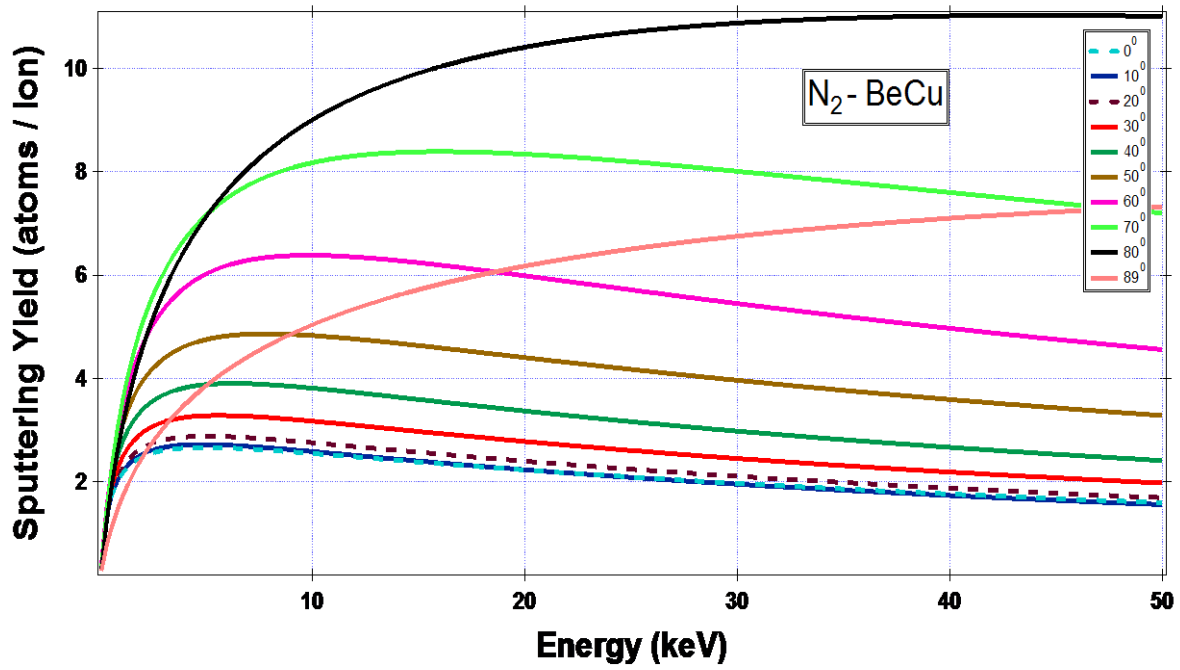


Figure (3-26): Energy dependence of S.Y of incident Nitrogen ions on BeCu alloy.

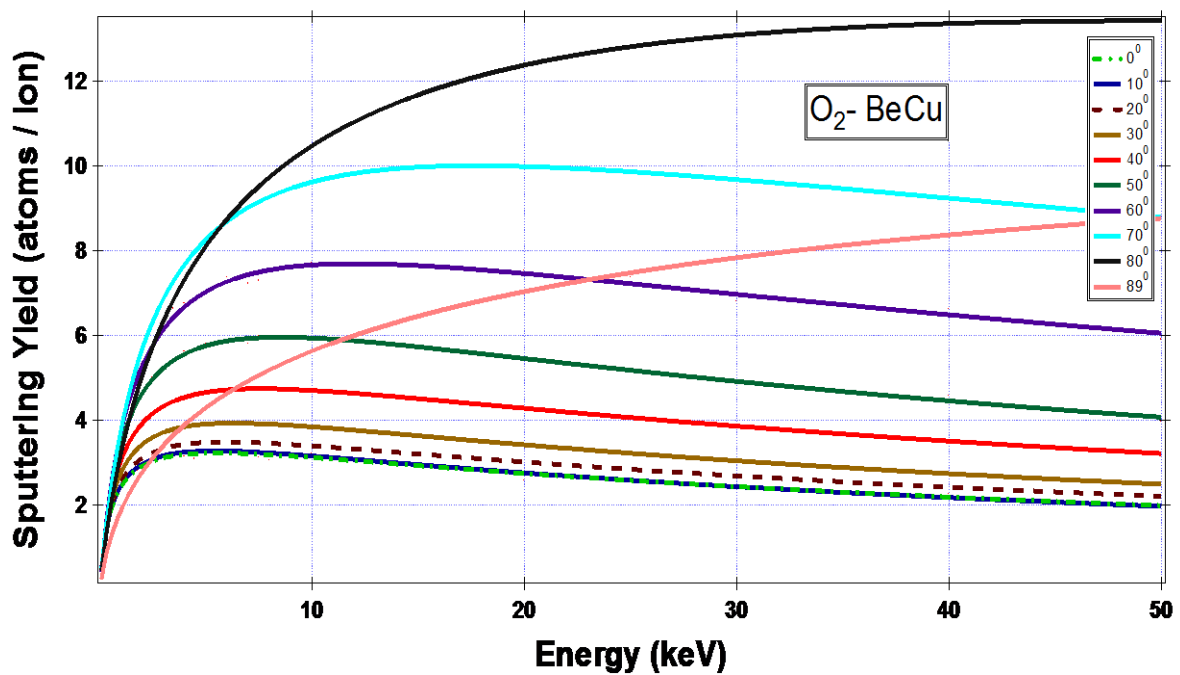


Figure (3-27): Energy dependence of S.Y of incident Oxygen ions on BeCu alloy.

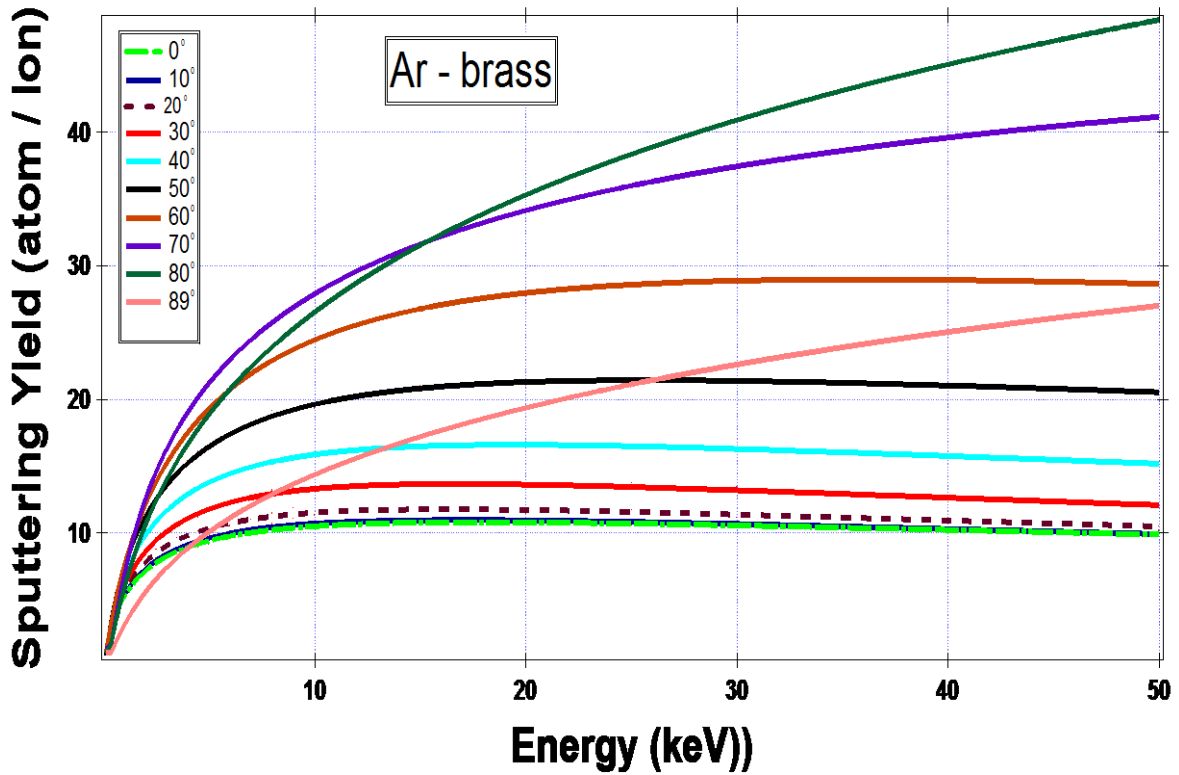


Figure (3-28): Energy dependence of S.Y of incident Argon ions on Brass alloy.

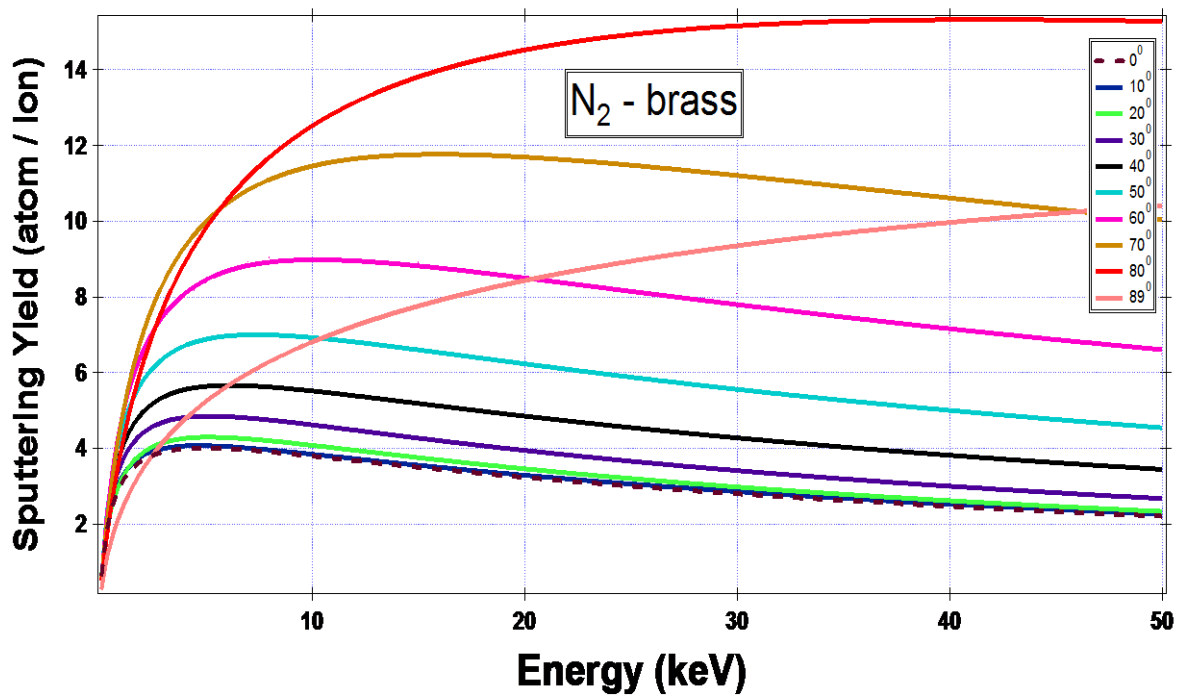


Figure (3-29): Energy dependence of S.Y of incident Nitrogen ions on Brass alloy.

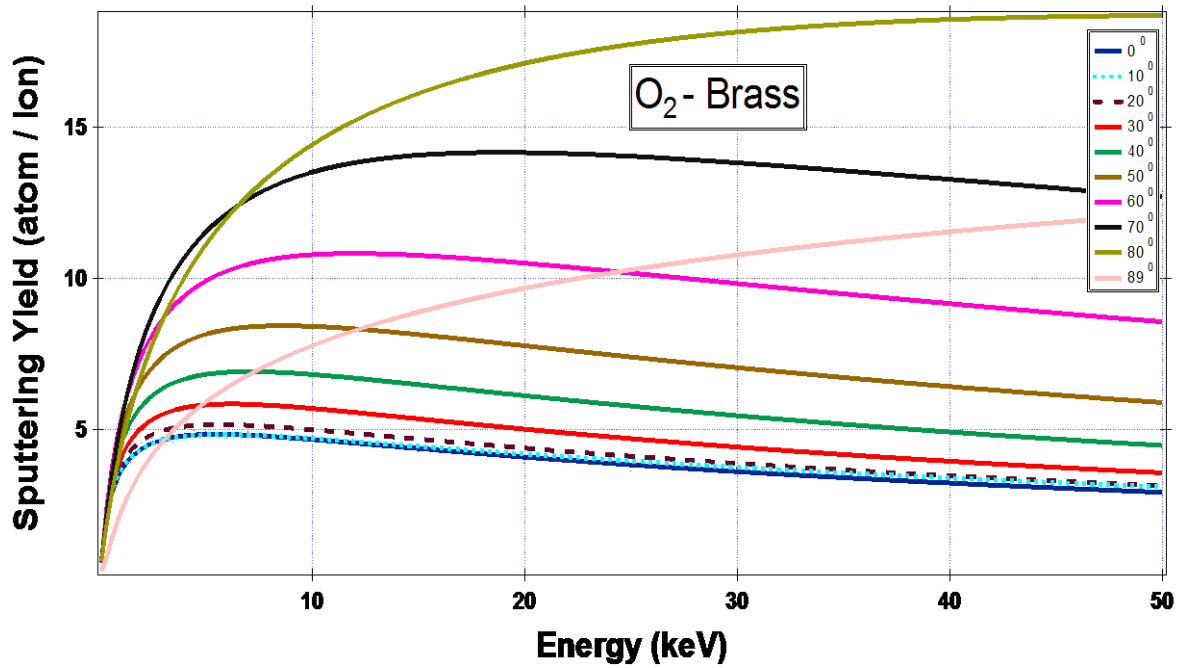


Figure (3-30): Energy dependence of S.Y of the incident for the bombarded by Oxygen ion on Brass alloy.

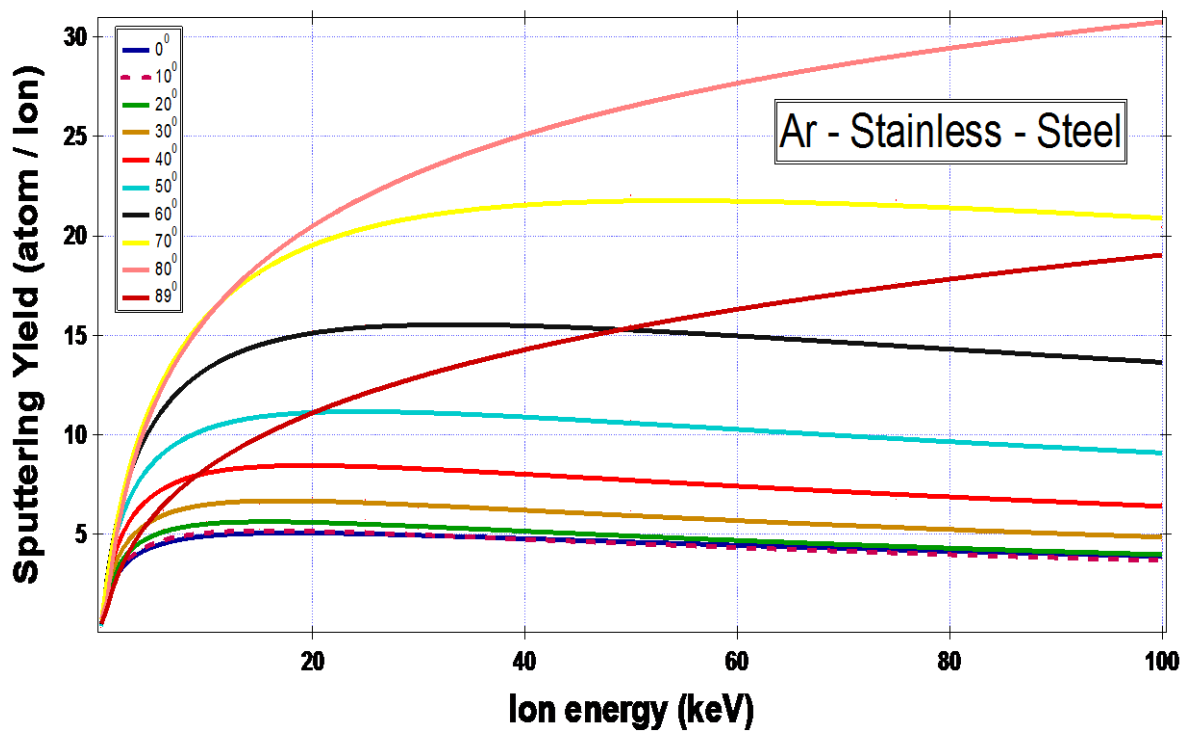


Figure (3-31): Energy dependence of S.Y of incident Argon ions on Stainless-Steel alloy.

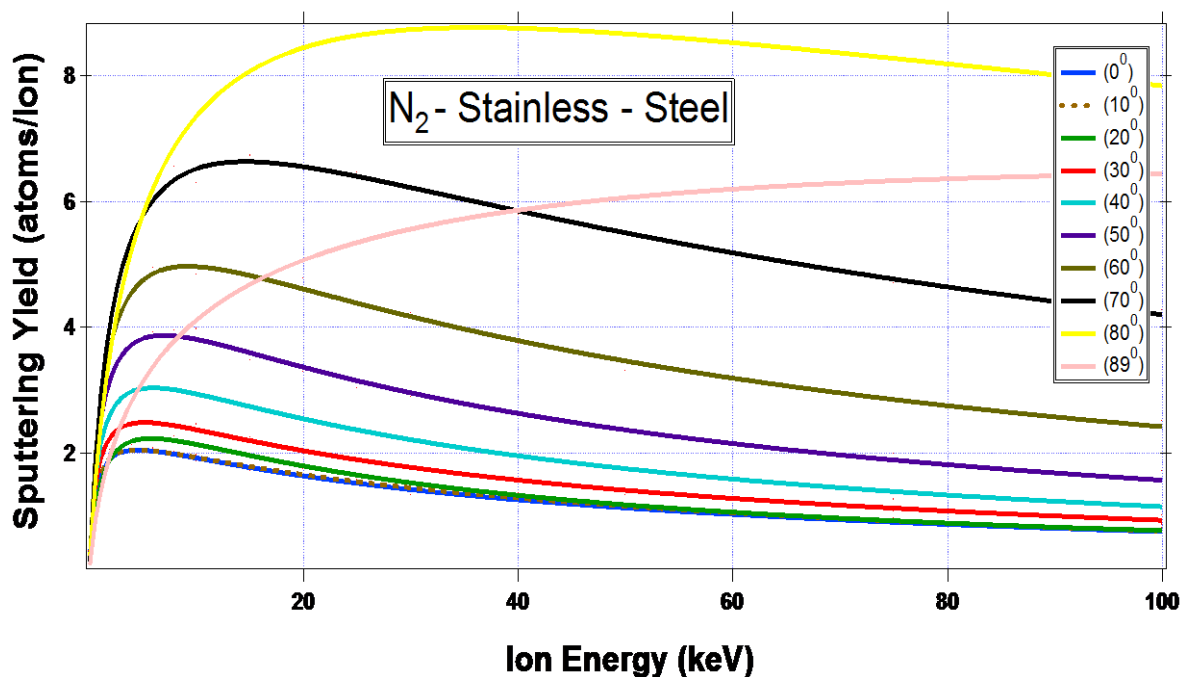


Figure (3-32): Energy dependence of S.Y of incident Nitrogen ions on Stainless-Steel alloy.

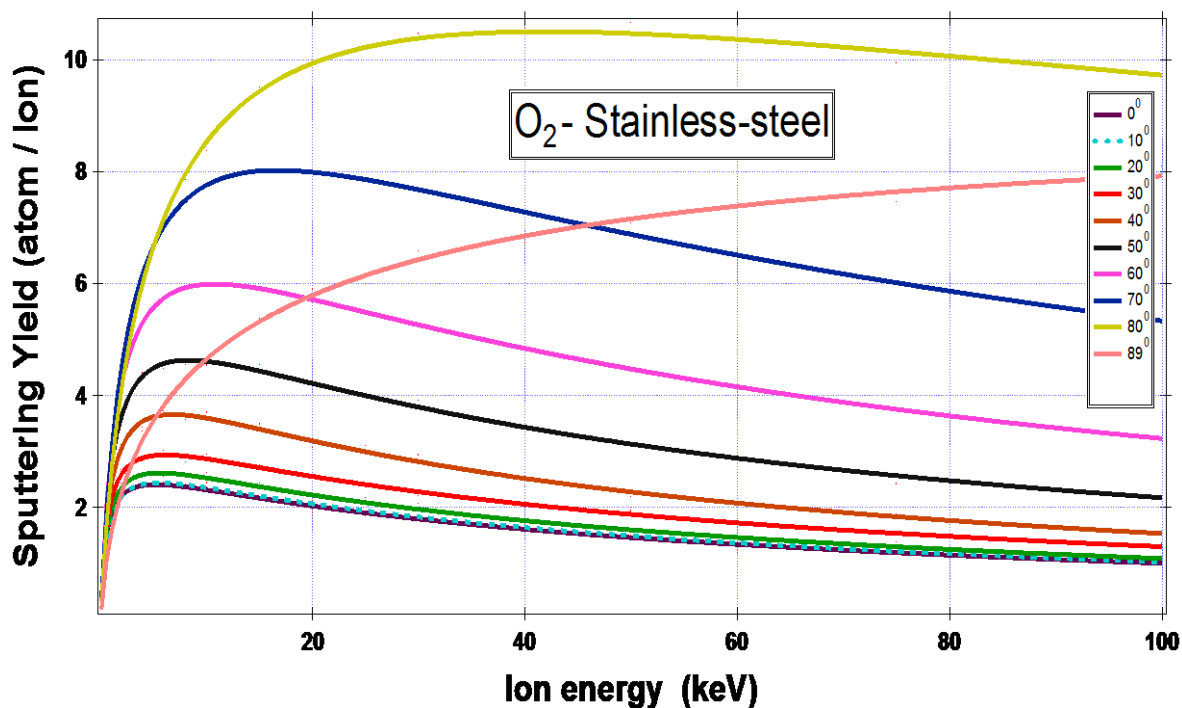


Figure (3-33): Energy dependence of S.Y of incident Oxygen ions on Stainless-Steel alloy.

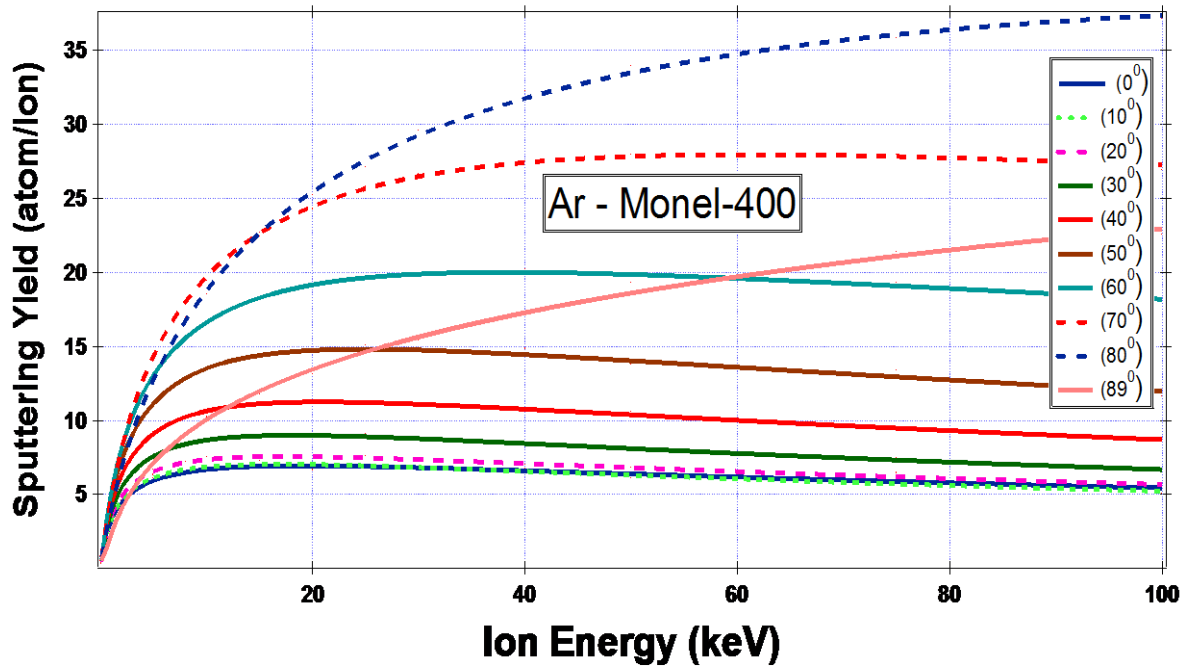


Figure (3-34): Energy dependence of S.Y of incident Argon ions on Monel-400 alloy.

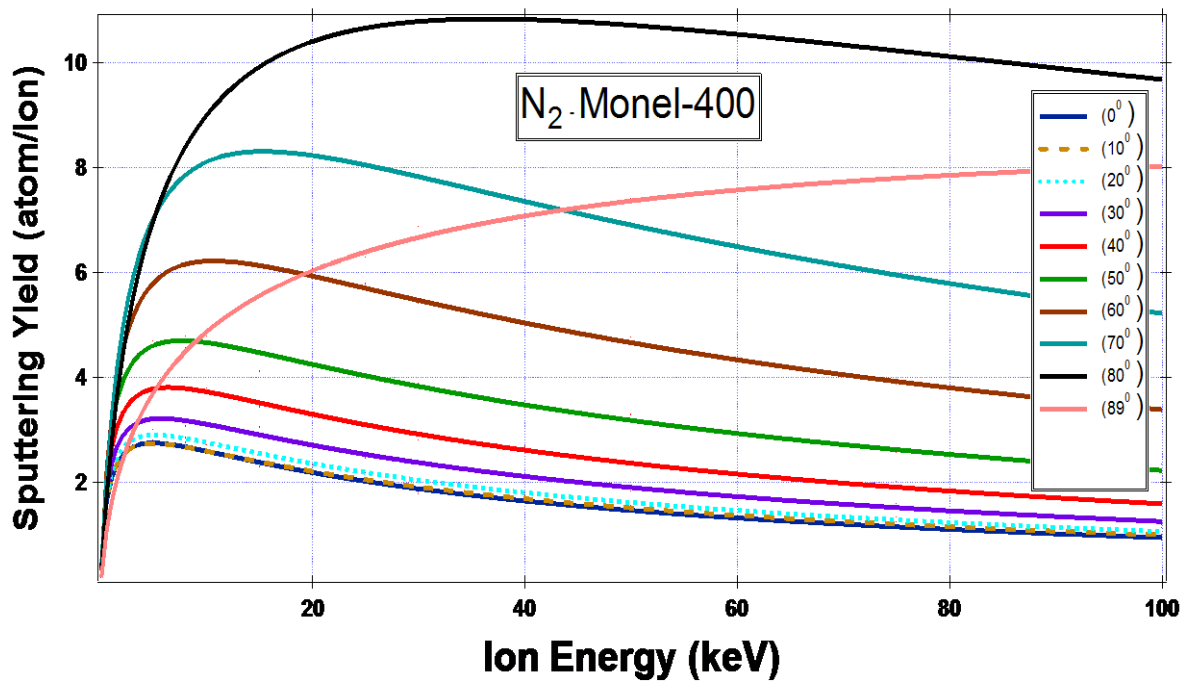


Figure (3-35): Energy dependence of S.Y of incident Nitrogen ions on Monel-400 alloy.

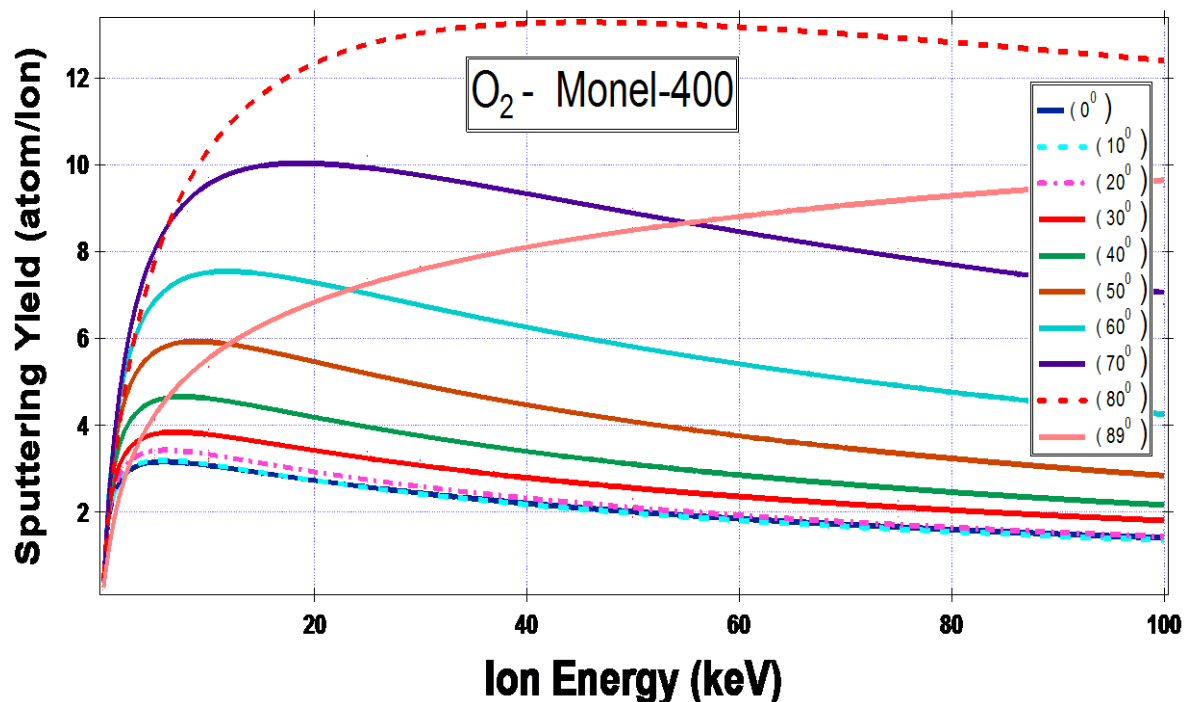


Figure (3-36): Energy dependence of S.Y. of incident Oxygen ions on Monel-400 alloy.

(3-4) The energy for sputtering yield maxima vs. angle of the incident ion

We Note from Figure (3-37) to (3-40) that ion energy vs. sputtering yield maxima, $E(S.Y_m)$ increases with increasing incident angle, this increase is slightly when angles less than (60°) , then increases significantly. For each of the (BeCu, Brass, Stainless-Steel, Monel-400) alloys, respectively. Observe that the argon ion is higher $E(S.Y_m)$ of other ions.

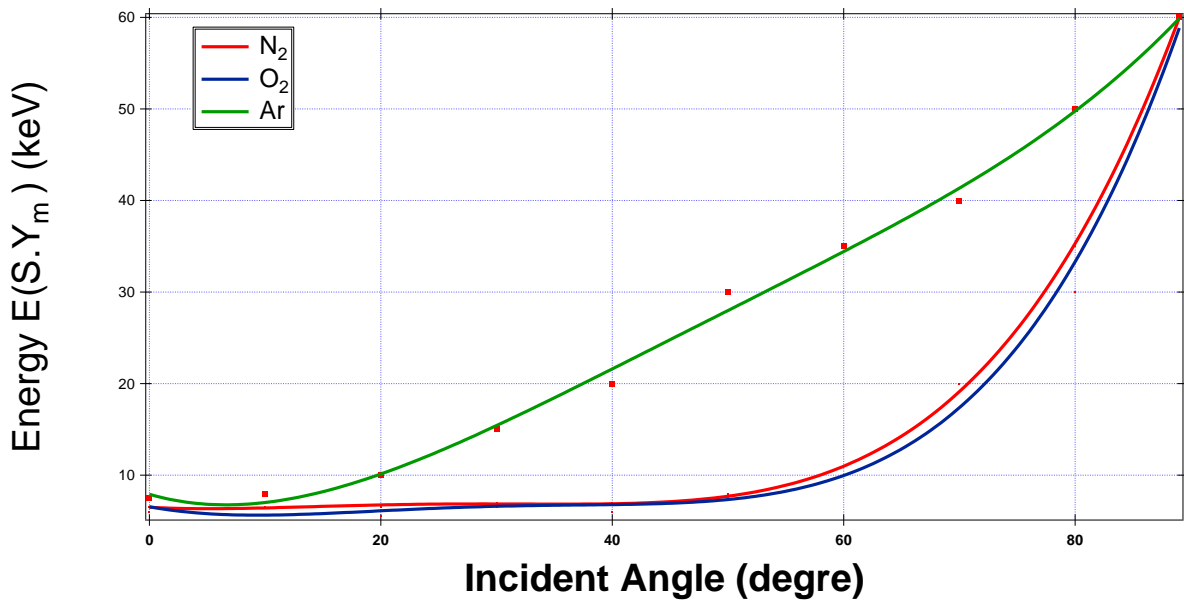


Figure (3-37): ion energy for S.Y maxima vs. angle. (BeCu alloy)

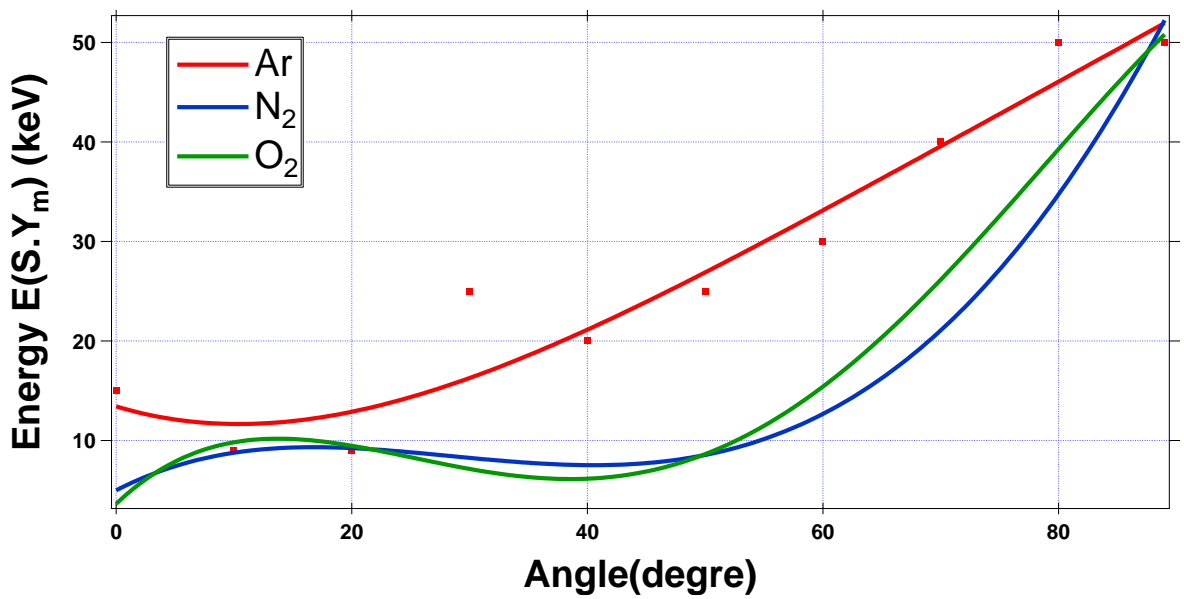


Figure (3-38): ion energy for E (S.Y_m) vs. ion incident angle. (Brass alloy)

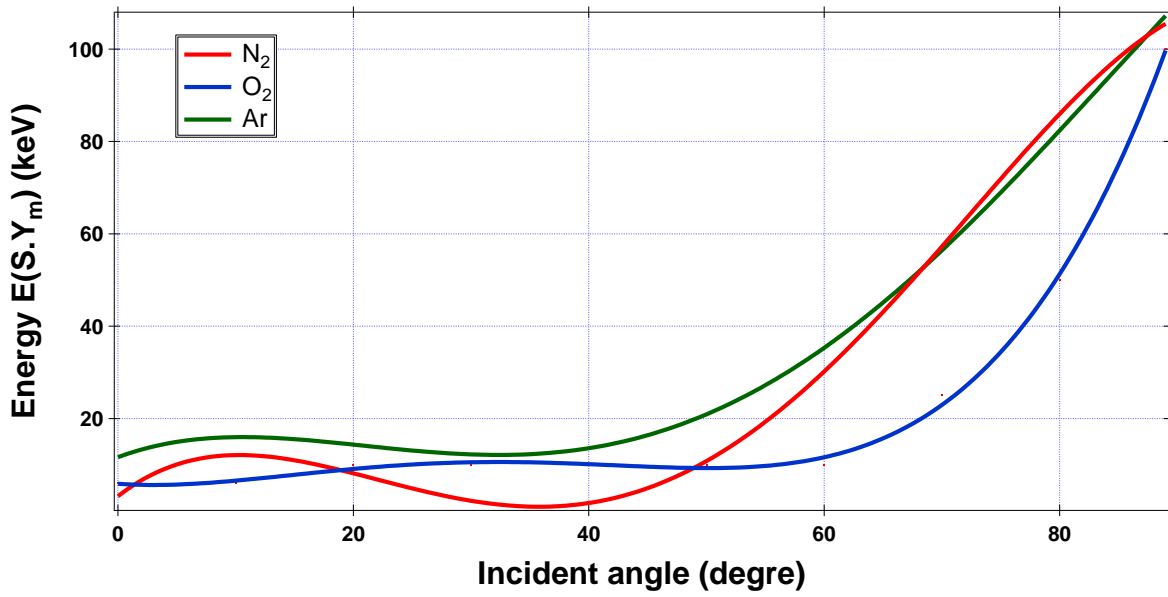


Fig. (3-39): ion energy for $E(S.Y_m)$ vs. ion incident angle. (Stainless-Steel alloy)

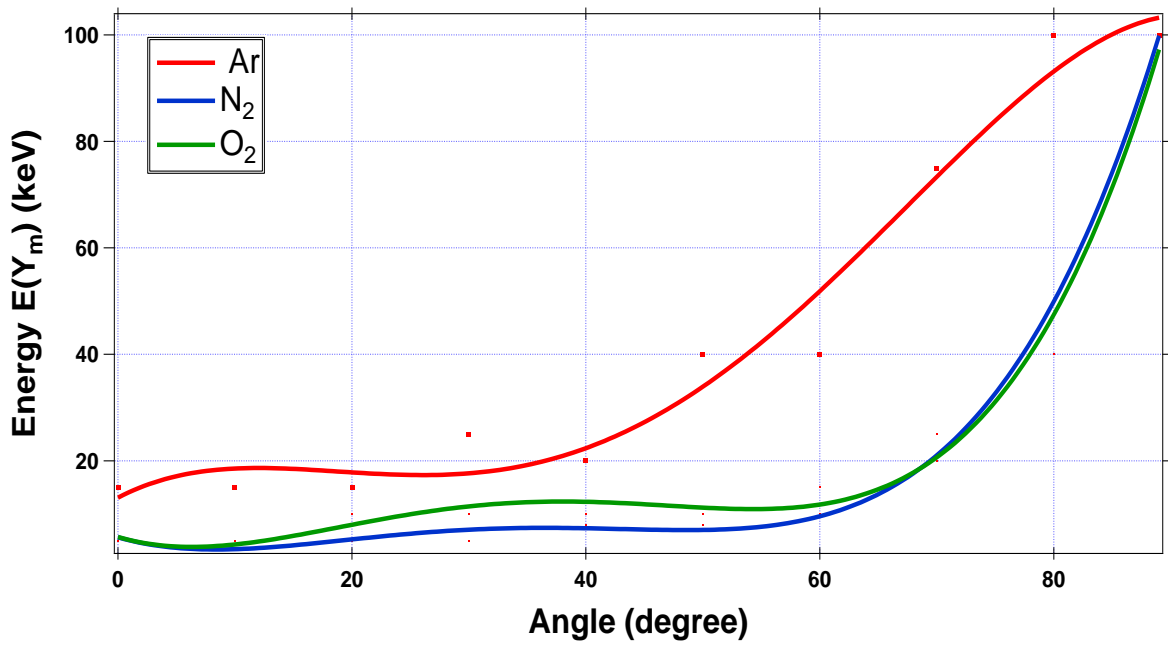


Figure (3-40): ion energy for $E(S.Y_m)$ vs. ion incident angle. (Monel-400 alloy)

(3-5) The influence of the atomic number of ions on the sputtering yield

Figures (3 - 41) to (3 – 44) illustrates the relationship between sputtering yield and an atomic number of ion bombardment, where we notice that sputtering yield increases with an increasing atomic number of ions (Ar, N₂, O₂), with ion energy 5 keV, incident angle (0°), width target 1000A⁰ and 5000 ions number bombardment the (BeCu, Brass, Stainless- Steel, Monel – 400) alloys. The fitting equation is (3-3) is given by:

$$Y = a + b Z \dots\dots\dots (3 - 3)$$

And table (3-25) gives the values of these parameters according to the different alloy.

Table (3-25): Parameters for equation (3-3) fitting for sputtering yield as a function of atomic number of incident ion (Z), bombarding of (Ar, N₂ and O₂) ion, target, in (BeCu, Brass, Stainless-Steel, Monel-400) alloy are shown in figures (3-41) – (3 – 44).

Alloy	<i>a</i>	<i>b</i>
BeCu	0.44831	0. 32194
Brass	1.1304	0.44429
Stainless-Steel	0.6094	0.21933
Monel – 400	0.775	0.29728

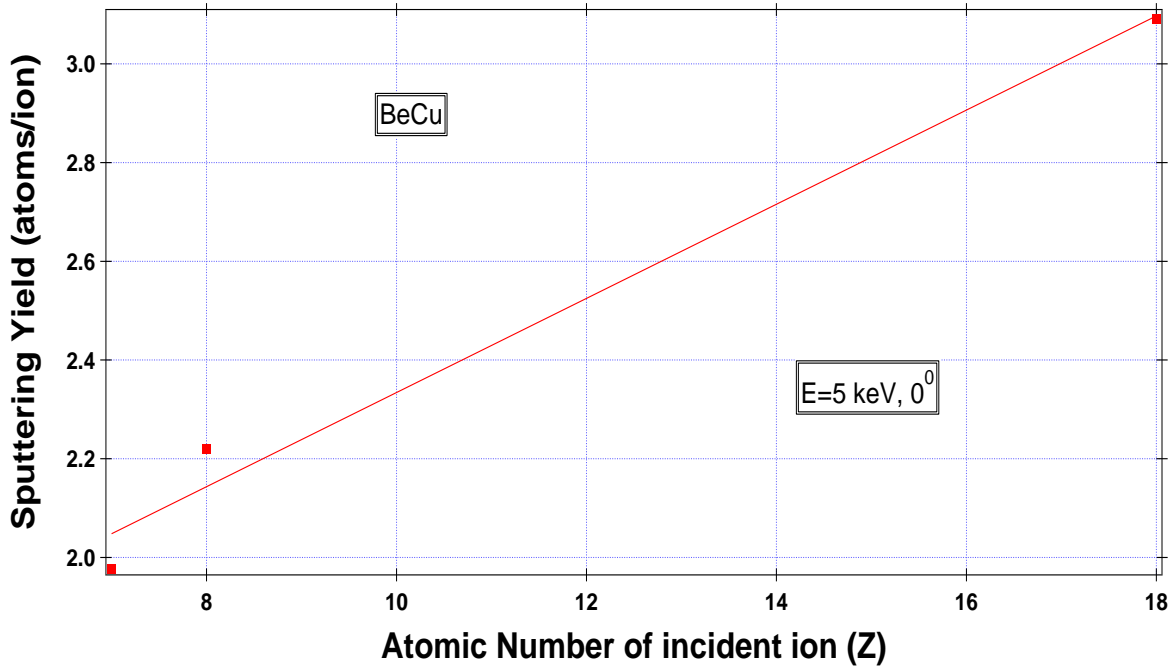


Figure (3 - 41): S.Y as a function atomic number of ions (N_2 , O_2 , Ar) that bombardment the BeCu alloy (Be 50%, Cu 50%).

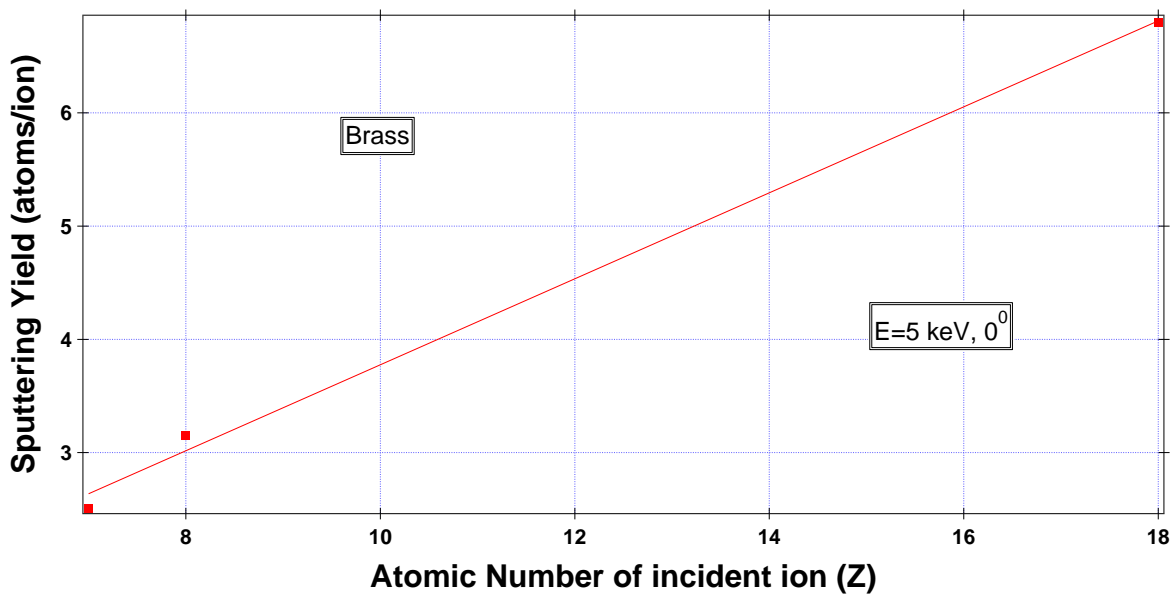


Figure (3 - 42): S.Y vs. atomic number of ions (O_2 , N_2 , Ar) that bombardment the Brass (Zn 33%, Cu 34%, Pb 33%).

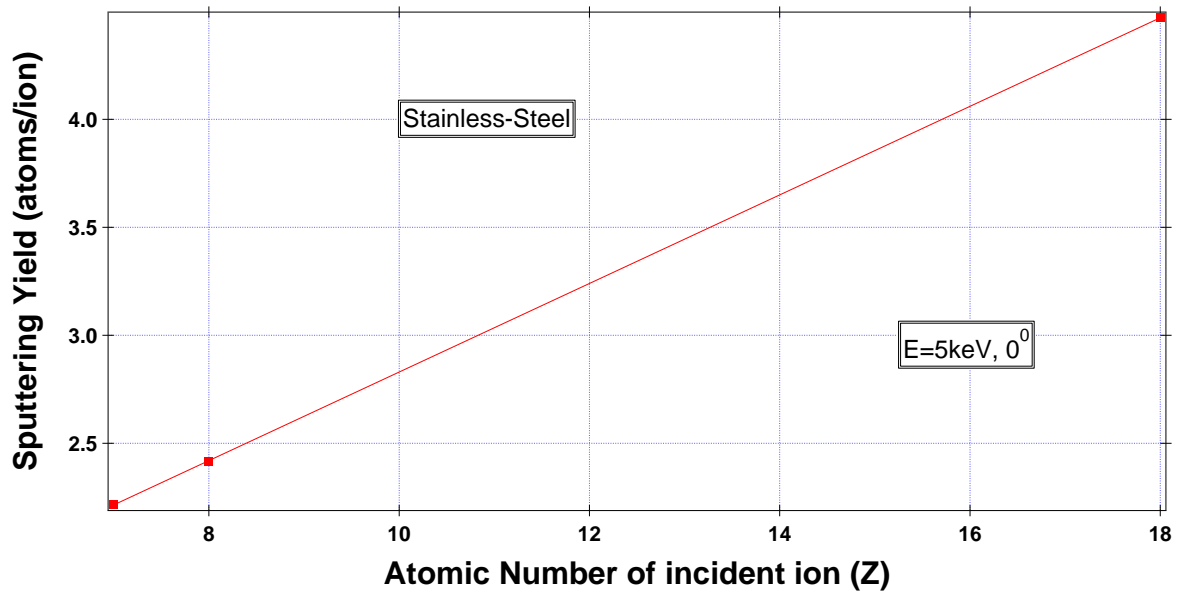


Figure (3 - 43): S.Y vs. atomic number of ions Argon, Nitrogen, and Oxygen that bombardment the Stainless - Steel (Cr 33%, Fe 34%, Ni 33%).

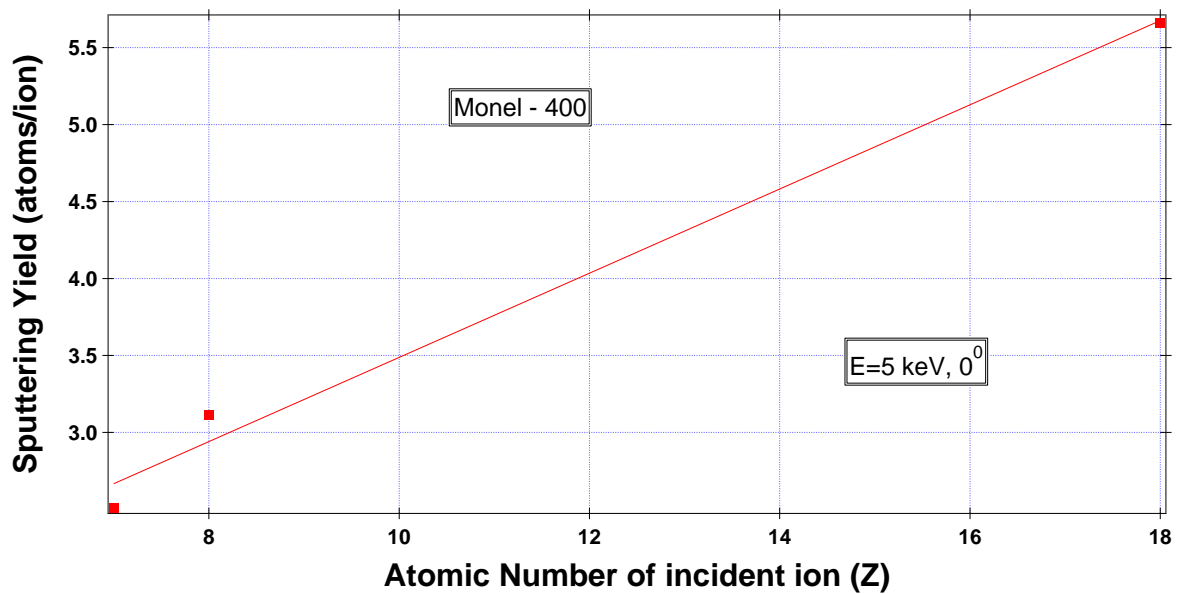


Figure (3 - 44): S.Y vs. atomic number of ions (N_2 , Ar, O_2) that bombardment the Monel - 400 alloy (Mn 25%, Fe 25%, Ni 25%, Cu 25%).

(3-6) The effect of concentration of the elements in the alloy on the sputtering yield

Elements content can be changed in alloys to control its elastic properties, but is still a simulation program study of the effect of element content on the sputtering in the alloy. We used the (MCs) methods to study the effects of elemental concentration, energy and angle the incident ions on the S.Y in the alloys. We got the results that the energy and angle of the incident ions have a significant impact on the S.Y in the alloys when the element concentration change in the alloys. The S.Y changes with the change of elemental concentration in the alloy, non-linearly in the target concentrations. As illustrated by the figures from (3-45) to (3-68).

Note in the figures (3-45) to (5-47) when increasing the concentration of beryllium element and decrease the concentration of copper element, the sputtering yield as a function of the of the ion incident angle decreases between the angle of 0° to 60° and increases when the angle is greater than 60° when the energy is constant at 0.5 keV.

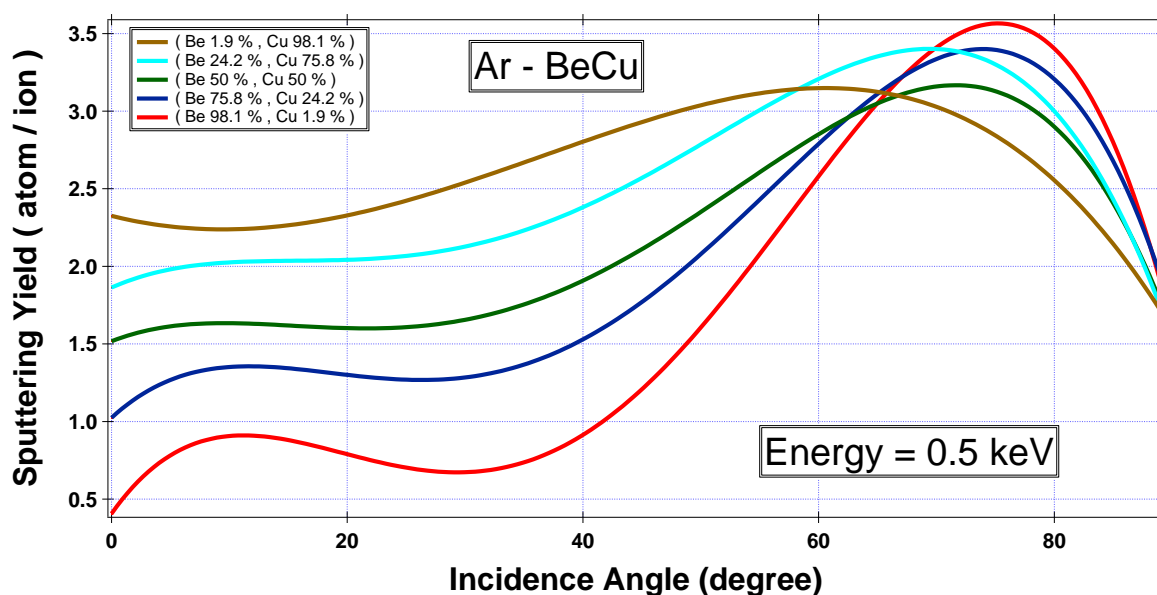


Figure (3-45): S.Y as a function incident angle (different concentration in BeCu alloy), bombarded by Argon ion.

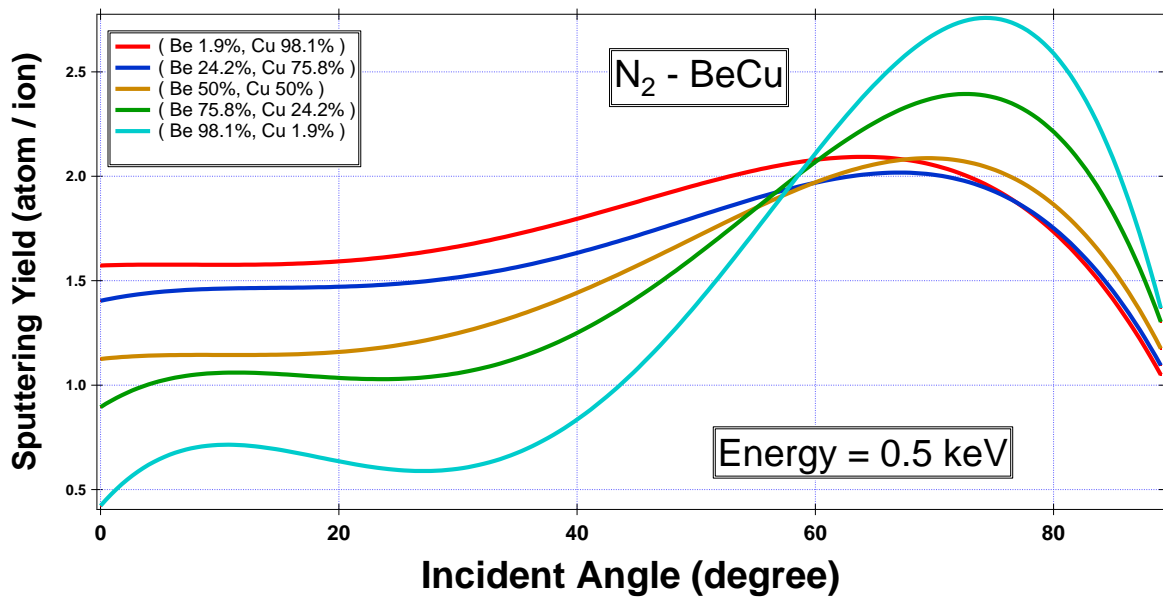


Figure (3-46): S.Y as a function of the incident angle (different concentration in BeCu alloy), bombarded Nitrogen ion.

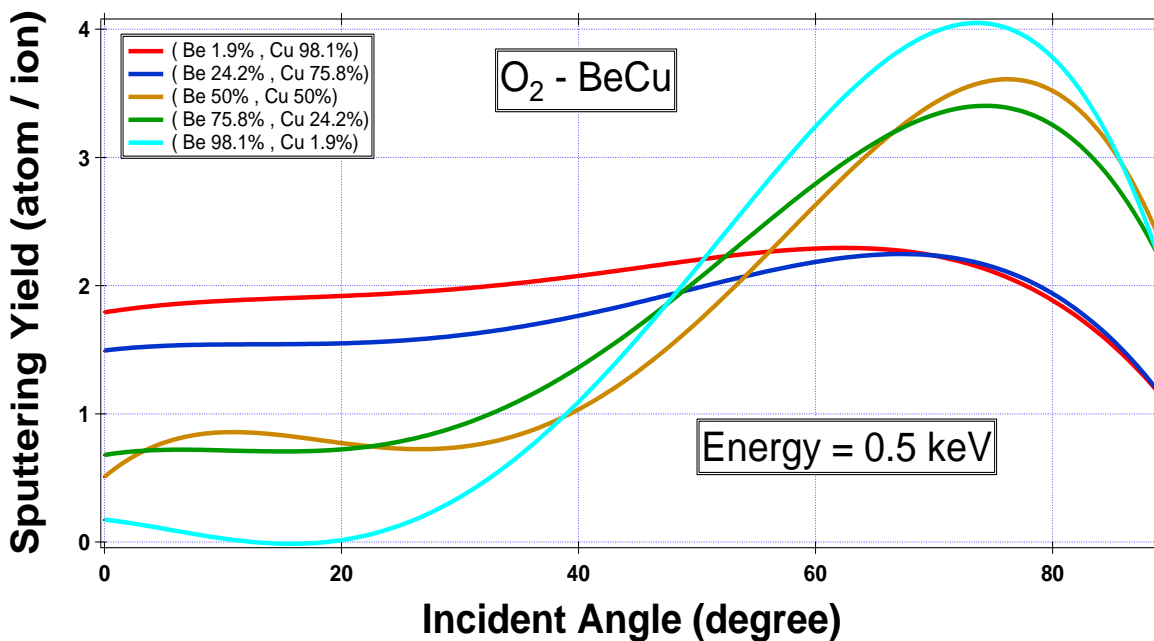


Figure (3-47): S.Y as a function of the concentration of the incident angle (different concentration in BeCu alloy), bombarded by Oxygen ion.

Note in the Figures (3-48) to (3-50) when increasing the concentration of beryllium element and decreasing the concentration of copper element, the sputtering yields as a function of the ion incident angle changes (decreases) when the angle is constant (0°).

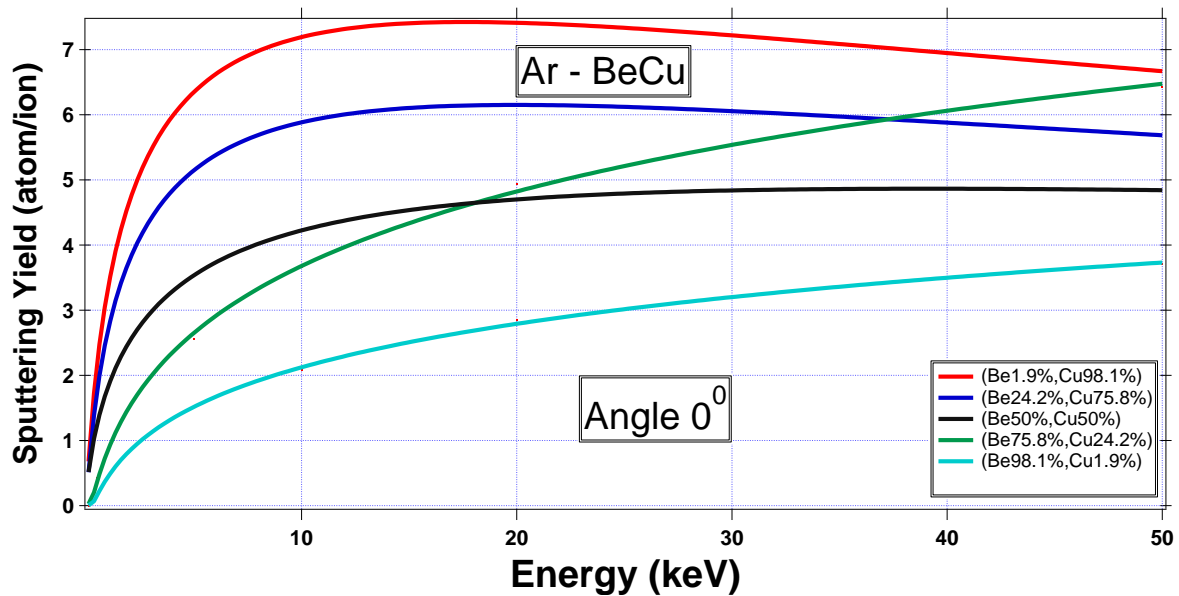


Figure (3-48): S.Y as a function of the ion energy (different concentration in BeCu alloy), bombarded by Argon ion.

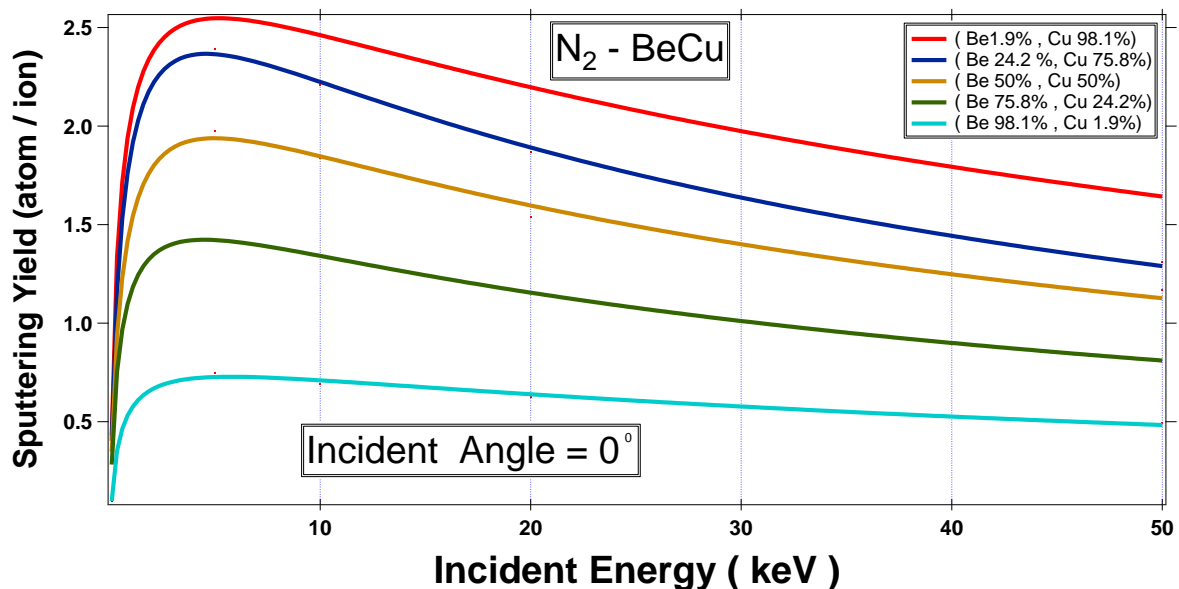


Figure (3-49): S.Y as a function of the concentration of the ion energy (different concentration in BeCu alloy), bombarded by Nitrogen ion.

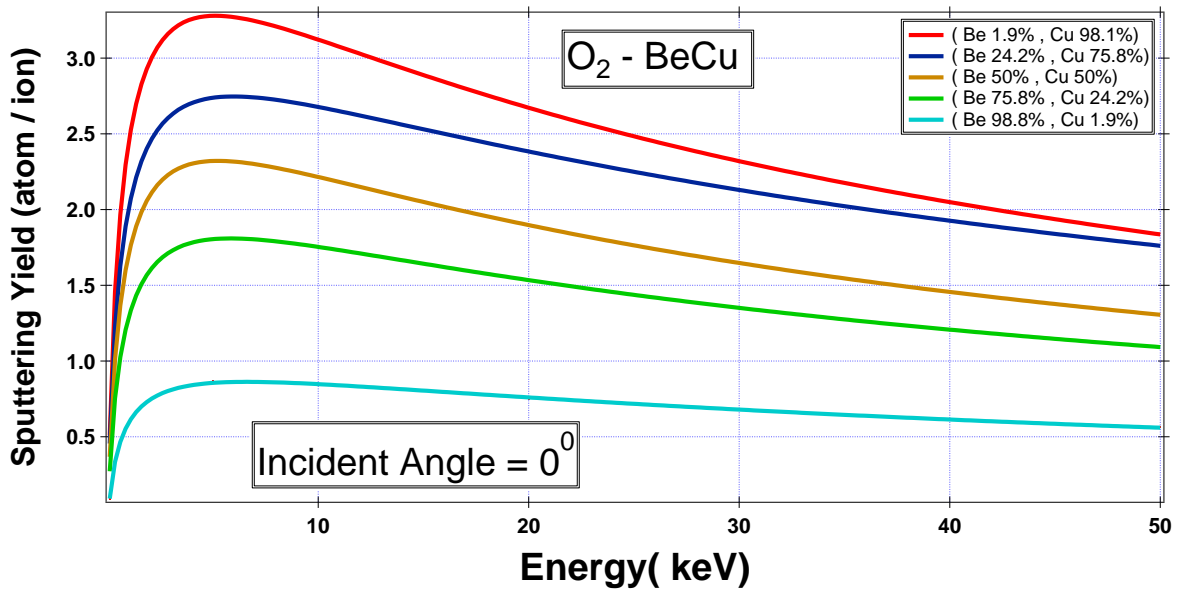


Figure (3-50): S.Y as a function of the ion energy (different concentration in BeCu alloy), bombarded by Oxygen ion.

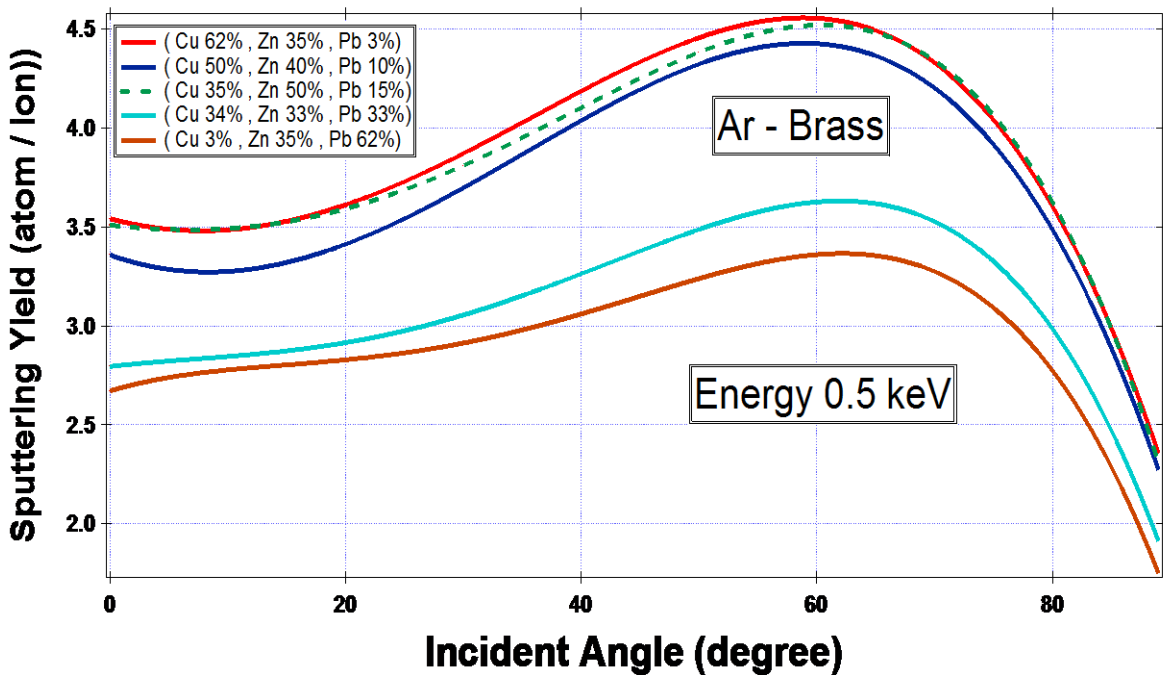


Figure (3-51): S.Y as a function of the incident angle (different concentration in the Brass alloy), bombarded by Argon ion.

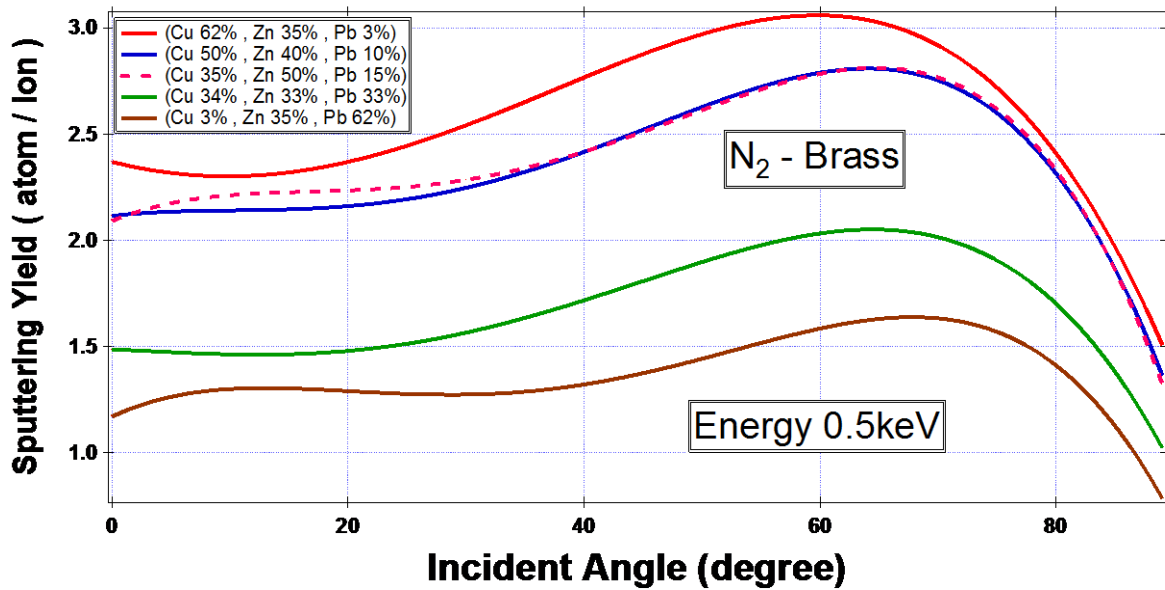


Figure (3-52): S.Y as a function of the incident angle (different concentration in the Brass alloy), bombarded by Nitrogen ion.

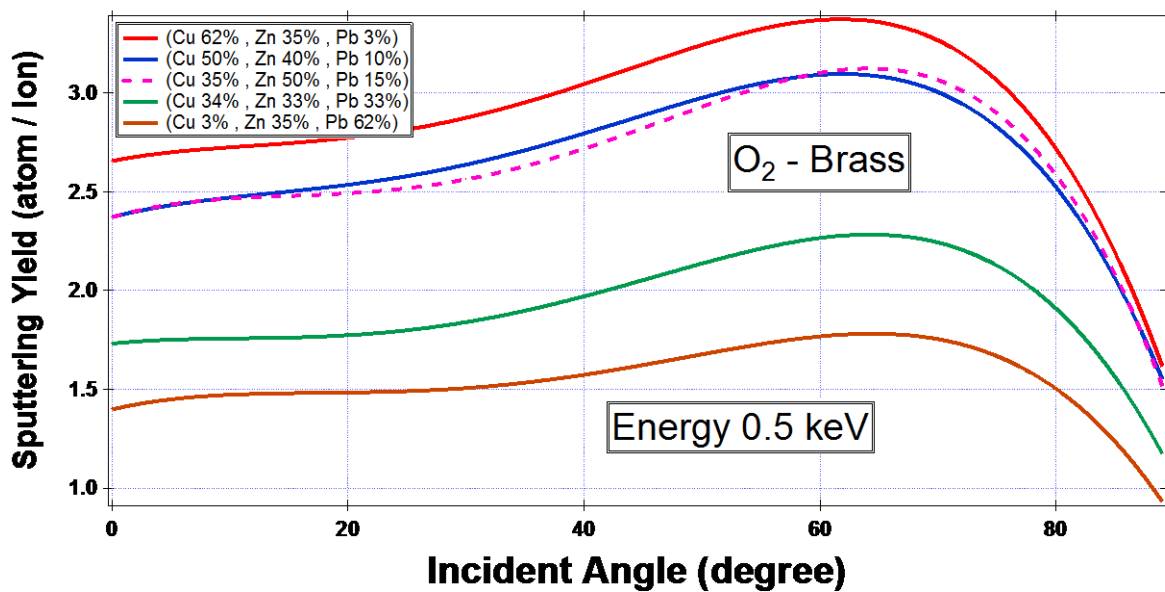


Figure (3-53): S.Y as a function of the incident angle (different concentration in the Brass alloy), bombarded by Oxygen ion.

Note in the Figures (3-54) to (3-56) when increasing the concentration of Pb element and decreasing the concentration of copper element, the sputtering yields as a function of the ion energy change (decreases) when the angle is constant (0°).

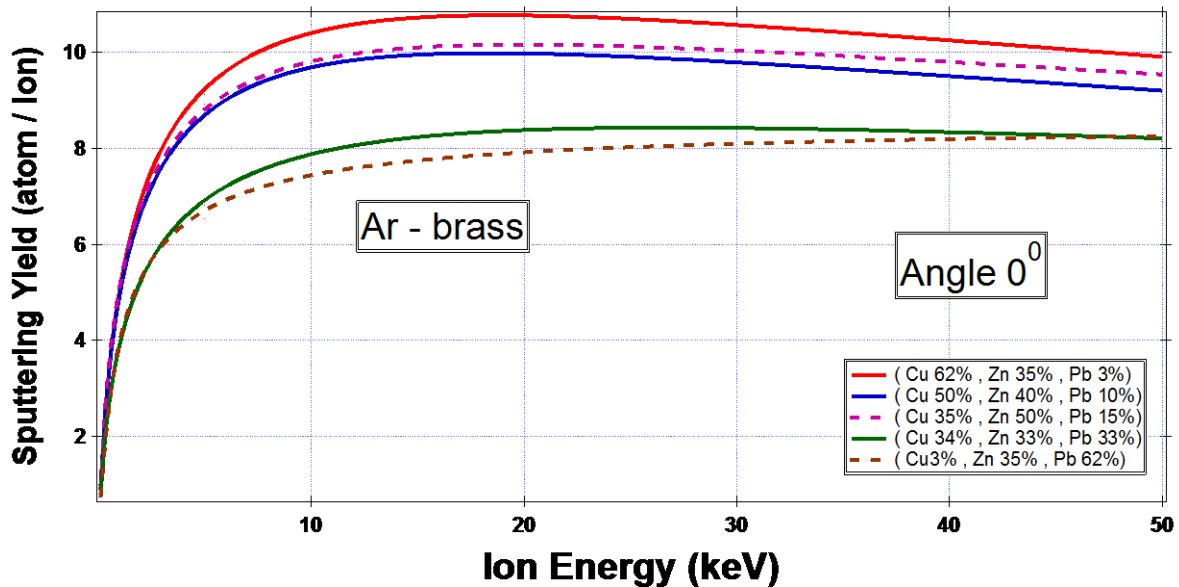


Figure (3-54): S.Y as a function of the ion energy (different concentration in the Brass alloy), bombarded by Argon ion.

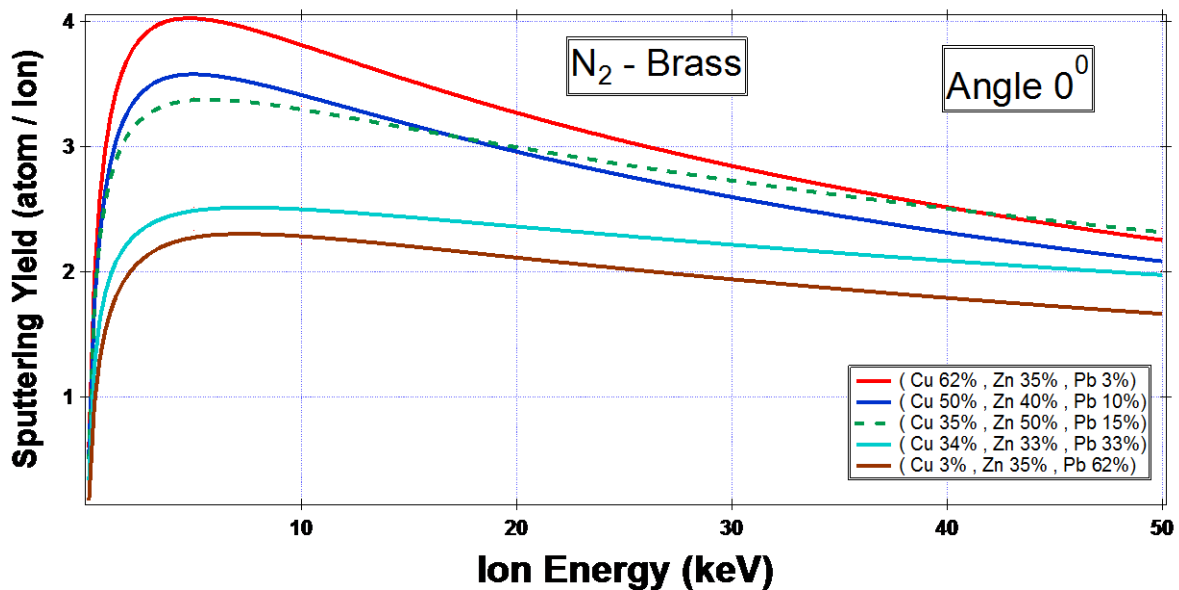


Figure (3-55): S.Y as a function of the ion energy (different concentration in the Brass alloy), bombarded by Nitrogen ion.

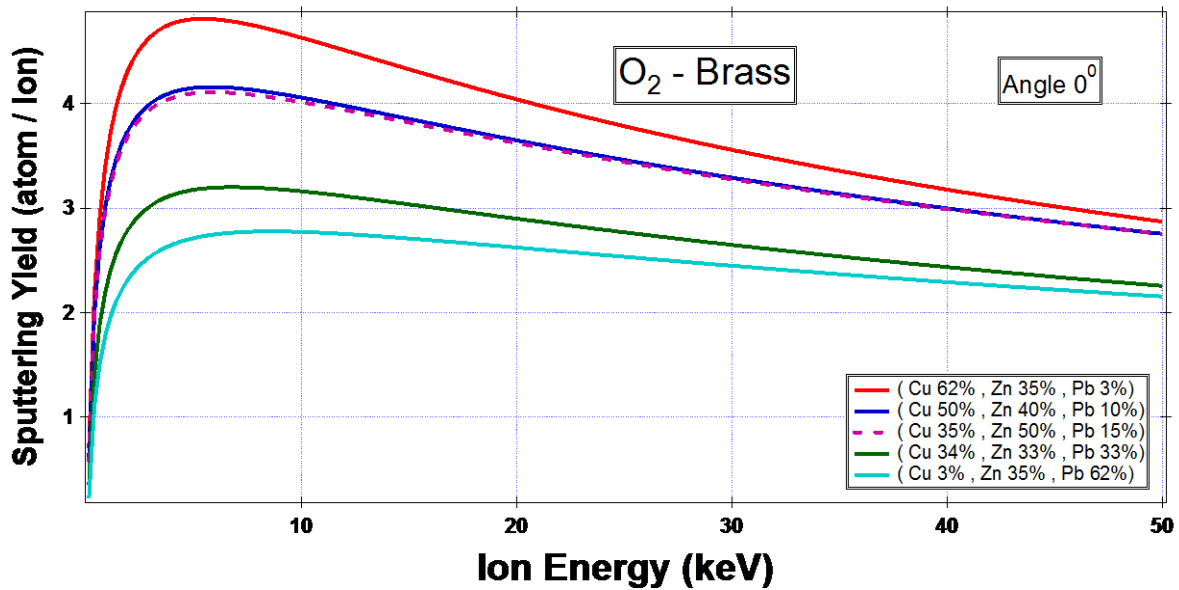


Figure (3-56): S.Y as a function of the ion energy (different concentration in the Brass alloy), bombarded Oxygen ion.

In the figures (3-57) to (3-59) we see the sputtering yield vs. ion incident angle when changing the concentrations of elements in the stainless-steel alloy the sputtering yield (decrease or increase) changes when the energy is at 0.5 keV.

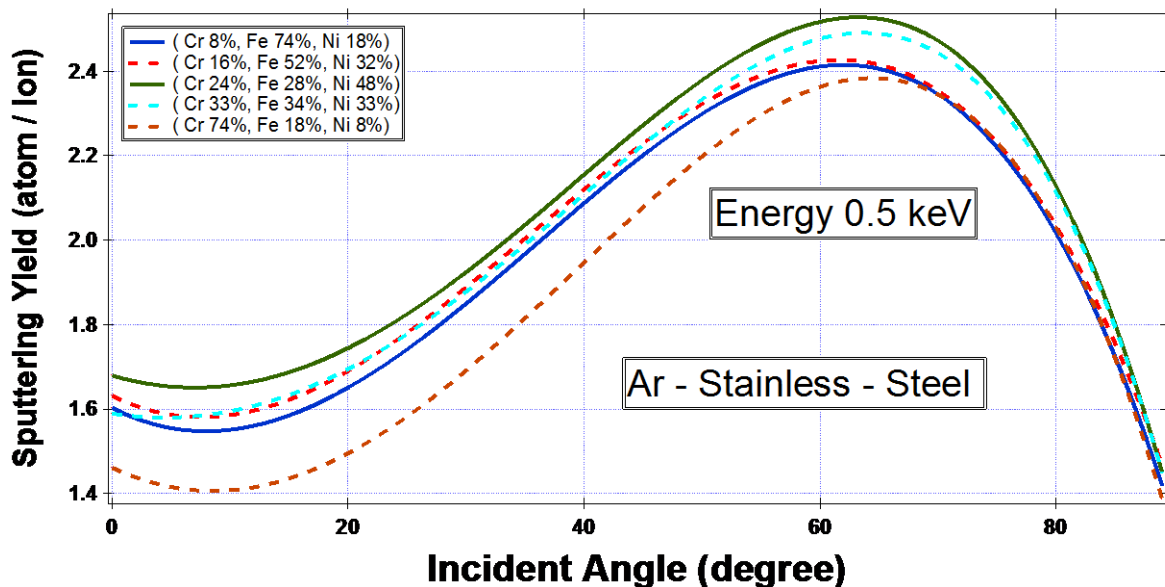


Figure (3-57): S.Y as a function of the incident angle (different concentration in the Stainless-Steel alloy), bombarded by Argon ion.

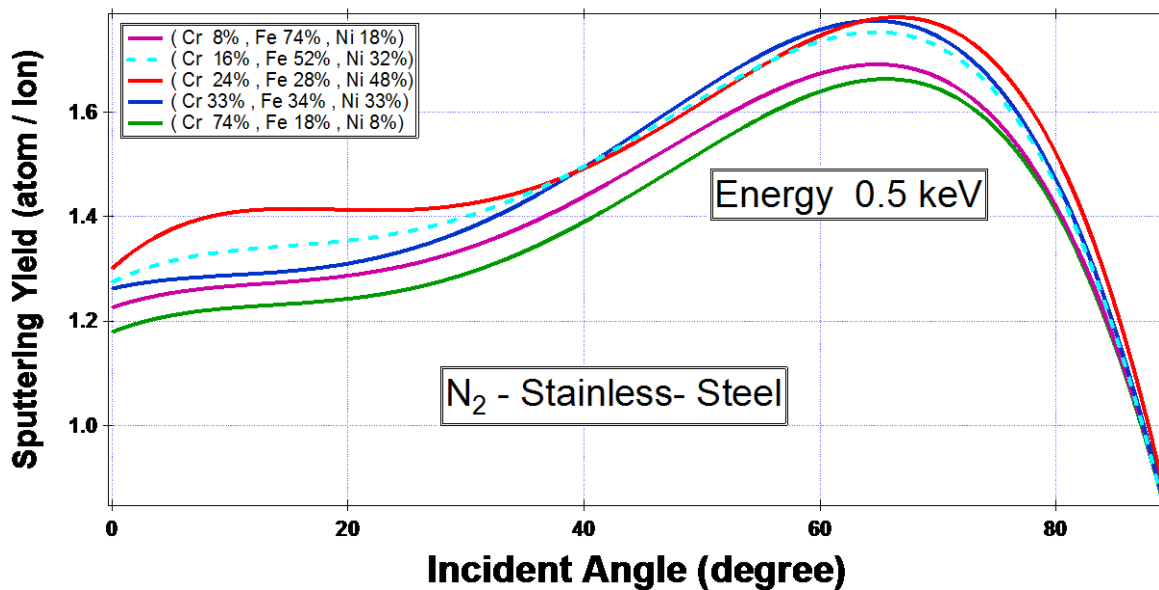


Figure (3-58): S.Y as a function of the incident angle (different concentration in the Stainless-Steel alloy), bombarded by Nitrogen ion.

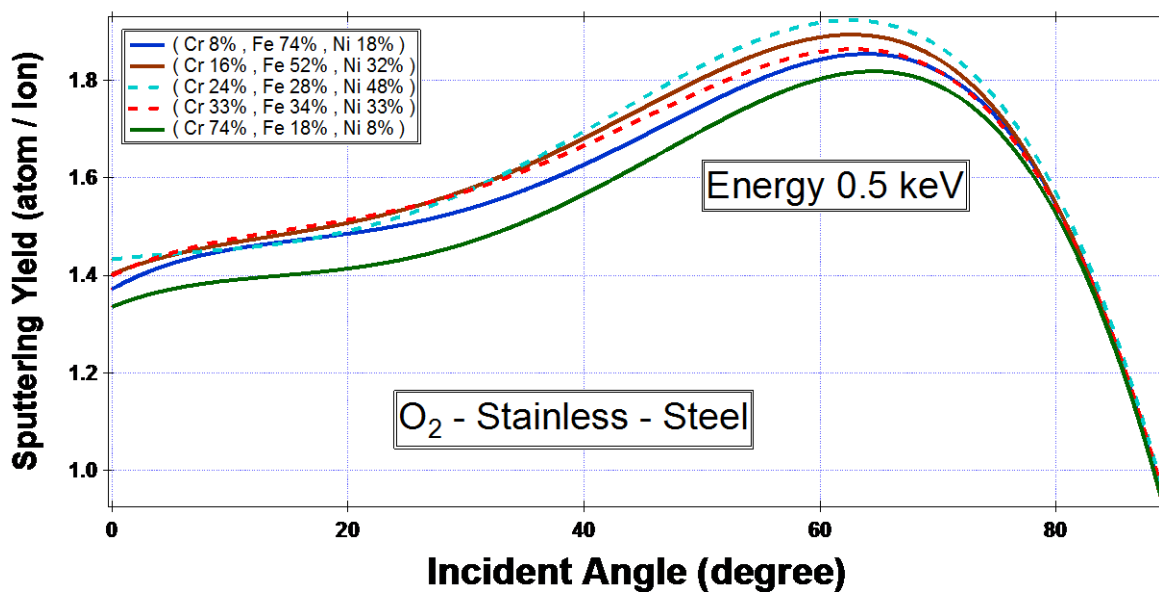


Figure (3-59): S.Y as a function of the incident angle (different concentration in the Stainless-Steel alloy), bombarded by Oxygen ion.

In the figures (3-60) to (3-62), the intermittent yield versus ion energy and the ion incident angle at (0°) the sputtering yield change (increase or decrease) with changing the concentration of the alloy elements.

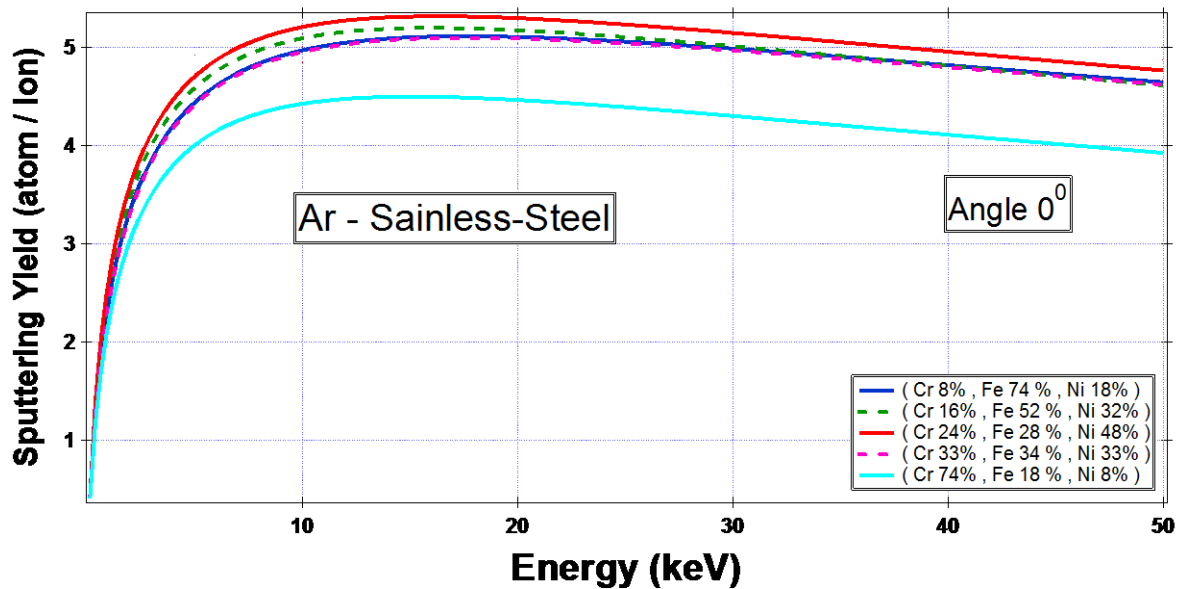


Figure (3-60): S.Y as a function of the ion energy (different concentration in the Stainless-Steel alloy), bombarded by Argon ion.

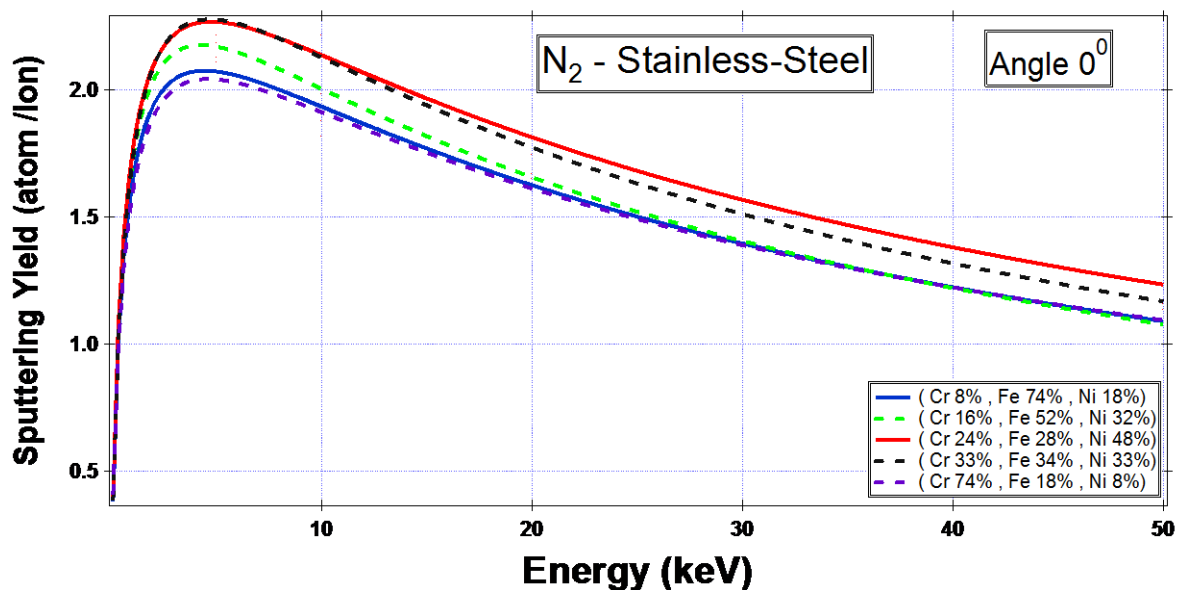


Figure (3-61): S.Y as a function of the ion energy (different concentration in the Stainless-Steel alloy), bombarded by Nitrogen ion.

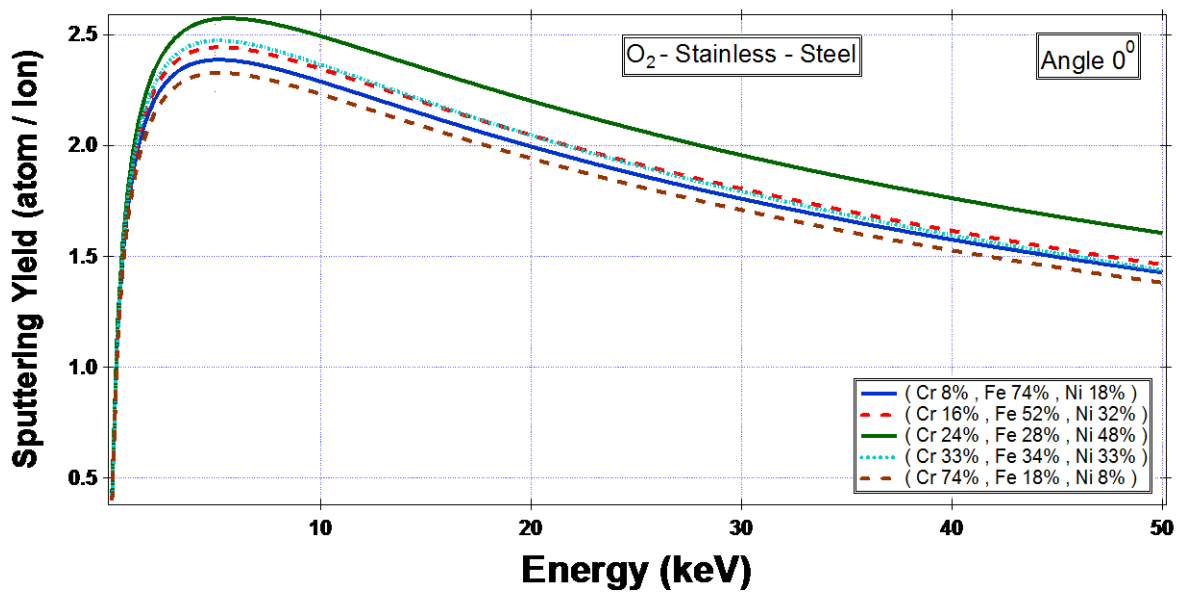


Figure (3-62): S.Y as a function of the ion energy (different concentration in the Stainless-Steel alloy), bombarded by Oxygen ion.

In the figures (3-63) to (3-65), the sputtering yield varies the ion incident angle the sputtering yield changes (increase or decrease) with changing the concentration of alloy elements. (energy 0.5 keV).

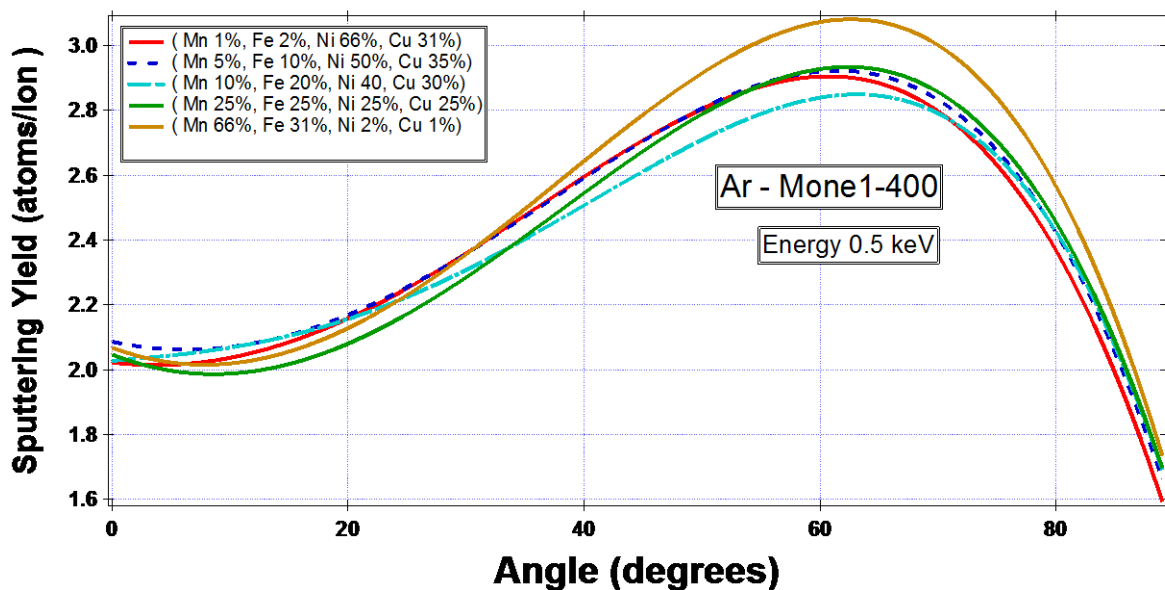


Figure (3-63): S.Y as a function of the incident angle (different concentration in the Monel-400 alloy), bombarded by Argon ion.

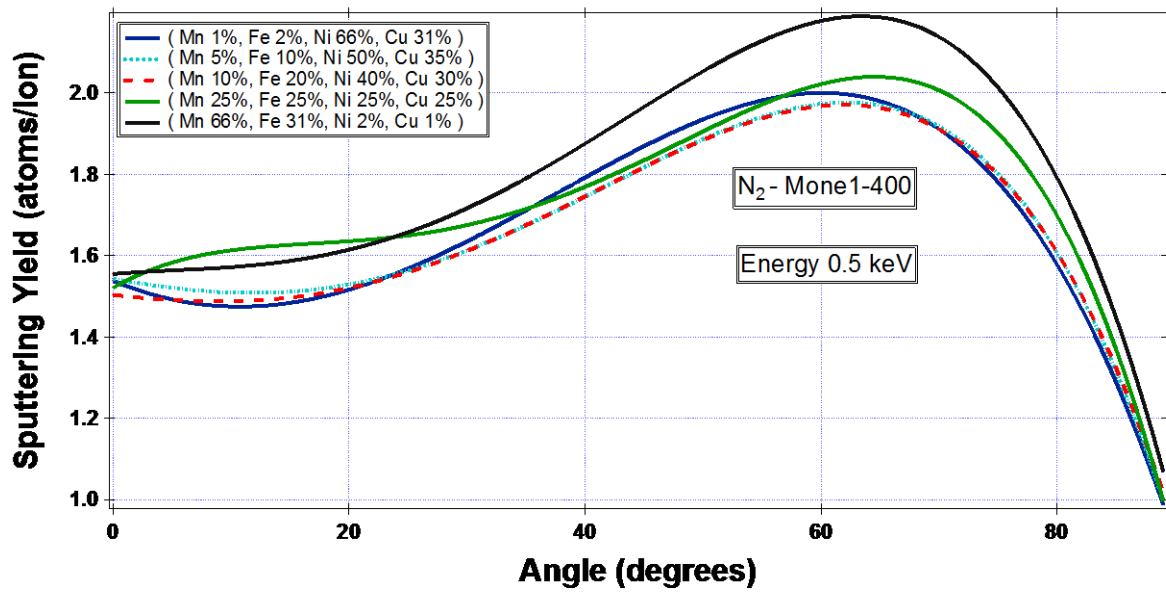


Figure (3-64): S.Y as a function of the incident angle (different concentration in the Monel-400 alloy), bombarded by Nitrogen ion.

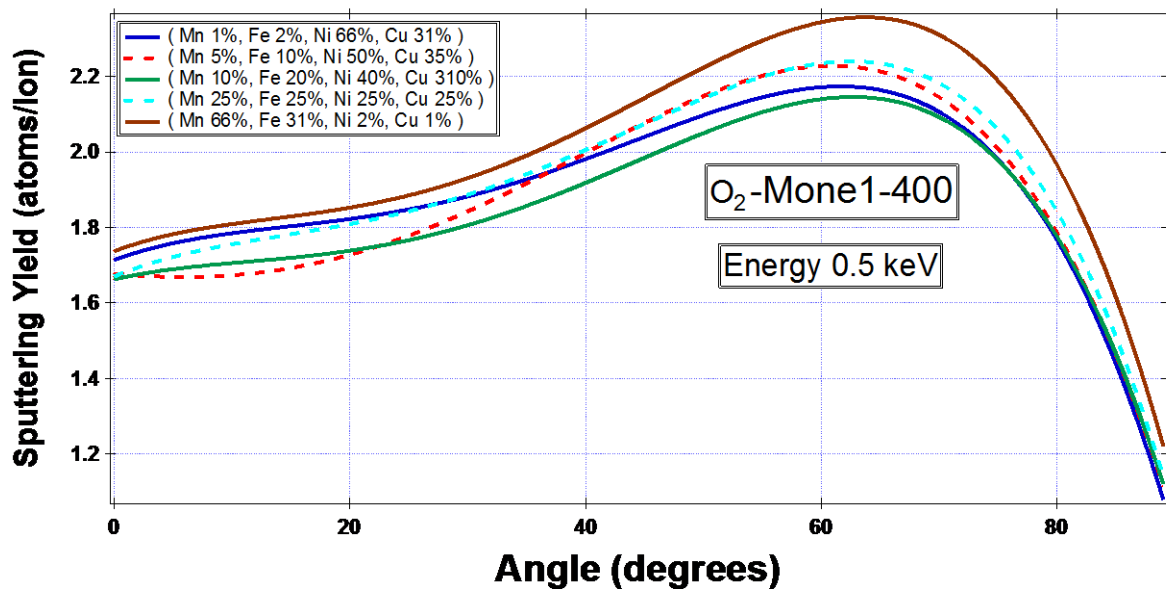


Figure (3-65): S.Y as a function of the incident angle (different concentration in the Monel-400 alloy), bombarded by Oxygen ion.

Figures (3-66) to (3-68), the sputtering yield varies the ion energy the sputtering yield changes (increase or decrease) with changing the concentration of alloy elements. Ion incident angle (0°).

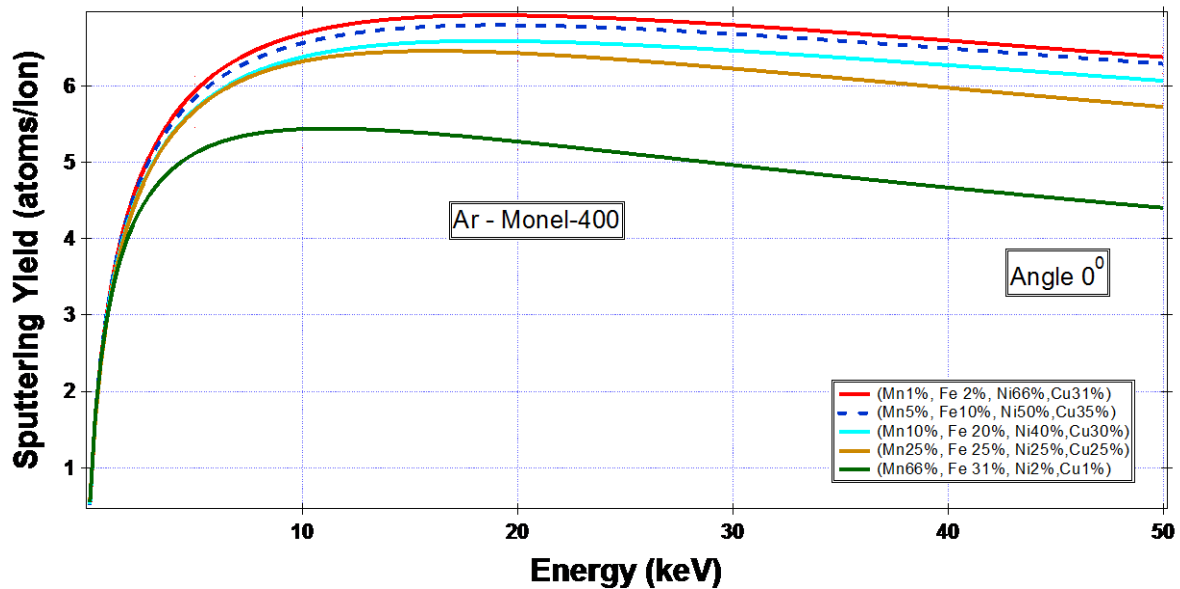


Figure (3-66): S.Y as a function of the ion energy (different concentration in the Monel-400 alloy), bombarded by Argon ion.

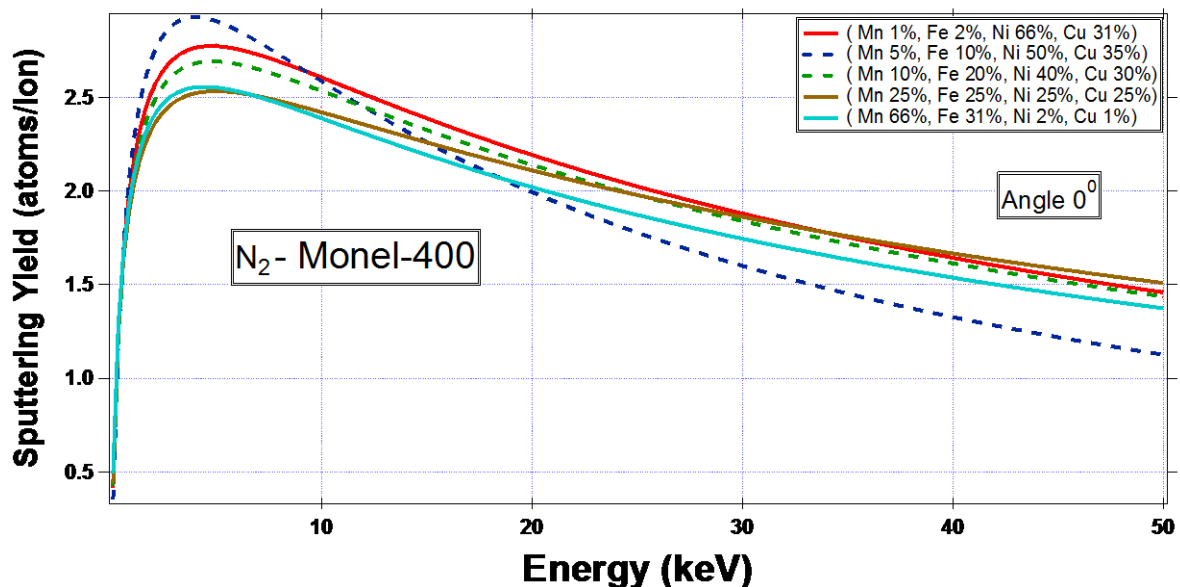


Figure (3-67): S.Y as a function of the ion energy (different concentration in the Monel-400 alloy), bombarded by Nitrogen ion.

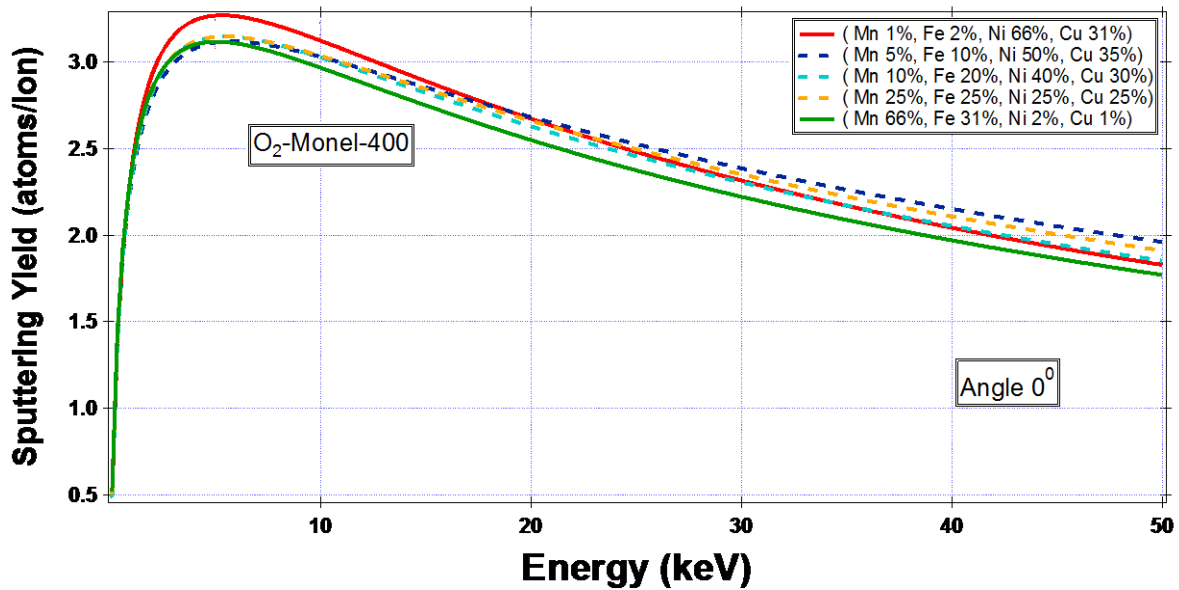


Figure (3-68): S.Y as a function of the ion energy (different concentration in the Monel-400 alloy), bombarded by Oxygen ion.

In the figures (3-68) to (3-75), a comparison is between the S.Y of the alloy on the one hand and the S.Y of the alloy elements on the other. When the number of Argon ions bombards 5000 and at a width alloy of 1000 Å. The sputtering yield of the alloy is not possible to be larger or less than the sputtering yield of the elements because each element in the alloy has a different atomic number, surface binding energy, and the concentration of the element in the alloy varies. This applies if the S.Y is vs. ion energy or vs. angle of the incident.

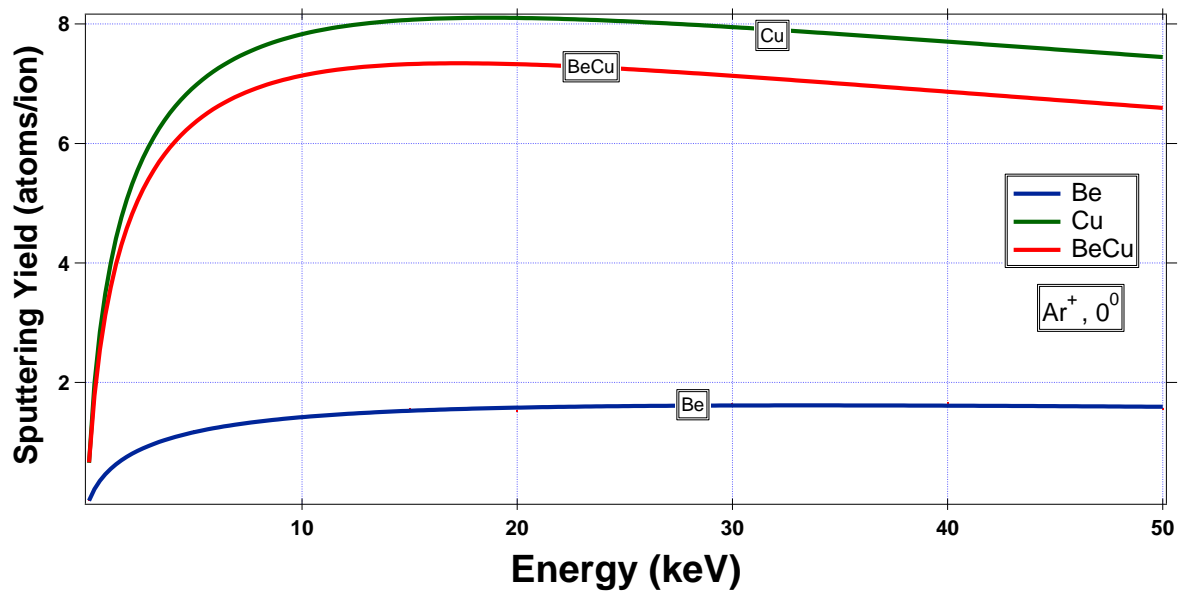


Fig. (3-69): sputtering yield dependence of ion Energy of Cu, Be, and BeCu under Ar^+ bombardment.

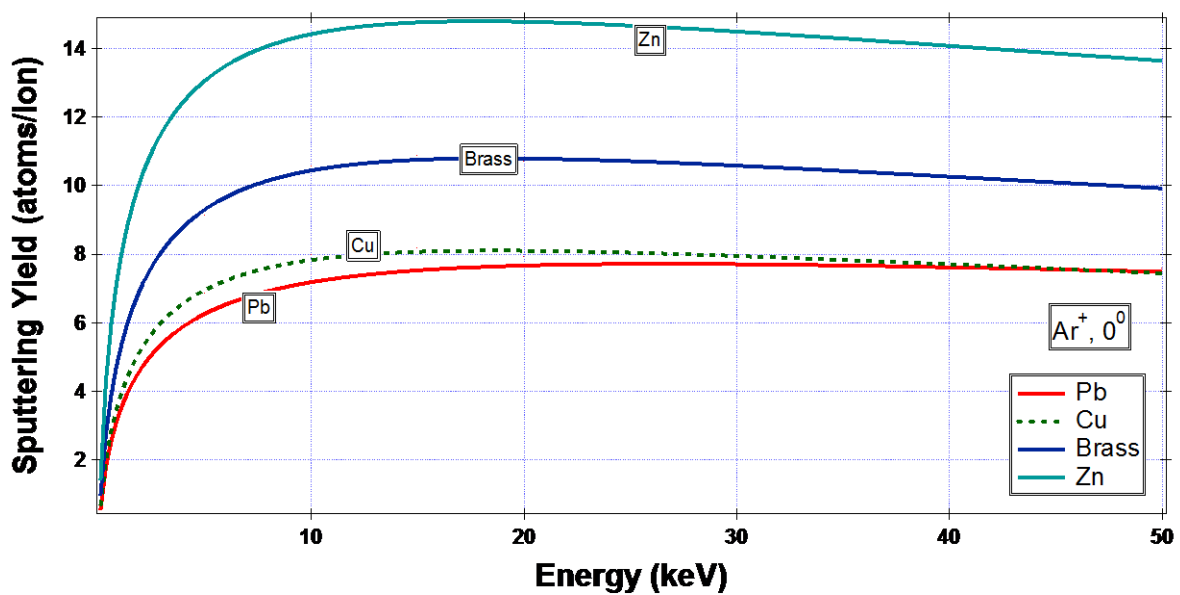


Fig. (3-70): Sputtering yield dependence of ion Energy of (Cu, Zn, Pb, and Brass Alloy) under Ar^+ bombardment.

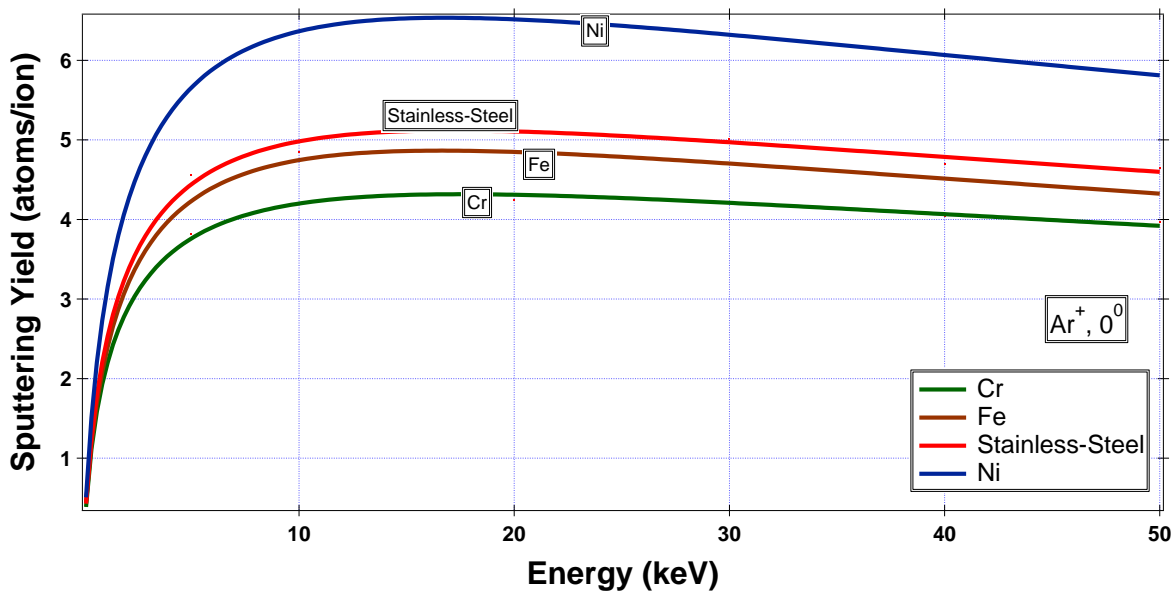


Fig. (3-71): Sputtering yield dependence of ion Energy of (Cr, Fe, Ni, and Stainless - Steel Alloy) under Ar⁺ bombardment.

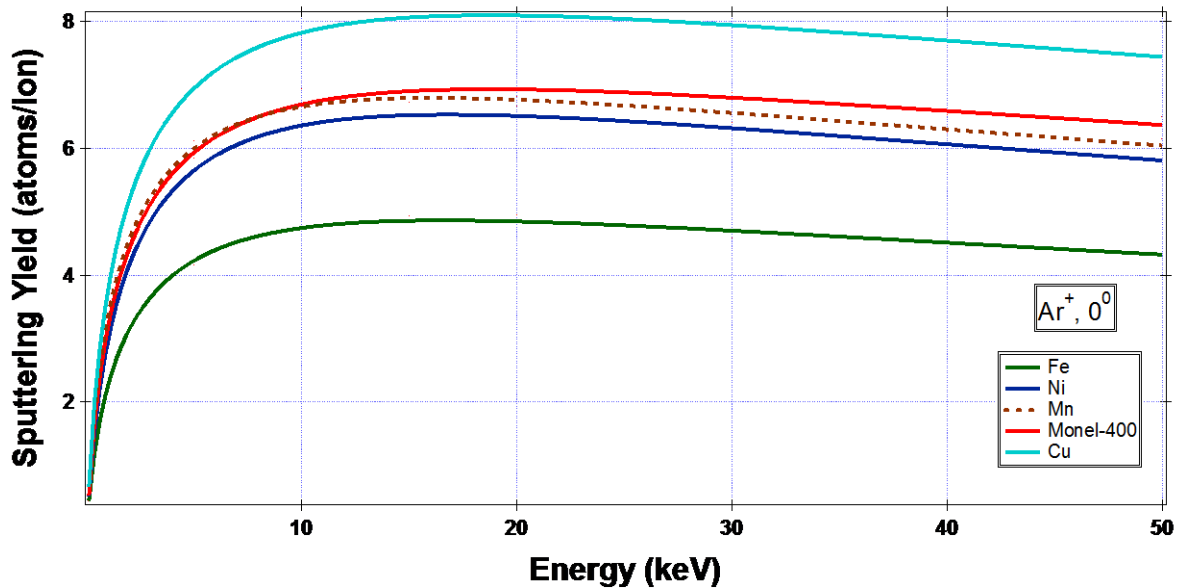


Fig. (3-72): Sputtering yields dependence of ion Energy of Cu, Fe, Ni, Mn, and Monel - 400 Alloy under Ar⁺ bombardment.

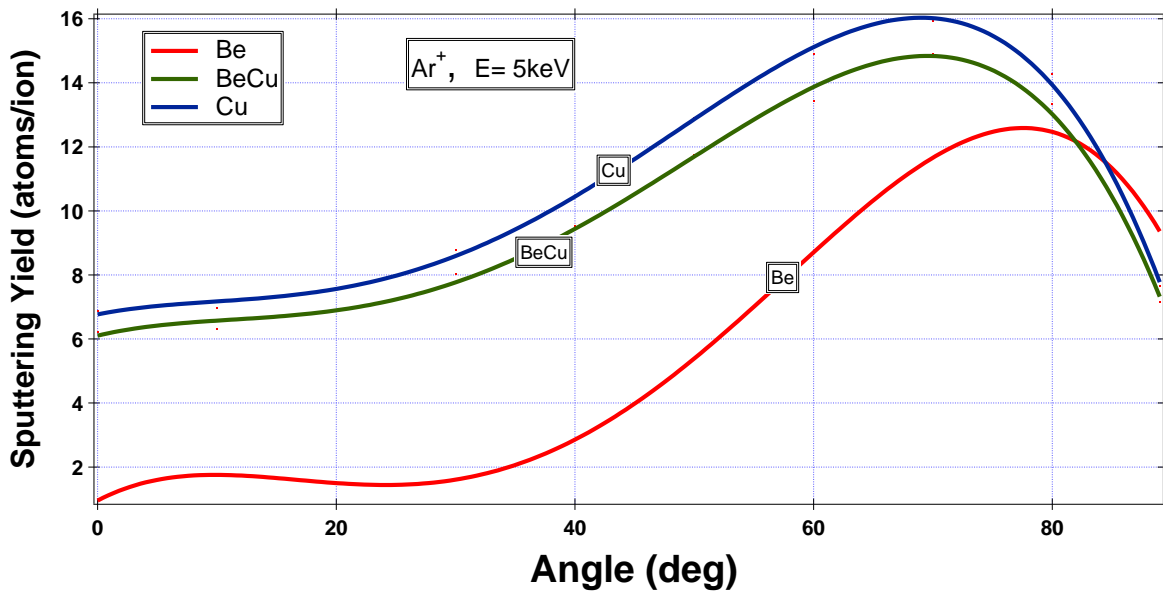


Fig. (3-73): Sputtering yields dependence of Angle incident of Cu, Be, and BeCu Alloy under Ar^+ bombardment.

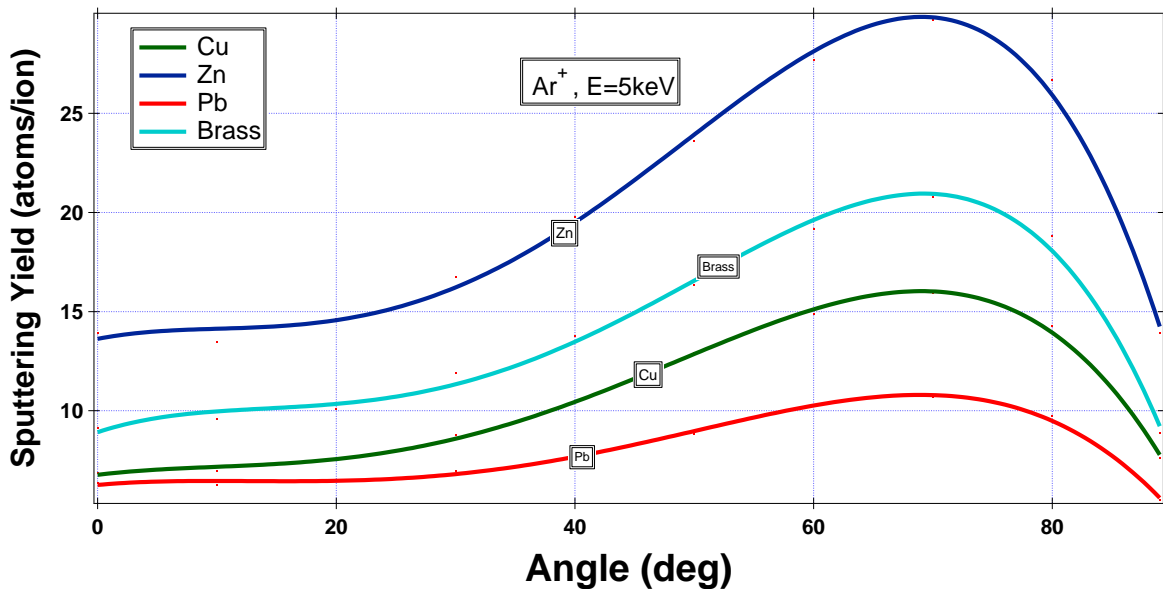


Fig. (3-74): Sputtering yields dependence of Angle incident of Cu, Zn, Pb, and Brass Alloy under Ar^+ bombardment.

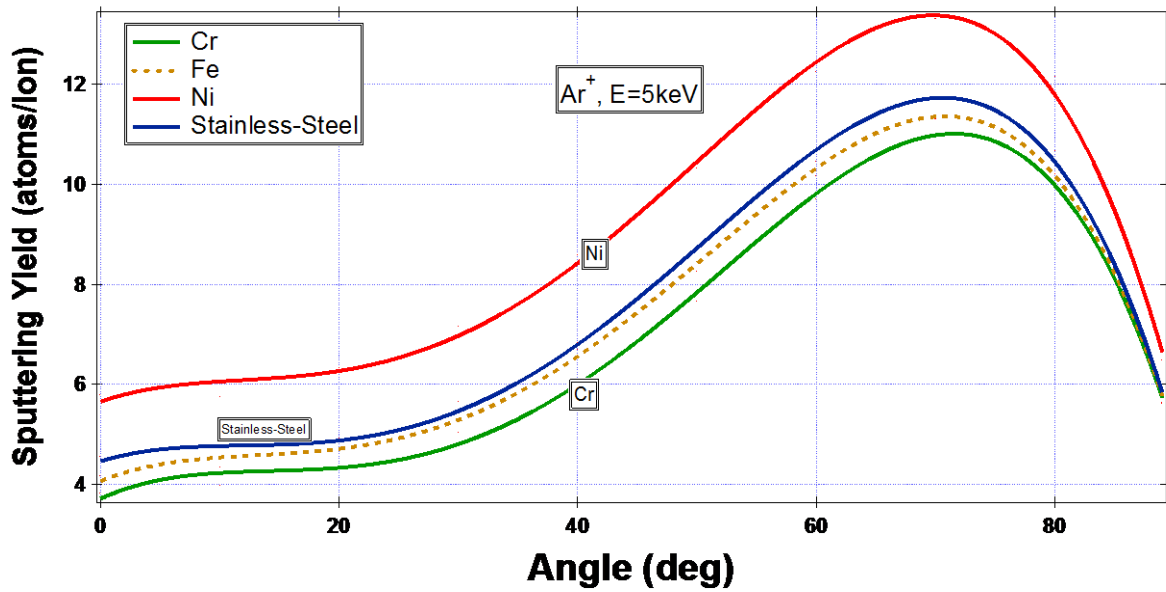


Fig. (3-75): Sputtering yields dependence of Angle incident of Cr, Ni, Fe, and Stainless-Steel Alloy under Ar⁺ bombardment.

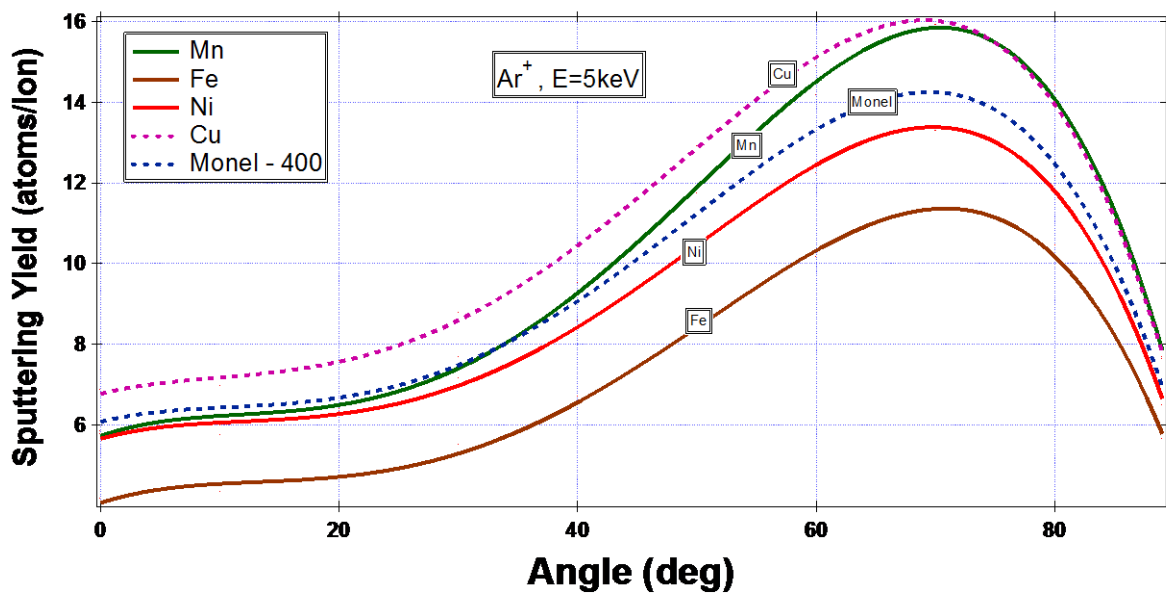


Fig. (3-76): Sputtering yields dependence of Angle incident of Cu, Ni, Fe, Mn, and Monel-400 Alloy under Ar⁺ bombardment.

(3-7) Effect of the surface binding energy (SBE) on the sputtering yield

Surface binding energy (SBE) is the energy that must be overcome to remove the atoms from the surface of the target. The estimation of this energy for one element targets. By default, TRIM will provide the energy table (SBE) for each element in particular for the sputtering process. Special lists are available to show you the binding of slight changes in (SBE) on the S.Y

Surface binding energy is a factor that determines the sputter yield. Increasing and decreasing these values about the well –known surface binding energy value would lead to variation in the sputter yield. In fact, any slight variation of surface binding energy leads to a change in the calculation the sputter yields. Whether to increase or to decrease, lead to a large and noticeable change in sputtering yield. The sputter yield decreases with increasing the surface binding energy. There is an inverse linear dependence between U_b and the sputter yield. as in figure (3-77) to (3-79).

Table (3-26) shows the elements involved in these alloys (targets).

The elements	Symbols	Atomic numbers	Atomic Mass	Surface binding energy (SBE) (eV)
Beryllium	Be	4	9.012182	3.38
Chromium	Cr	24	51.94051	4.12
Manganese	Mn	25	54.938044	2.98
Iron	Fe	26	55.93494	4.34
Nickel	Ni	28	57.93534	4.46
Copper	Cu	29	62.9296	3.52
Zinc	Zn	30	65.38	1.35
Lead	Pb	82	207.2	2.03

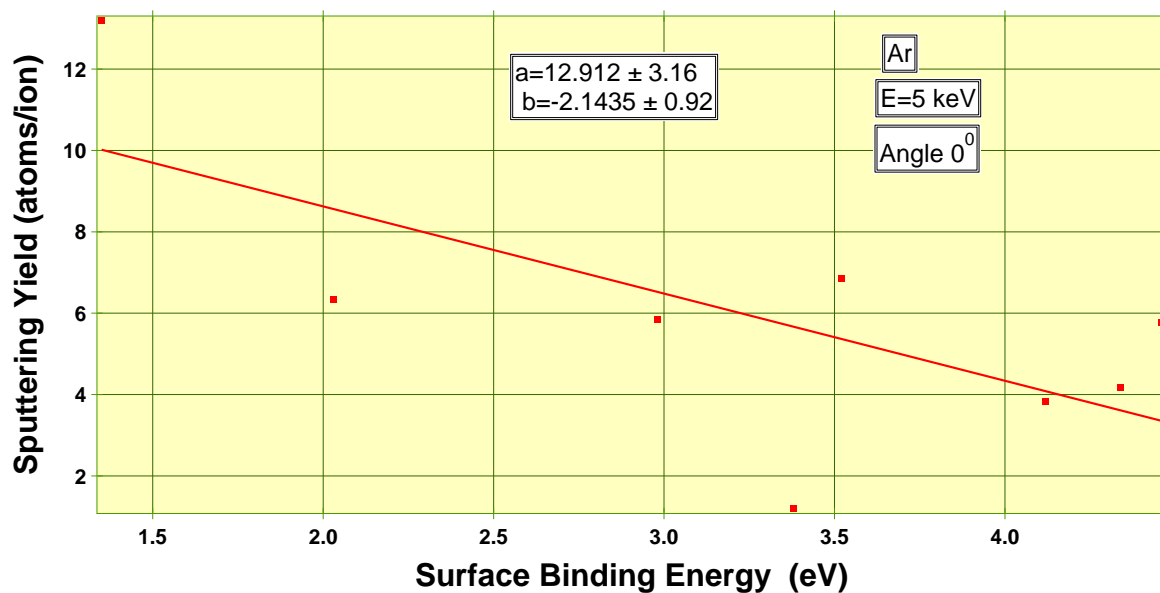


Figure (3-77): Sputtering yield vs. (SBE) of the target material (Be, Cr, Mn, Fe, Ni, Cu, Zn, Pb) bombarded by Ar^+ ions

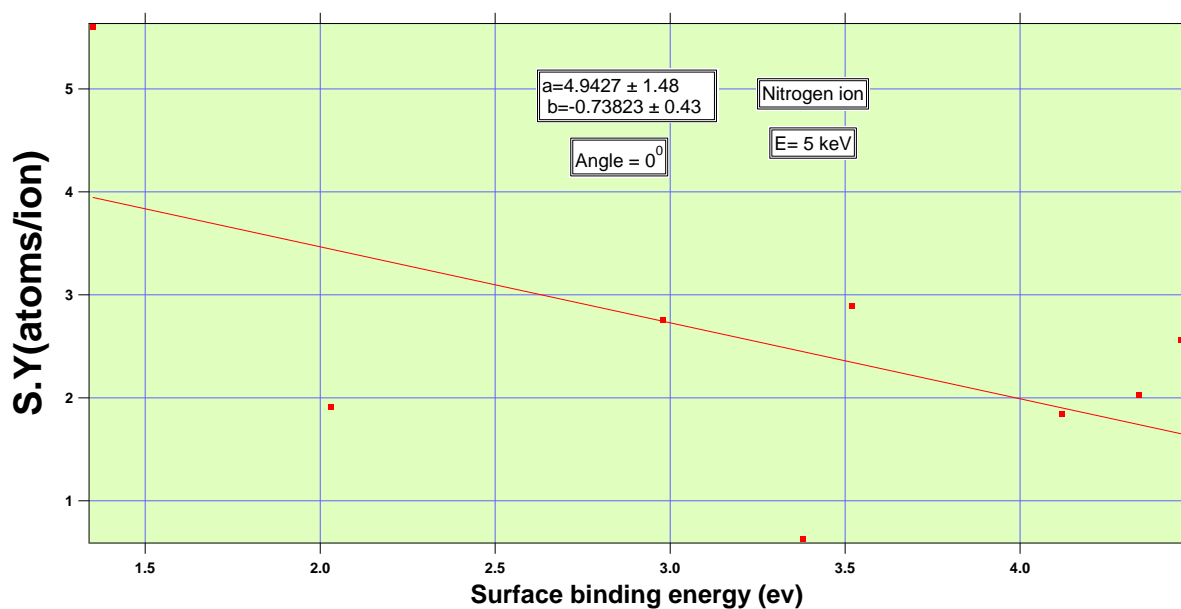


Figure (3-78): Sputtering yield vs. (SBE) of the target material (Be, Cr, Mn, Fe, Ni, Cu, Zn, Pb) bombarded by Nitrogen ions

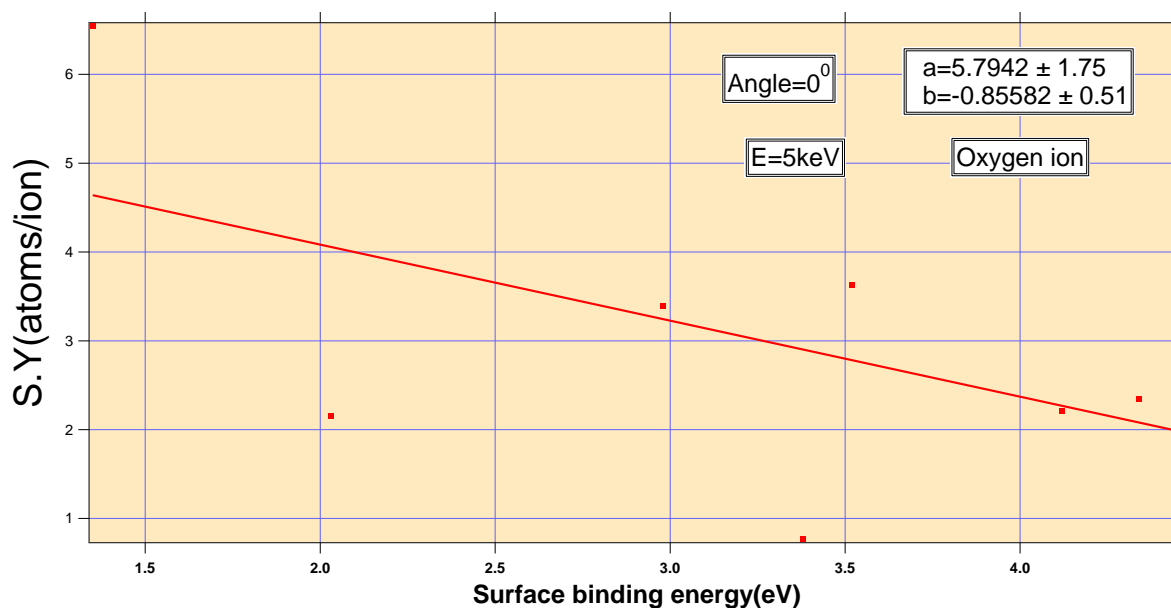


Figure (3-79): Sputtering yield vs. (SBE) of the target material (Be, Cr, Mn, Fe, Ni, Cu, Zn, Pb) bombarded by Oxygen ions

(3-8) Influence of the threshold energy (E_{th}) on the sputtering yield

The threshold energy, E_{th} , must meet the condition, that the maximum transferable energy in a collision is larger than the surface binding energy. The threshold energy cannot be determined directly. It can be obtained by extrapolating the sputtering yields to low energy. The threshold energy depends on the angle of incidence. It has been shown by simulations, that this dependence is stronger for heavy projectiles than for light incident ions.

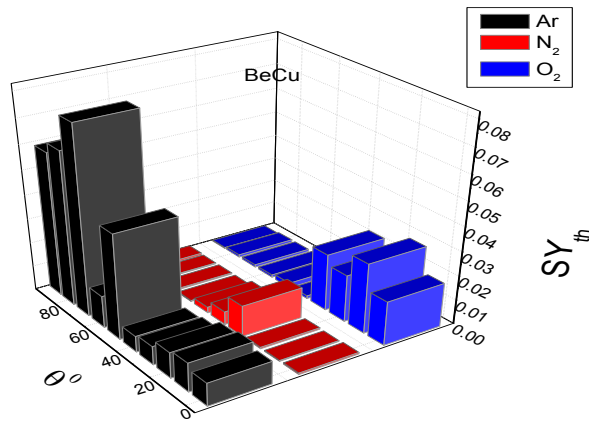


Figure (3-80): incident ion angle vs. sputtering threshold energy for alloy elements BeCu (Be, Cu) target materials bombarded by (Ar, N_2 , and O_2) ions.

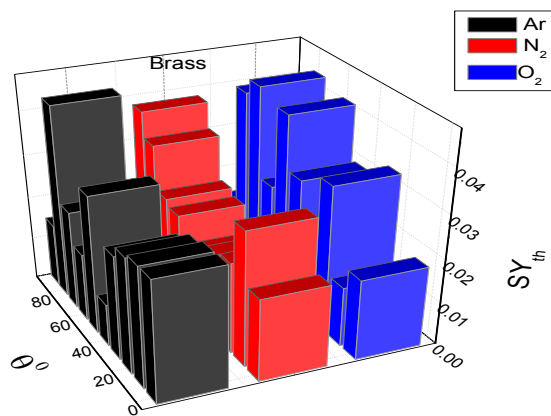


Figure (3-81): incident ion angle vs. sputtering threshold energy for alloy elements Brass (Cu, Zn, Pb) target materials bombarded by (Ar, N_2 , and O_2) ions.

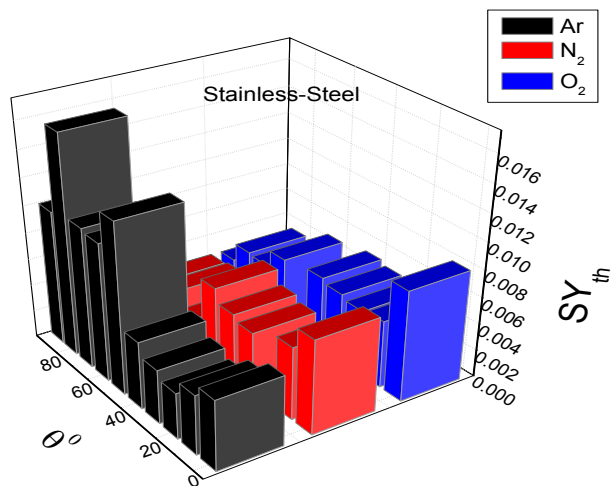


Figure (3-82): incident ion angle vs. sputtering threshold energy for alloy elements Stainless-Steel (Cr, Fe, Ni) target materials bombarded by (Ar, N_2 , and O_2) ions.

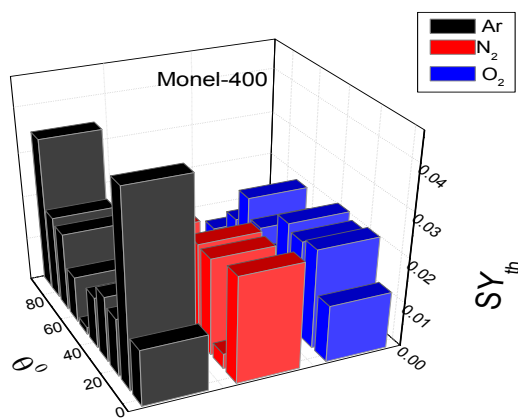


Figure (3-83): incident ion angle vs. sputtering threshold energy for alloy elements Monel-400 (Mn, Fe, Ni, Cu) target materials bombarded by (Ar, N_2 , and O_2) ions.

(3-9) The effect of the target atomic number on the sputtering yield

Figure (3-84) shows the plots of sputter yield vs. of the atomic number of alloy elements (Be, Cr, Mn, Fe, Ni, Cu, Zn, Pb) bombarded by (Ar, N₂, and O₂) ion for a width target of 1000 Å, ion energy of (0.5 KeV), and a number of ions of 5000 at incident ion angles (0°)

It is noted that the maximum sputter yield of Zinc (Zn) target (with atomic number $Z = 30$) is higher than the others element. The minimum sputtering yield is to Beryllium (Be) ($Z = 4$). That means the sputter yield increases with increasing the target atomic numbers of the elements of the alloys (Z).

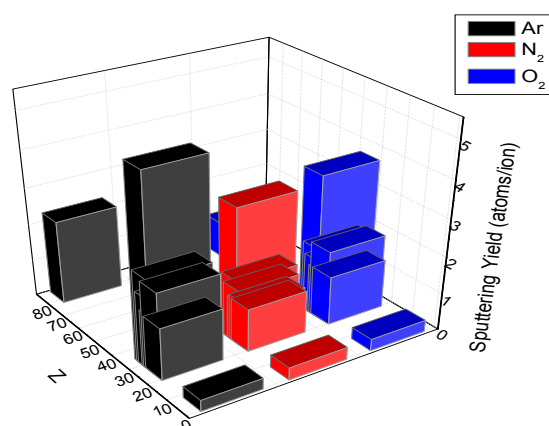


Figure (3-84): Sputtering yield vs. atomic number target for (Be, Cr, Mn, Fe, Ni, Cu, Zn, Pb) bombarded by (Ar, N₂, and O₂) ions.

(3-10) The effect of the target atomic Mass on the sputtering yield

Figure (3-85) shows the plot with using origin8 Program of sputter yield vs. atomic Mass for target elements for (Be, Cr, Mn, Fe, Ni, Cu, Zn, Pb) bombarded by (Ar, N₂, and O₂) ions in the incident ion Energy 0.5 KeV using TRIM simulation data.

Figure (3-85) shows that the sputtering yield of Zinc (Zn) target (with atomic Mass = 65.38) is higher than the other elements. The minimum sputtering yield is to Beryllium (Be) (with atomic Mass = 9.012182). This means the sputter yield increases with increasing the target atomic Mass of the elements of the alloys.

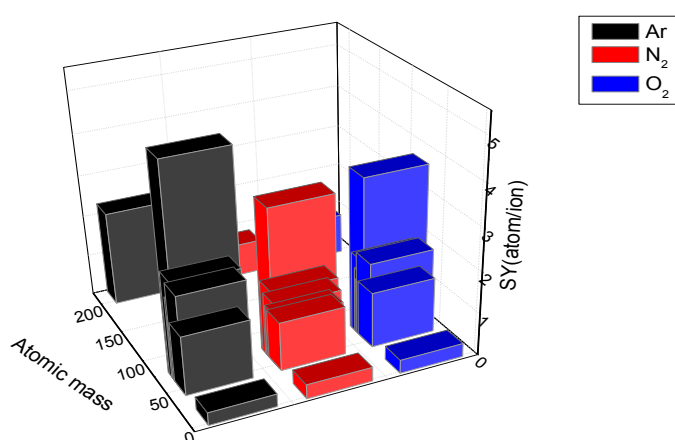


Figure (3-85): Sputtering yield vs. atomic Mass target for (Be, Cr, Mn, Fe, Ni, Cu, Zn, Pb) bombarded by (Ar, N₂, and O₂) ions.

(3-11) Conclusions

1. The S.Y increase with increasing the incident ion energy. When the ion energy is greater than the threshold energy, there is a gradual increase in the yield, and when ion energy greater than 8 keV, there is a small increase in sputter yield and then begins to decline.

2. The S.Y yield has a slight increase from the incident angle of (0°) to (60°) and then a significant increase typically between (60°) to (80°) of incident angle. after crossing the maximum, it decreases rapidly at larger angles (80°).
3. Sputtering yield increases linearly with an increasing atomic number of incident ions (Ar, N₂ , O₂).
4. The S.Y changes with the change of elemental concentration in the alloy, the change non-linearly in the target concentrations.
5. Surface binding energy is a factor that determines the sputter yield. Increasing and decreasing these values about the well –known surface binding energy value would lead to variation in the sputter yield. There is an inverse linear dependence between surface binding energy and the sputter yield.
6. Energy sputters yield maximum, E (S.Ym) increase with increasing incident ion angle, this increase is slight when angles less than 60° . Then increases significantly. That the argon-ion is higher E (S.Ym) of other ions.
7. A slight increase of the angle of incidence yields to a gradual increase in the normalized sputter yield reaching to the highest point of the angle 70° and then it drops rapidly towards low values as it approaches 89° .
8. The sputter yield increases with increasing the target atomic numbers of the elements of the alloys.
9. The sputter yield increases with increasing the target atomic Mass of the elements of the alloys.
10. According to our findings in this work we suggest:
 - a) The alloy consists of elements (iron, nickel, and chrome).

- b) The ratio of the elements of iron, nickel, and chrome in the alloy in the following form where the iron and nickel by 35% for each one of the ratios of chrome is 30%.
11. The results reveal a relatively higher sputtering yield for Brass alloy than BeCu and Monel – 400. And less sputtering yield at Stainless-Steel alloy made of elements (Cr, Fe, Ni). As shown in the tables of (3-27) to (3-32).

Table (3-27): Max. Sputter yields vs. Energy for Argon ion.

Figure	Target (Alloy)	Max. Sputter Yields (atoms/ion)	Energy (keV)
(3-25)	BeCu	33.6736	50
(3-28)	Brass	48.31	50
(3-31)	Stainless-Steel	26.98	50
(3-34)	Monel – 400	33.9146	50

Table (3-28): Max. Sputter yields vs. Energy for Nitrogen ion.

Figure	Target (Alloy)	Max. Sputter Yields (atoms/ion)	Energy (keV)
(3-26)	BeCu	10.9158	50
(3-29)	Brass	15.3644	40
(3-32)	Stainless-Steel	9.0758	40
(3-35)	Monel – 400	11.202	50

Table (3-29): Max. Sputter yields vs. Energy for Oxygen

Figure	Target (Alloy)	Max. Sputter Yields (atoms/ion)	Energy (keV)
(3-27)	BeCu	13.2028	50
(3-30)	Brass	18.4358	40
(3-33)	Stainless-Steel	10.6518	50
(3-36)	Monel – 400	13.4090	40

Table (3-30): Max. Sputter yields vs. Incident Angle for Argon ion.

Figure	Target (Alloy)	Max. Sputter Yields (atoms/ion)	Incident Angle (deg)
(3-1)	BeCu	14.89	70
(3-4)	Brass	20.76	70
(3-7)	Stainless-Steel	11.75	70
(3-10)	Monel – 400	14.3	70

Table (3-31): Max. Sputter yields vs. Incident Angle for Nitrogen ion.

Figure	Target (Alloy)	Max. Sputter Yields (atoms/ion)	Incident Angle (deg)
(3-2)	BeCu	7.11	70
(3-5)	Brass	9.84	70
(3-8)	Stainless-Steel	5.76	80
(3-11)	Monel – 400	7.01	80

Table (3-32): Max. Sputter yields vs. Incident Angle for Oxygen ion.

Figure	Target (Alloy)	Max. Sputter Yields (atoms/ion)	Incident Angle (deg)
(3-3)	BeCu	8.19	70
(3-6)	Brass	11.47	70
(3-9)	Stainless-Steel	6.56	80
(3-12)	Monel – 400	7.84	70

(3-12) Suggestions for future work

Given the importance of alloys in equipment and devices used mainly in our lives, so recent research tends to focus on them, we suggest the following:

1. Study of Ferro alloys and bombarded with the same ions that were made in this study (Non – ferrous alloys), namely argon, nitrogen, and oxygen.
2. Change the proportions of the constituent elements of the alloys and find out the most influential element in calculating the sputtering yield.

3. Study the effect of changing ions bombarding the alloys to be light, medium and heavy and compare the results to see the impact of ion mass on the alloys themselves.



REFERENCES

References

- [1] D. M. Mattox, (2003). "The Foundations of Vacuum Coating Technology", Noyes Publications, New York. USA.
- [2] W. R. Grove, (1952). "On the Electrochemical Polarity of Gases", Philosophical Transactions Royal Society, (London), Vol (142), p. 87.
- [3] F. Keywell, (1955). "Measurements and Collision-Radiation Damage Theory of High Vacuum Sputtering", Physical Review, Vol. 97, N. 6, pp. 1611-1619,
- [4] P. Sigmund, (1981). "Sputtering by Ion Bombardment: Theoretical Concepts", Sputtering by Particle Bombardment I, Springer-Verlag, Berlin.
- [5] J. F. Ziegler and J. P. Biersack. SRIM 2003 (Program and Documentation). <http://www.srim.org>.
- [6] J. P. Biersack, & L. G. Haggmark, (1980). A Monte Carlo computer program for the transport of energetic ions in amorphous targets. Nuclear Instruments and Methods, 174 (1-2), 257-269.A.
- [7] J. F. Ziegler, & J. P. Biersack, (2008). SRIM-2008, Stopping power and range of ions in matter. Nuclear energy agency of the OECD (NEA). Inis Issue 49. Volume 40. D-14109 Berlin (Germany).
- [8] G. F Knoll, (1999). Radiation detection and measurement (3rd ed.). New York: Wiley. ISBN 978-0-471-07338-3.
- [9] V. Swaminathan, A. Jayaraman, (2001), Semiconductors, Raman Spectroscopy of in Encyclopedia of Materials: Science and Technology,
- [10] W. Robert (1984). CRC, Handbook of Chemistry and Physics. Boca Raton, Florida: Chemical Rubber Company Publishing. pp. E110. ISBN 0-8493-0464-4.

- [11] W. D. Callister, & D. G. Rethwisch, (2007). *Materials science and engineering: an introduction* (Vol. 7, pp. 665-715). New York: John Wiley & Sons.
- [12] B. D. Fahlman, (2011). *Materials chemistry* (2. ed.). Dordrecht [u.a.]: Springer. ISBN 978-94-007-0692-7.
- [13] P. Lacombe, B. Baroux, and G. Beranger (1990). *Les aciers inoxydables*. Les Editions de Physique. ISBN 2-86883-142-7.
- [14] "Monel" *Encyclopedia Britannica*. Retrieved (2014).
- [15] R. Behrisch, (1981), "Sputtering by Particle Bombardment I: Physical Sputtering of Single-Element Solids", vol. 47, pp17 of *Topics in Applied Physics*. Springer-Verlag, New York.
- [16] P. D. Townsend, J. C. Kelly, and N. E. W. Hartley. (1976). "Ion Implantation, Sputtering and Their Applications". Academic Press, New York.
- [17] C. Alexander, (1999). "The Neutral Source for the Exosphere of Ganymede from Sputtering and Sublimation Processes Combined", American Geophysical Union Fall meeting, San Francisco, CA,
- [18] R. A. Baragiola, (2004). "Sputtering: Survey of Observations and Derived Principles", *Philosophical Transactions Royal Society of London A.*, Vol. 362, pp. 29-53.
- [19] N. Laegreid, & G. K. Wehner, (1961). Sputtering yields of metals for Ar⁺ and Ne⁺ ions with energies from 50 to 600 eV. *Journal of Applied Physics*, 32 (3), 365-369.
- [20] P. K. Hafft. (1976), "On the sputtering of binary compounds" Copenhagen, Denmark.

- [21] Z. L. Liao and et. al. (1977). "Surface-layer composition changes in sputtered alloys and compounds". California.
- [22] P. Sigmund, (1979). Recoil implantation and ion- beam- induced composition changes in alloys and compounds. *Journal of Applied Physics*, 50 (11), 7261-7263.
- [23] T. Okutani, M. Shikata, , & R. Shimizu, (1980). Investigation on surface compositions of Cu - Ni alloy under Ar⁺ ion bombardment by ISS and in situ AES measurements. *Surface Science*, 99 (3), L410-L418.
- [24] G. Betz, M. Opitz, & P. Braun, (1981). Dynamic surface composition changes in binary alloys under ion bombardment. *Nuclear Instruments and Methods*, 182, 63-66.
- [25] L. Rivaud, A. H. Eltoukhy, & J. E. Greene, (1982). Low energy ion bombardment enhanced diffusion, segregation, and phase transformations in Cu: In alloys. *Radiation Effects*, 61 (1-2), 83-92.
- [26] M. P. Seah, (1981). Pure element sputtering yields using 500–1000 eV argon ions. *Thin Solid Films*, 81 (3), 279-287.
- [27] Y. Yamamura, N. Matsunami, & N. Itoh, (1983). Theoretical studies on an empirical formula for sputtering yield at normal incidence. *Radiation Effects*, 71 (1-2), 65-86.
- [28] R. S. Li, L. X. Tu, & Y. Z. Sun, (1985). Energy dependence of the surface composition changes in Au - Cu alloys under Ar⁺ ion bombardment. *Surface Science*, 163 (1), 67-78.
- [29] K. W. Pierson, J. L.Reeves, T. D. Krueger, C. D. Hawes, & C. B. Cooper,. (1996). The total sputtering yield of Ag/Cu alloys for low energy argon ions. *Nuclear Instruments and Methods in Physics*

Research Section B: Beam Interactions with Materials and Atoms, 108 (3), 290-299.

- [30] M. Kustner, , W. Eckstein, , E. Hechtel, , & J. Roth, (1999). Angular dependence of the sputtering yield of rough beryllium surfaces. *Journal of Nuclear materials*, 265 (1-2), 22-27.
- [31] W. Eckstein, and R. Preuss, (2003). New fit formulae for the sputtering yield. *Journal of nuclear materials*, 320 (3), 209-213.
- [32] M. P. Seah, C. A. Clifford, F. M. Green, & I. S. Gilmore, (2005). An accurate semi-empirical equation for sputtering yields I: for argon ions. *Surface and Interface Analysis: An International Journal devoted to the development and application of techniques for the analysis of surfaces, interfaces and thin films*, 37 (5), 444 - 458.
- [33] T. A. Cassidy, & R. E. Johnson, (2005). A Monte Carlo model of sputtering and other ejection processes within a regolith. *Icarus*, 176 (2), 499-507.
- [34] M. P. Seah, & T. S. Nunney, (2010). Sputtering yields of compounds using argon ions. *Journal of Physics D: Applied Physics*, 43 (25), 253001.
- [35] V. I. Bachurin, S. A. Krivelevich, E. V. Potapov, A. B. Churilov, (2007). "Study of the interaction of Ar⁺ and Nitrogen ions with the Silicon dioxide surface". *V* (1), p (136)
- [36] Huda M. Tawfeek, Mustafa K. Jassim, Firas M. Hady, Rafah I. Nori. (2015), "A Computer Simulation Study of Sputtering Yield of GaAs Target Bombarded by Argon Ions". *Diyala Journal for Pure Sciences*. *V* (11) N (4), pp 132 – 141.

- [37] H. Gu, J. Cui, D. D. Niu, A. Wellbrock, W. L. Tseng, & X. J. Xu, (2019). Monte Carlo calculations of the atmospheric sputtering yield on Titan. *Astronomy & Astrophysics*, 623, A18.
- [38] L.I. Maissel and R. Glang, editors, (1970). "Handbook of Thin Film Technology", chapter (3). McGraw-Hill, New York.
- [39] M. Nakles, J. Pierru, J. Wang, & M. Domonkos, (2004). Experimental and Modeling Studies of Low Energy Ion Sputtering in Ion Thrusters. In 39th AIAA/ASME/SAE/ASEE Joint Propulsion Conference and Exhibit (p. 5160).
- [40] J. Roth, J. B. Roberto, & K. L. Wilson, (1984). Erosion of carbon due to bombardment with energetic ions at temperatures up to 2000 K *Journ. Nucl. Mater*, 122 (123), 1447.
- [41] G. K. Wehner, (1975). In *methods of surface analysis*, Ed. A. W. Zanderna. (Elsevier. New York)
- [42] H. H. Andersen, (1974), in: *physics of Ionized Gases*, Ed. V. V ujnovic (Inct. of physics, univ. of Zagreb, Yugoslavia, p. 361.
- [43] H. Oechsner, (1976), in: *physics of Ionized Gases*. Ed.B. Narinsek, (J. Stefan Inst. , Univ. of Ljubljant, Yugoslavia, p. 477.
- [44] P. K.Haff, , & Z. E. Switkowski, (1976). On the sputtering of binary compounds. *Applied Physics Letters*, 29 (9), 549-551.
- [45] Lucille, A. Giannuzzi and Fred, A. Stevie (2005) *Introduction to Focused Ion Beams: Instrumentation Theory, Techniques and practice*. Springer.
- [46] I.P. Jain. G. Agarwal, (2011), "Ion beam induced surface and interface engineering" *Surface Science Reports* 66. 77–172, Jaipur 302004, India.

- [47] K. A. Zoerb, (2007). Differential sputtering yields of refractory metals by ion bombardment at normal and oblique incidences (Doctoral dissertation, Colorado State University).
- [48] J.S. Dolaghen, (1991). "Monte Carlo Simulation of Molecular Redistribution in an Enclosure due to Sputtering", M.S. Thesis, Colorado State University, USA.
- [49] R. Behrisch, W. Heiland, W. Poschenrieder, P. Staib, & H. Verbeek, (1973). Ion surface interaction, sputtering, and related phenomena. Conference held at Munich, Germany, September 24--27, 1972 (No. CONF-7209125-). Gordon and Breach, Science Publishers, Inc., New York.
- [50] R. Behrisch, (1981). "Introduction and Overview", Sputtering by Particle Bombardment., Springer-Verlag, Berlin. Vol. 1, pp. 1-8,
- [51] V.S. Smentkowski, C. Wei, and K. Browall, (1999). "Summary of Sputter Yield Literature", General Electric Research and Development Centre, General Electric Company.
- [52] J. Jung, (2011). The effect of the sputtering parameters on the ITO films deposited by RF magnetron sputtering. The University of Texas at San Antonio.
- [53] T. T. Emons. J. Li, L. F. Nazar, J. Am. Chem. (2002). Soc.124, 8516
- [54] N. Bohr, & K. Dan, (1948). Vidensk, Selsk. Mat. Fys. Medd, 18 (8).
- [55] Olivier B. Duchemin. (2001). An Investigation of Ion Engine Erosion by Low Energy Sputtering. PhD thesis, California Institute of Technology, Pasadena, CA.
- [56] J. Orloff, M. Utlaut, and L. Swanson, (2003). High Resolution Focused Ion Beams: FIB and its Applications, Kluwer Academic/Plenum Publishers, NY,

- [57] International Fusion Research Council (IFRC), (2005) Status Report on Fusion Research, Nucl. Fusion V (52), pp1–28,.
- [58] H.E. Wilhelm, (1985), "Quantum-statistical analysis of low-energy sputtering". Australian Journal of Physics, V (38), N (2), pp125–133.
- [59] M. P. Seah, C. A. Clifford, F. M. Green, & I. S. Gilmore, (2005). An accurate semi-empirical equation for sputtering yields I: for argon ions. Surface and Interface Analysis: An International Journal devoted to the development and application of techniques for the analysis of surfaces, interfaces and thin films, 37 (5), 444-458.
- [60] P. Sigmund, (1987), Mechanisms and theory of physical sputtering by particle impact, Nucl. Instruments Methods Phys. Res. B27 1–20.
- [61] N. Matsunami, Y. Yamamura, Y. Hikawa, N. Itoh, Y. Kazumata, S. Miyagawa, K. Morita, R. Shimizu, and H. Tawara, (1984). At. Data Nucl. Data Tables 311-80
- [62] P. Sigmund, (1969). Theory of sputtering. I. Sputtering yield of amorphous and polycrystalline targets. Physical review, 184 (2), 383.
- [63] J. Lindhard, V. Nielsen, M. Scharff, & P. V. Thomsen, (1963). Integral equations governing radiation effects. Mat. Fys. Medd. Dan. Vid. Selsk, 33 (10), 1-42.
- [64] N. Matsunami, Y. Yamamura, Y. Itikawa, N. Itoh, Y. Kazumata, S. Miyagawa, & R. Shimizu, (1981). A semiempirical formula for the energy dependence of the sputtering yield. Radiation Effects, 57 (1-2), 15-21.
- [65] P. Sigmund, (1981), Topics in Applied Physics 47: Sputtering by Particle Bombardment I. R. Behrisch (Berlin: Springer) p 9-71
- [66] C. Anders, & H. M. Urbassek, (2005). Effect of binding energy and mass in cluster-induced sputtering of van-der-Waals bonded systems. Nuclear Instruments and Methods in Physics Research

Section B: Beam Interactions with Materials and Atoms, 228 (1-4), 84-91.

- [67] M. P. Seah, T. S. Nunney. (2010), “Sputtering yields of compounds using argon ions”. *Journal of Physics D: Applied Physics*, IOP Publishing, 43 (25), pp. 253001.

الخلاصة :

تمت دراسة سلوك حاصل التريز للسبائك المعدنية (Stainless- ، Monel-400 ,Brass ، BeCu) والتي تم قصفها بأيونات (Ar و N₂ و O₂) باستخدام برنامج TRIM (نقل الأيونات في المواد)، وهو برنامج يستخدم خوارزمية مونت كارلو لمحاكاة عملية التريز. كان اختيار السبائك المستخدمة في هذه الدراسة بسبب أهميتها الكبيرة واستخداماتها في العديد من التطبيقات المهمة مثل أدوات القياس الدقيقة والفضاء.

كان عرض السبيكة المستخدمة في هذه الدراسة هو 1000 أنكستروم وعدد الأيونات هو 5000 بسبب نتائجنا المستحصلة ثبت أن أي تغيير في عدد الأيونات يؤدي إلى تغييرات طفيفة وليست كبيرة في حاصل التريز وان استخدام 5000 أيون في الواقع يقلل من وقت العمليات الحسابية.

أظهرت النتائج أن الدراسة النظرية لحساب حاصل التريز من السبائك المعدنية التي تم قصفها بأيونات مختلفة (Ar, N₂, O₂) في الحالات الطبيعية ومائلة تعتمد بشكل أساسي على عدة عوامل مهمة وهي : طاقة الايون، زاوية السقوط ، العدد الذري والكتلي للأيونات الساقطة ، العدد الكتلي والذري للهدف ، وتركيز العناصر المستخدمة في السبائك. تشير النتائج التي تم الحصول عليها في هذه الدراسة إلى أن حاصل التريز يعتمد بشكل مباشر على هذه المعلمات. ان تغيير طفيف في زاوية السقوط من حزمة الأيون والطاقة يؤدي إلى تغيير كبير وواضح في حاصل التريز.

اظهرت هذه الدراسة وجود زيادة في حاصل التريز بزيادة العدد الذري لأيونات القصف على السبائك المستهدفة ، وهي الأركون والنيتروجين والأوكسجين. كذلك الاعتماد غير الخطي لحاصل التريز على تركيز العناصر المستخدمة في السبائك المستهدفة. كما أظهرت النتائج أن التغيير الطفيف في الطاقة السطحية للهدف (زيادة ونقصان على حد سواء) يؤدي إلى تغيير كبير وهام في حاصل التريز. ولتوضيح الرسوم البيانية بين المتغيرات تم استخدام برامج عالمية مثل ORIGIN 8 و IGOR. بالإضافة إلى ذلك، تم تضمين نتائج العمليات الحسابية الموجودة في معاملات المنحنى في المعادلات شبه التجريبية لجميع المتغيرات.



جمهورية العراق

وزارة التعليم العالي والبحث العلمي

جامعة بغداد

كلية التربية للعلوم الصرفة – ابن الهيثم

قسم الفيزياء

دراسة حاسوبية لحاصل ترزيد السبائك المعدنية

(BeCu, brass, stainless –steel, and monel-400)

بقصفها بواسطة أيونات (Ar, N₂, and O₂)

مختلفة عند سقوطها المباشر والمائل

رسالة

مقدمة إلى مجلس كلية التربية للعلوم الصرفة (ابن الهيثم) جامعة بغداد

وهي جزء من متطلبات نيل شهادة الماجستير في علوم الفيزياء

تقدم بها

نعيم ناهي عبد علي

بكالوريوس في علوم الفيزياء (1997)

بأشراف

م.د. أيناك أحمد جواد